UNIVERSITY OF MINNESOTA
ST. ANTHONY FALLS LABORATORY
Engineering, Environmental and Geophysical Fluid Dynamics

PROJECT REPORT 461

Pressure Loss Coefficients of 6, 8 and 10-inch Steel Pipe Fittings

By
Chengwei (Alex) Ding, Luke Carlson, Christopher Ellis and Omid Mohseni

Prepared for
American Society of Heating, Refrigerating and Air-Conditioning Engineers, Inc.
(Final Report on ASHRAE Research Project No. 1116-TRP)

February 2005
Minneapolis, Minnesota

Executive Summary

The scope of this study includes the testing of 6, 8 and 10-inch wrought steel fittings with flowing water to determine their head loss coefficient values. The fittings comprise long elbows, reducing and expansion elbows, Tees, reducing Tees, concentric reducers and expansions. Sixty fittings from seven manufacturers (four manufacturers per fitting) were tested at specified ranges of flow velocities to determine their head loss coefficients. In addition, an uncertainty analysis was conducted to determine the errors associated with the test set-up, the instrumentation, and the procedures used for these tests. The head loss coefficients of the fittings and their ranges are presented in this report as a function of upstream flow velocity and the Reynolds number.

The results of the study show that the K-value of long elbows is smallest for larger pipe fittings and increases as the pipe fitting size decreases. For branching flows in Tees, the K-value of the straight leg is very similar to those in reducing Tees. However, for branching flows in reducing Tees, the K-value of the branching leg varies with size and the percent reduction in flow area. The K-values of reducers and expansions show a weak dependence on upstream velocity. They are dependent on both the fitting size, and the percent reduction and expansion of the flow area.

Acknowledgements

The work reported herein was supported by the American Society of Heating, Refrigerating and Air-Conditioning Engineers, Inc. (ASHRAE). Mr. Al Black and Michael Vaughn were the project officers. We would like to thank the ASHRAE Technical Committee TC6.1 for their continued support in sponsoring this project. We would also like to thank Professor William Rahmeyer of the Utah State University for his voluntary support in sharing valuable information regarding previous test experiences. We would like to thank Mike Plante, Brett Otteson and Benjamin Erickson from St. Anthony Falls Laboratory for their help with the test set-up, the instrumentation and the photos.

Table of Contents

List of Figures

List of Tables

1. Introduction

Passing a fluid through a pipe fitting often results in a net energy loss which is usually associated with a drop in pressure. The pressure drop or head loss is caused by friction between the fluid and the fitting wall, flow separation and associated turbulence, regions with secondary flows, and non-uniform flow distribution downstream of the fitting. The fitting head loss is often quantified by a non-dimensional coefficient, the K-value, multiplied by a velocity head. The fitting head loss, which is called minor loss in text books and in many fluid mechanics publications, plays an important role in sizing pumps and piping and optimizing system cost versus system energy use in heating, ventilating and air-conditioning (HVAC) systems.

A frequently used source of K-values is the ASHARE Handbook Fundamentals (ASHRAE, 1997). Many of the sources of this data date to testing performed about 80 years ago. In addition to uncertainties regarding the measurement and calibration techniques used in those old experiments, the fittings in the current market have different geometry and roughness than those tested in the past. Recent testing conducted on several types and sizes of pipe fittings have shown that the older published K-values were often overestimated and result in over sizing the pumps for a piping system. Therefore, experienced practitioners have expressed a need for more accurate and complete data on K-values.

The scope of this study is testing of 6, 8 and 10-inch wrought butt welded steel fittings with flowing water to determine their K-values. The fittings comprise 90^{o} long elbows, reducing and expansion elbows, Tees, reducing Tees, concentric reducers and expansions. Sixty fittings from seven manufacturers (four manufacturers per fitting) were tested at a specified range of flow velocities. A total of 1,256 tests were conducted in this study.

In this report, a brief review of the existing data is given in section 2. The methodology is then described in section 3 and the test results in section 4. An uncertainty analysis conducted on these tests is presented in section 5, and the fitting characteristics are presented in section 6.

2. Existing Data on Pipe Fittings

One of the earliest works on fitting head loss was done in late nineteen century by Freeman (1941). His work was all testing on threaded and flanged elbows, Tees, reducing Tees and reducers. He conducted experiments on 2½ to 8-inch fittings. His test set-up included multiple fittings in series. It is not clear how he accounted for the flow disturbances caused by upstream fittings on the downstream ones.

Similarly, Gieseke and Badgett (1932) conducted a series of tests in the early 1900s with multiple pipe fittings installed in series. In 1979, the Hydraulic Institute Engineering Data Book was published with K-values for pipe fittings. However, the origin of the data presented in the handbook is not clear.

In addition to the list cited above, there are manuals published by manufacturers (Crane, 1952; Crane 1979; Weldbend, 1996). The sources of the data are not clear but it seems that the data are from Freeman (1941) and Gieseke and Badgett (1932).

In 1981, Hooper introduced the two K-method to estimate the K-values as a function of the Reynolds number. No new data were introduced. The method was based on the data collected by Freeman (1941) and Piggot (1950).

Idelchik (1994) presents a broad range of experimental data for a variety of fittings. The handbook is very difficult to follow and there is a significant problem with definitions. The handbook, however, shows that it is possible to have negative K-values in a Tee with mixing flow.

Miller (1990) presented series of plots and equations with correction factors for estimating K-values of a variety of fittings over a broad range of sizes. He classified the presented data using three classes. Class 1 includes data which are based on experimental tests usually from two or more sources which had been cross-checked. Class 2 encompasses data from isolated research programs where no detailed cross-checking was possible, or the data were from two or more research program but outside of the expected experimental accuracy. Class 3 includes data either from less reliable sources or data

applied outside of their tested range. The data were presented as curves and equations as a function of the Reynolds Number. Only the data presented for regular 90^{o} elbow were Class 1 data, and the rest of the data were either Class 2 or Class 3. Miller shows that in Tees under some conditions, the K-value becomes negative.

Rahmeyer (1990a, 1990b) conducted a series of tests at Utah Water Research Laboratory on a range of 2 to 4-inch threaded and forged weld fittings for ASHRAE. Rahmeyer also conducted a series of tests on 12, 16, 20 and 24-inch forged steel weld fittings. The current study which has been conducted on 6, 8 and 10-inch fittings was conducted to complement the tests performed at Utah Water Research Laboratory. In addition to providing updated data for pipe fittings in the 6 to 10-inch range, the current study provides loss coefficients for reducing elbows and reducing Tees which have never been previously tested.

3. Methodology

3.1. Hydraulics of Loss Coefficients

The pressure loss coefficient of fittings, K, is defined from the Darcy equation as follows

$$K = \frac{h_m}{V_1^2 \diagup 2g} \tag{3.1}$$

where h_m is the fitting head loss, V_1 is the average upstream velocity at the inlet of the fitting, and g is the gravitational acceleration (32.2. ft/sec^2). To determine the head loss of a fitting, Bernoulli's equation between a point upstream and a point downstream of the fitting can be utilized as follows

$$\frac{P_1}{\gamma} + \frac{V_1^2}{2g} = \frac{P_2}{\gamma} + \frac{V_2^2}{2g} + \sum_i \frac{f_i \, L_i}{D_i} \frac{V_i^2}{2g} + h_m \tag{3.2}$$

where P is pressure, γ is the specific weight of water, f is the Darcy-Weisbach friction loss coefficient of the pipe connected to the fitting, D is the pipe diameter where the pressure P is measured, L is the length of the pipe between the fitting and the pressure measurement location, and subscripts 1 and 2 refer to the upstream and downstream pressure measurement locations, respectively.

Every fitting produces secondary flow and turbulence which affects the flow pattern downstream of the fitting. Therefore, to correctly utilize equation 3.2 for estimating the fitting head loss, the pipe length downstream of the fitting needs to be long enough for the local effects of the fitting on the downstream velocity profile to dissipate. This length is described in section 3.2.6. The fitting head loss h_m can thus be estimated by rearranging equation 3.2 as

$$h_m = \frac{P_1 - P_2}{\gamma} + \frac{V_1^2 - V_2^2}{2g} - \sum_i \frac{f_i \, L_i}{D_i} \frac{V_i^2}{2g} \tag{3.3}$$

The term $(P_1\text{-}P_2)/\gamma$ can be estimated using pressure taps at points 1 and 2 and a pressure

transducer between the two points to measure the differential pressure. The average velocities, V_1 and V_2, can be estimated by measuring the flow rates and the pipe cross-sectional areas at those locations. The head loss due to pipe friction, the last term on the right hand side of equation 3.3, can be determined either by estimating the Darcy-Weisbach friction factor as a function of the pipe Reynolds number using the Moody Diagram, or by directly measuring the friction head loss of a unit length of the straight pipe as a function of flow rate. In this study, the latter method was used to eliminate the uncertainties with the Moody Diagram, the pipe diameter and pipe friction variability of which affect the friction head loss. Therefore, equation 3.3 cab be rewritten as

$$h_m = \frac{P_1 - P_2}{\gamma} + \frac{V_1^2 - V_2^2}{2g} - \sum_i L_i F_i(Q) \tag{3.4}$$

where $F(Q)$ is the straight pipe friction loss function. The notation Σ indicates the sum of the head losses due to friction of straight pipes upstream and downstream of the fitting, which could be from different materials, e.g. steel pipe upstream and PVC pipe downstream. In the following sections, the modified forms of equation 3.4 for each fitting are presented.

3.1.1. Flow in Elbows

For elbows, the upstream and downstream cross-sectional areas are the same; therefore the velocity does not change from point 1 to point 2. Equation 3.4 is then modified as follows.

$$h_m = \left(\frac{P_1 - P_2}{\gamma} \right) - \sum_i L_i F_i(Q) \tag{3.5}$$

3.1.2. Flow in Reducing Elbows, Reducers and Expansions

For reducing elbows, reducers and expansions, the upstream and downstream velocities differ; therefore, the fitting head loss is estimated using the following equation.

$$h_m = \left(\frac{P_1 - P_2}{\gamma} \right) + \frac{Q^2}{2g} \left(\frac{1}{A_1^2} - \frac{1}{A_2^2} \right) - \sum_i L_i F_i(Q) \tag{3.6}$$

where A_1 and A_2 are the pipe cross-sectional areas at the upstream and downstream pressure measurement locations, respectively.

3.1.3. Flow in Branching Tees

There are two fitting head losses associated with branching Tees. One is the straight thru-flow head loss, and the other is the branch flow head loss (Figure 3.1). Referring to Figure 3.1, the conservation equations for a branching Tee are as follows.

$$Q_1 = Q_2 + Q_3 \tag{3.7}$$

$$h_{m_{1-2}} = \left(\frac{P_1 - P_2}{\gamma} \right) + \frac{1}{2g} \left(\frac{Q_1^2}{A_1^2} - \frac{Q_2^2}{A_2^2} \right) - \sum_i L_i F_i(Q_i) \tag{3.8}$$

$$h_{m_{1-3}} = \left(\frac{P_1 - P_3}{\gamma} \right) + \frac{1}{2g} \left(\frac{Q_1^2}{A_1^2} - \frac{Q_3^2}{A_3^2} \right) - \sum_i L_i F_i(Q_i) \tag{3.9}$$

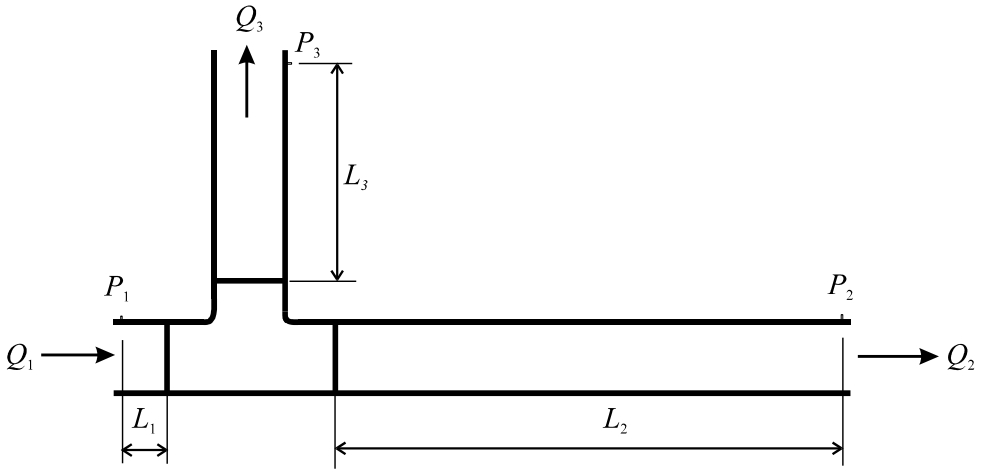

Figure 3.1. Schematic for flow paths through a branching Tee

3.1.4. Flow in Mixing Tees

Figure 3.2 shows the flow paths of a mixing Tee. Referring to Figure 3.2, the conservation equations for a mixing Tee are as follows.

$$Q_2 = Q_1 + Q_3 \tag{3.10}$$

$$h_{m_{1-2}} = \left(\frac{P_1 - P_2}{\gamma}\right) + \frac{1}{2g}\left(\frac{Q_1^2}{A_1^2} - \frac{Q_2^2}{A_2^2}\right) - \sum_i L_i F_i(Q_i) \tag{3.11}$$

$$h_{m_{3-2}} = \left(\frac{P_3 - P_2}{\gamma}\right) + \frac{1}{2g}\left(\frac{Q_3^2}{A_3^2} - \frac{Q_2^2}{A_2^2}\right) - \sum_i L_i F_i(Q_i) \tag{3.12 }$$

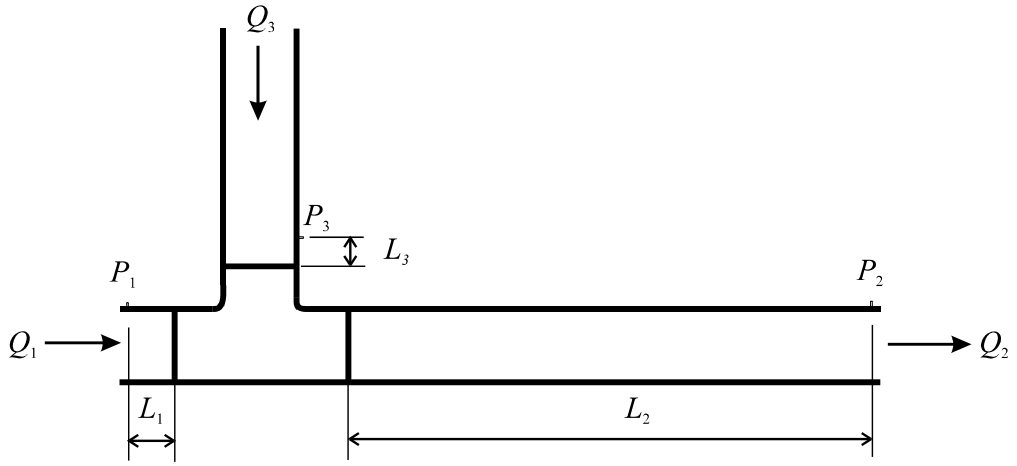

Figure 3.2. Schematic for flow paths through a mixing Tee

3.2. Test Set-ups and Procedures

3.2.1. General Layout

A testing layout was designed to provide a relatively convenient means for installing, aligning, sealing and testing the required fittings. The piping was located directly adjacent to the inlet of the SAFL weigh tanks to allow for in-place calibration of all orifices, and all discharge was to the tanks. Plan and elevation views are shown in Figure

3.3. There was one location where all fittings were tested. The main pipes in the testing set-up are labeled in Table 3.1 and shown in Figure 3.3.

Table 3.1. Main pipes arrangements

Pipe	Pipe Function	Valve	Valve Function
A	Supply	A	Supply
B	Supply or Drain	B	Supply
C	Drain	C	Drain
		D	Drain

Pipe B was reversible. With valve B open, and valve D closed, pipe B was a supply pipe and the flow was toward the test section. With valve B closed and valve D open, pipe B was a drain pipe and the flow was away from the test section. This arrangement made it possible to test Tees in mixing and branching flows in one installation. In order to decrease the system head loss, supply and drain pipes were 10 or 12 inch steel pipes. The pipes were reduced to the necessary diameter, and required upstream and downstream lengths were provided.

3.2.2. Water Supply and Control of Discharge

Water supply for the test rig was taken from the SAFL supply channel. The supply channel, approximately six feet deep and nine feet wide, runs the length of SAFL (250 feet) and connects uncontrolled to the pool of the Mississippi River above the St. Anthony falls. Due to the large cross-sectional area of the channel, it approximates a constant head source of water for the experiments. The total head available for testing was approximately 18 to 21 feet, dependent on the Mississippi River pool elevation. The connection of the test rig to the supply channel is shown in Figure 3.4.

In addition to valves A and B on the upstream side of the test section, valves C and D were located downstream of the test section and were used for additional flow adjustment. The drain pipe C discharged to the SAFL weigh tanks.

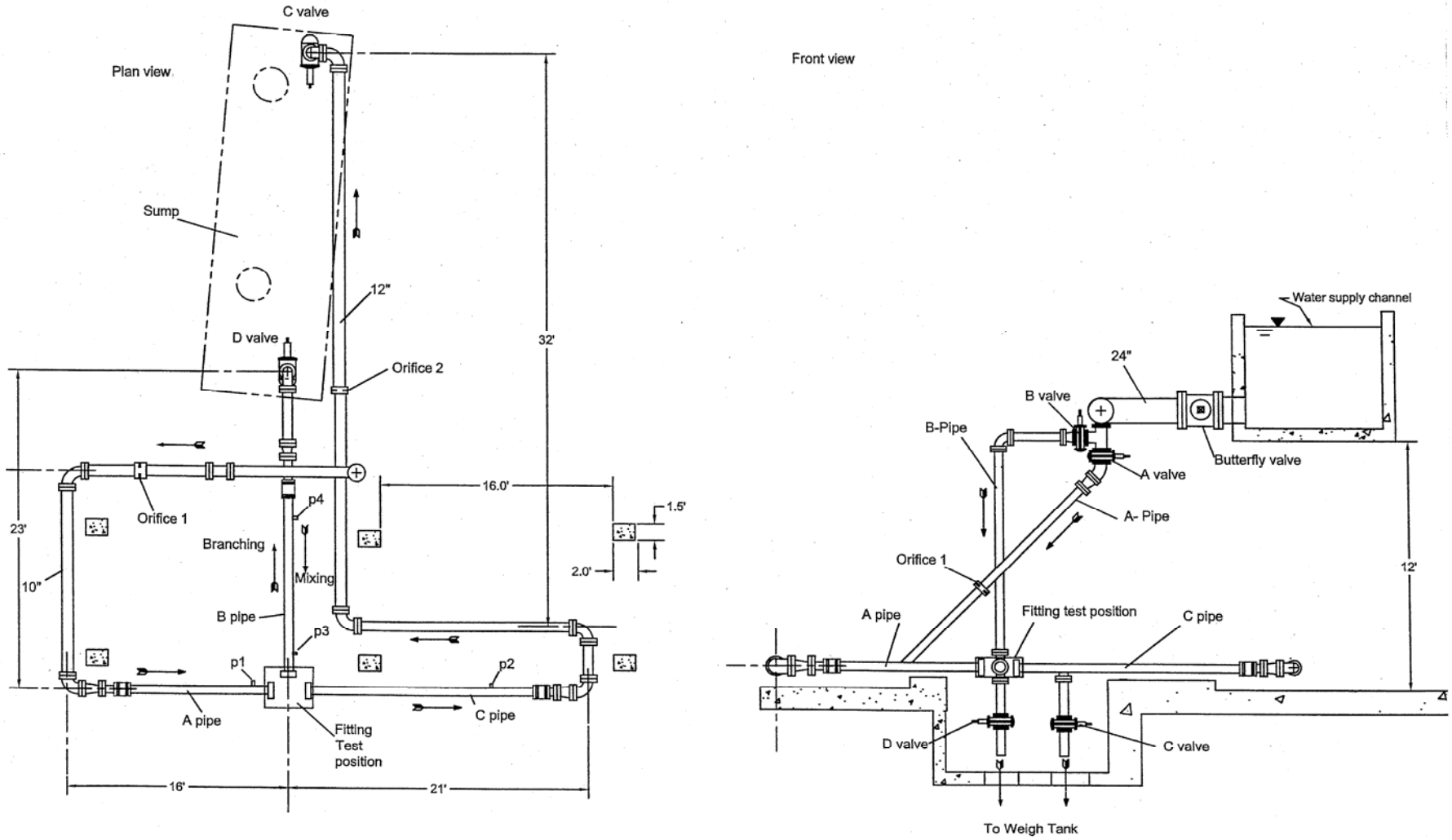

Figure 3.3. Plan view (left) and elevation (right) of pipe configuration.

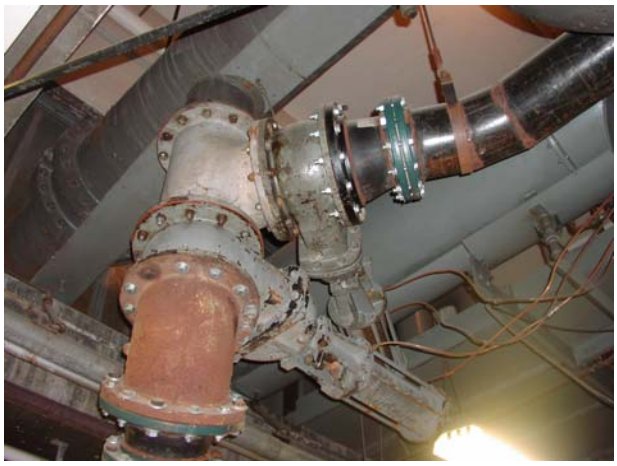

Figure 3.4. 24-inch tap from supply channel, 12-inch pipe and Tee to Pipe B (upper right) and Pipe A (bottom left). Note hydraulic-actuated gate valves on each pipe for control of flow rates.

3.2.3. Discharge Rate Measurement

The SAFL weigh tanks served as the primary standard for discharge measurements (Figure 3.5). The tanks were recently calibrated using NIST traceable standards and can measure discharges accurately up to approximately 16 cfs. Uncertainty associated with weigh tank measurements are flow rate and test duration dependent but are typically better than 0.5%. This facility was used to perform in place calibration of flow meters (orifices) at two locations in the testing setup as defined in Table 3.2. Figure 3.6 shows the results of the orifice calibrations for 6-inch fittings.

Table 3.2. Locations of orifices for flow measurements

Orifices	Pipe	Use
O1	A (Supply)	Total flow measurement, Flow proportion for mixing Tee
O2	C (Drain)	Total flow measurement, Flow proportion for branching Tee

One orifice was used at each meter location. Each orifice was sized so as to cause a differential pressure of 90″ of water to occur at the maximum discharge. Two Validyne differential transducers were used to measure this differential pressure, one having a range of 0″-90″ of water and the other having a range of 0″-14″ of water. For discharges between the maximum and 35% of maximum, the larger transducer was used. For

discharges below 35% of maximum, the smaller transducer was used. In this way, pressure measurement uncertainty for the lowest discharges was reduced by a factor of 6.4 over what would result if only the 90″ transducer were to be used for all flows. The 0.25% accuracy of the Validyne transducers translates to a pressure measurement uncertainty of 0.035″ of water for the 14″ transducer. It should be noted that each orifice was needed to measure from the maximum flow to 25% of the minimum total flow during the testing of branching and mixing flows in tees. This is a flow range of 1:40, corresponding to a pressure range of 1:1600 (0.0625%), which is beyond the accurate range of a single transducer. Using two selectable transducers reduced the flow range associated with each transducer to no more than 1:10 or a pressure range of 1:100 (1%).

The differential pressures across the flow meters (orifices) were measured using a Scanivalve controlled, an automatically calibrated transducer connected to a data acquisition system (see Section 3.2.8).

3.2.4. Pipe Configurations for Fitting Types

The supply and drain pipes are named as indicated in the above drawing with pipes A and B being the upstream pipes and C the downstream pipe. The arrangements for each of the fitting types are given in Table 3.3.

Figure 3.5. The St. Anthony Falls Weigh Tanks

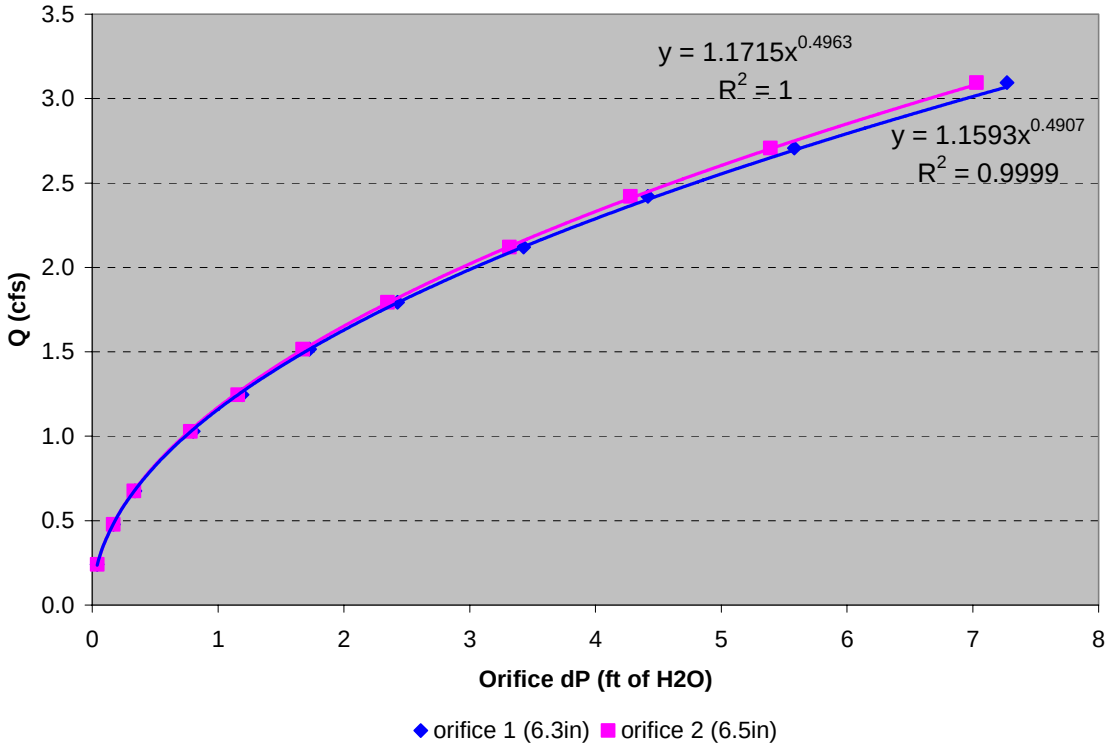

Figure 3.6. Calibration of 6-inch orifice flow meters against the weigh tanks

3.2.5. Pipe-Fitting Installation and Sealing

Fittings were installed as depicted in Figure 3.7. Flanges were welded to each pipe to form a seating surface for each fitting joint and to assist in alignment. Sealing was accomplished by an O-ring compressed into the void left by the chamfer on the pipe fitting (Figure 3.8). For Tees, the fitting was connected to the piping by through-bolts on flanges at Legs 1 and 2 and a U-bolt wrapped around the elbow to the flange at Leg 3. Adjustability of pipe length was built into each of pipes A, B and C at the end distant from the fitting. Reducers (and straight pipe for pipe friction testing) were attached to the flanges of pipes A and C with the same through-bolt arrangement.

Table 3.3. Testing set-ups

Fitting Type	K-Value Measured	Supply Pipe (Leg of Tee)	Upstream Pressure	Drain Pipe (Leg of Tee)	Downstream Pressure	Discharge Measurement O1 = Pipe A O2 = Pipe C
Concentric Reducer	Reducing	A	P1	C	P2	O2
Concentric Reducer	Expanding	A	P1	C	P2	O2
Long Radius Ell		B	P3	C	P2	O2
Reducing Ell	Reducing	B	P1	C	P4	O1
Reducing Ell	Expanding	B	P3	C	P2	O2
Tee	Branching	A(1)	P1	C(2) and B	P2 P4	O1 and O2
Tee	Mixing	A(1) B(3)	P1 P3	C(2)	P2	O1 and O2
Reducing Tee	Branching	A(1)	P1	C(2) B(3)	P2 P4	O1 and O2
Reducing Tee	Mixing	A(1) B(3)	P1 P3	C(2)	P2	O1 and O2

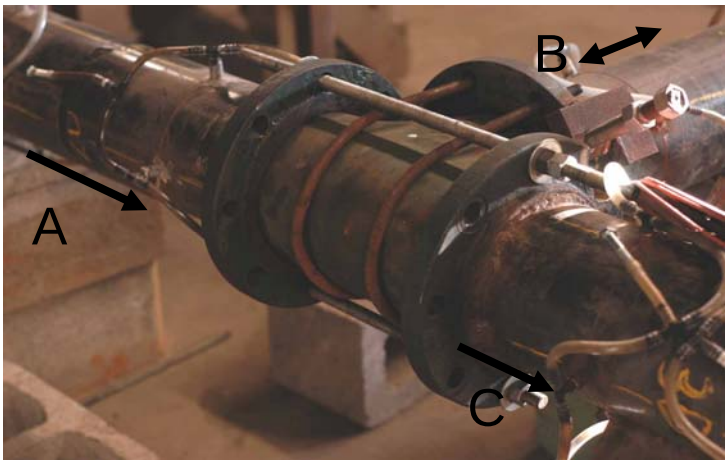

Figure 3.7. An installed 6″ Tee fitting

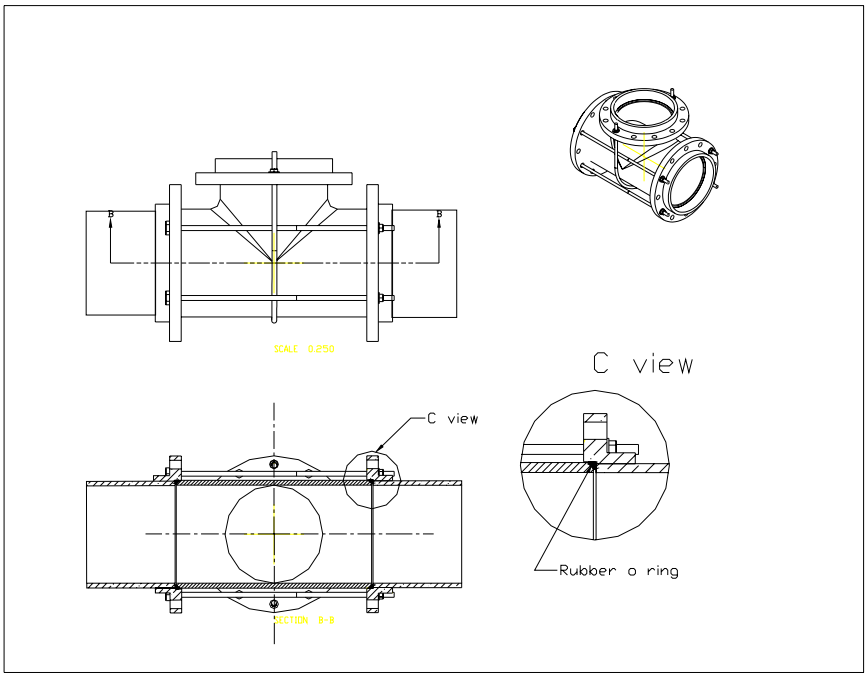

Figure 3.8. Tee fitting set-up

3.2.6. Upstream and Downstream Pipe Lengths and Pressure Measurement Locations

The test layout was designed to achieve a minimum straight pipe length equal to about 20 pipe diameters downstream of the test section and 10 pipe diameters upstream of the test section. Four pressure measurement locations were required to measure loss coefficients. The locations are shown in Figure 3.3 and explained in Table 3.4.

Table 3.4. Locations of the pressure taps

Pressure Tap	Location and Use
P1	Pipe A, ~ 1.5D upstream of the test section. Measurement of pressure loss in fittings; measurement of pressure loss in Pipe C.
P2	Pipe C, 20 diameters downstream of the test section. Measurement of pressure loss in fittings; measurement of pressure loss in Pipe C.
P3	Pipe B, ~ 1.5D upstream of the test section. Measurement of pressure loss in fittings; measurement of pressure loss in Pipe B.
P4	Pipe B, 20 diameters downstream of the test section. Measurement of pressure loss in fittings; measurement of pressure loss in Pipe B.

Measurement of friction head loss was conducted on pipe B as a supply pipe and used for flow in the opposite direction when it was operated as a drain pipe.

3.2.7. Pressure Tap and Tubing Design Couplings

Pressure taps consisted of 1/16-inch holes drilled through the pipe wall. The taps were de-burred on the inside of the pipe. Four taps were installed at quarter points of the pipe circumference at each measurement location and interconnected. A single tube conveyed this pressure to the pressure transducer. 1/16-inch I.D. Urethane tubing was used throughout the pressure measurement system.

3.2.8. Pressure Measurement

Differential pressure (DP) measurements for both of the flow meters (orifices) and for the fitting loss were made using Validyne Model DP15 transducers. The transducers measuring the orifices DP had ranges of 90 and 14 inches of water while that measuring the fitting loss had a range of 30 inches of water. Validyne DP15 transducers have a stated accuracy of 0.25% of their range. Thus, the expected accuracy of the orifice transducers were 0.225 inches (0.019 ft) and 0.035 inches (0.029 ft) of water while that of the fitting loss transducer was 0.075 inches (0.006 ft) of water. Both transducers were automatically calibrated before each fitting loss and flow rate measurement using a Scanivalve hydraulic switch and an array of known differential pressures. Three to five known differential pressures, from 0.0 ft to the upper range limit of each transducer, were measured 5 to 10 seconds, averaged, and then used to perform a quadratic best fit of the calibration measurements (Figure 3.9). This calibration was then used to convert the transducer output while measuring fitting loss and orifice DP from voltage to pressure. Before beginning fitting loss testing, this system was used (with the weigh tanks as described above) to calibrate the two flow meters (orifices). Once calibrated, the orifice coefficients (derived using a best-fit method, i.e. from Figure3. 6) were used to convert the measured orifice DPs to flow rate. The testing routine measured each orifice DP for 3 to 6 times for 5 to 10 seconds each time and the fitting DP for the same number of seconds six times. Following these measurements, the 0.0 ft DP reference and one mid-range DP reference was also measured to check for drift and any other change in

calibration. If these last "check" measurements were accurate to within the expected limits, the measurement was assumed accurate within the specifications. Incorporating automatic 3 to 5 point calibration before every measurement and 2 point verification after each measurement improved transducer accuracy to better than stated by the manufacturer, typically to better than 0.1% of full scale. Root mean square error of the 3 to 5 point calibration best fit was typically 0.05% of full scale.

A differential pressure manometer using Red Meriam was occasionally used in parallel with the pressure transducers as an analog check of the system and as an aid to quick adjustment of flow.

3.2.9. Data Acquisition System

Data acquisition was performed by a PC based system running LabView and using a National Instruments PCI-MIO-16XE-50 A/D card. This A/D card is a 16 bit board with programmable gain. Since the Validyne transducers have their own signal conditioners (Validyne CD23) which output +/- 10 VDC full scale, the range of the A/D card was set to this same range and thus had a resolution of 0.3 mV and an accuracy of about 1 mV. The 0.25% accuracy of the Validyne transducers corresponds to an output accuracy of 25 mV. Thus, the A/D board is about 25 times more accurate than the pressure transducers and was never a significant contributor to overall error. A/D measurements were made over an interval sufficient to capture unchanging statistics (approximately 5 seconds) at a rate of 1 kHz. In addition to performing the measurement of the pressure transducer outputs, the A/D board also exerted digital control over the Scanivalve hydraulic switch (causing it to step and auto home) as well as monitor the actual Scanivalve position. The LabView application allowed the operator to hit a button and initiate the automated measurement routine including the transducer calibration, flow rate and fitting loss measurement sequence, reference validation, and data reduction and storage.

The particular strengths of this measurement system included:

1. Auto-calibration of pressure transducers before each measurement and auto-verification following each measurement

2. Rapid and simultaneous measurement of fitting loss and flow rate so that even somewhat unsteady flow conditions did not affect the validity of the measurements

3. Accurate measurement of the mean and standard deviation of differential pressure, not subject to manual observation of fluctuating manometer levels.

A display screen from the LabView application showing the data acquisition components is shown in Figure 3.10.

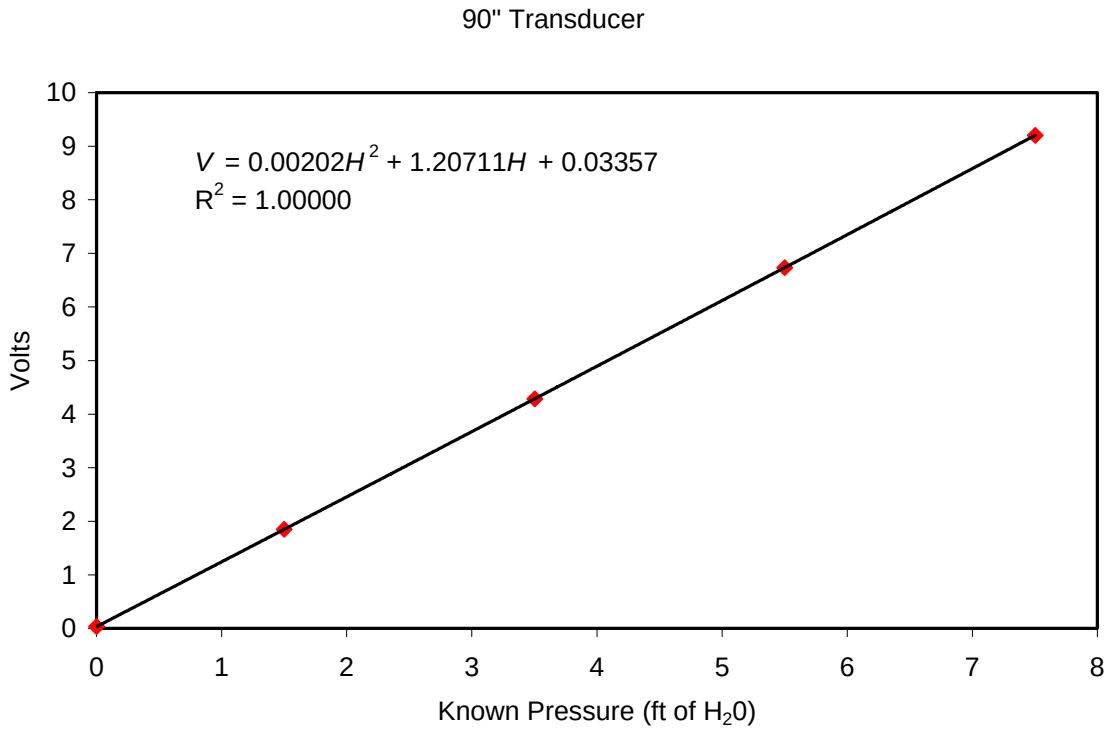

Figure 3.9. 90″ transducer calibration

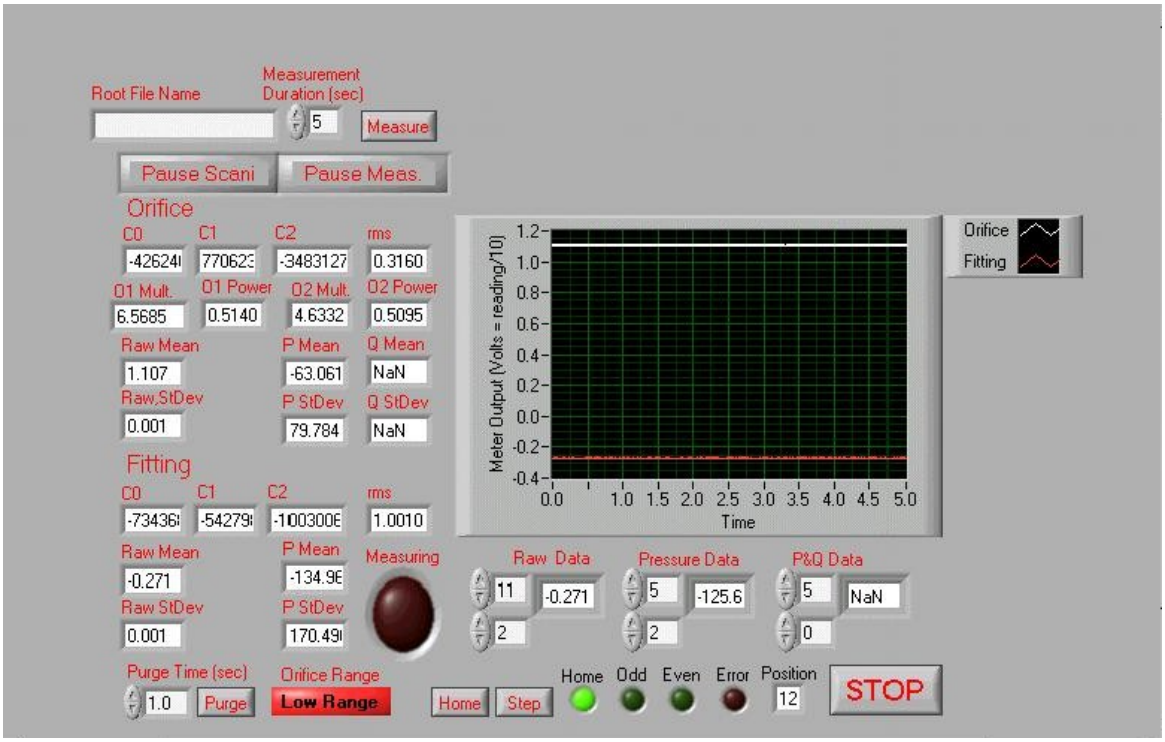

Figure 3.10. LabView screen showing the data acquisition components

3.3. List of Fittings and Number of Tests

There were a total of 1,256 tests conducted in this study, which included five types of fittings from four manufacturers. The list of the tests per fitting type is summarized in Table 3.5. Five complete tests (for the entire range of flows) were also conducted on one 6-inch elbow from one manufacturer to test the repeatability of the test procedure.

On the basis of the data obtained at Utah Water Research Laboratory for similar pipe fittings, we expected the variability in K-values for different samples of the same fitting from the same manufacturer to be significantly less than the variability in K-values for samples of the same fitting from different manufacturers. To verify this, five samples of 6-inch elbows, and five samples of 6-inch mixing and branching Tees from one manufacturer were tested. The K-values obtained from five samples of one manufacturer were compared with the K-value of the median of those samples and the K-values obtained from three other manufacturers; one sample per manufacture. The results showed that, except in very few cases, the variability in K-values for samples of the same

fitting from one manufacturer was substantially less than the variability in K-values for samples of the same fitting from different manufacturers. It should be noted, however, for a small number of cases, variability among samples was comparable to inter-manufacturer variability, but these cases involved very low flow rates where testing uncertainty is large in any case.

Table 3.5. Number of tests per fitting type

Fitting Type	Number of Tests
Long Ell	160
Tee	448
Reducing Tee	408
Reducing Ell	120
Concentric Reducer	120
TOTAL	1,256

3.4. Test Conditions and Range of Discharges

A total of 68 fittings were tested and 1,256 individual determinations of K-values were made. The total discharge range used for the testing is shown in Table 3.6. For a small number of high head loss test conditions, the maximum discharge tested was rather less than that indicated in Table 3.6 due to limitations of total head availability.

Table 3.6. Maximum and minimum flow rates tested

Diameter [in]	Minimum Discharge [cfs]	Maximum Discharge [cfs]
6	0.3	3.0
8	0.7	7.0
10	1.1	11.0

3.5. General Test Procedure

The general test procedure was as follows:

1. Calibrate orifice meters using weigh tanks over range of fitting test discharges.

2. Measure friction loss in Pipe C with a straight pipe blank in test section.
3. Measure friction loss in Pipe B (supply, in conjunction with elbow test).
4. Install and align the pipe fitting.
5. Fill pipes and eliminate leaks and trapped air.
6. Purge all pressure lines and fill pressure references.
7. Measure water temperature.
8. Establish discharge through a fitting; allow to stabilize while observing discharge measurement from orifice meter.
9. Run data acquisition routine to measure pressure loss through fitting and downstream pipe and pressure drop across orifice meter. Program samples each pressure for about 5 seconds at 1 kHz. Each measurement consists of:
    - Auto-calibration of pressure transducers.
    - Simultaneous discharge measurement and fitting loss measurements.
    - Verification of calibration following loss and discharge measurement.
    - Automatic saving of data files.
    - Manual check of differential manometers.
    - Manual data collection, file saving, notes.

4. Results

4.1. Water Analysis

As part of the experimental method validation, a sample of test water from the Mississippi River was analyzed to determine its kinematic viscosity. A no. 50 capillary tube viscometer was used for the analysis. The average kinematic viscosity of the sample was measured to be 1.288×10^{-5} ft^2/sec at 71.6 ^{o}F (22 ^{o}C). This value is about 19% larger than that reported for pure water at 22 ^{o}C, which is 1.038×10^{-5} ft^2/sec. The difference is likely due to the presence of suspended and soluble materials found in the Mississippi River. The sample was taken in winter and could be different from one taken in summer. In winter, the Mississippi River is at low flow and effluents discharged into the river, e.g. salt water due snowmelt, end in river in relatively high concentrations. In summer, the river is more frequently subject to effluent discharges from urban stormwater and agricultural runoff in the Mississippi River headwater. However, the river flow varies significantly in summer and fall. For the period of June to December, 2003, during which time the tests were conducted, the Mississippi River flow at the USGS station at Anoka, about 9 miles upstream of St. Anthony Falls Laboratory, varied from 1500 cfs to 28000 cfs. Therefore, it would be difficult to project the Mississippi River water viscosity from a single measurement when the Mississippi River flow was at 3000 cfs.

Viscosity is also a function of water temperature, which was measured during each test. Due to lack of reliable data on Mississippi River water viscosity, published values of pure water viscosity at the tested temperatures were used to calculate the Reynolds number.

4.2. Repeatability

To assess the repeatability of the test set-up and the apparatus used to measure the pressure differential and flow rates, the same fitting was tested five times. After each test, the fitting was removed from the test set-up and then re-placed in the test section and tested again. In this way, not only measurement uncertainty, but also non-reproducibility due to testing technique (purging of pipes and tubes, installation of fitting, etc.) would be addressed. Figure 4.1 shows the average fitting head loss of five tests conducted on a 6-

inch long radius elbow for the range of flows. The error bars show the range of values for the five tests. It is evident that the tests were repeatable. The maximum variability was about 3 to 5 percent of the mean at velocities smaller than 4 fps, and at velocities larger than 4 fps, the maximum variability was less than 2%.

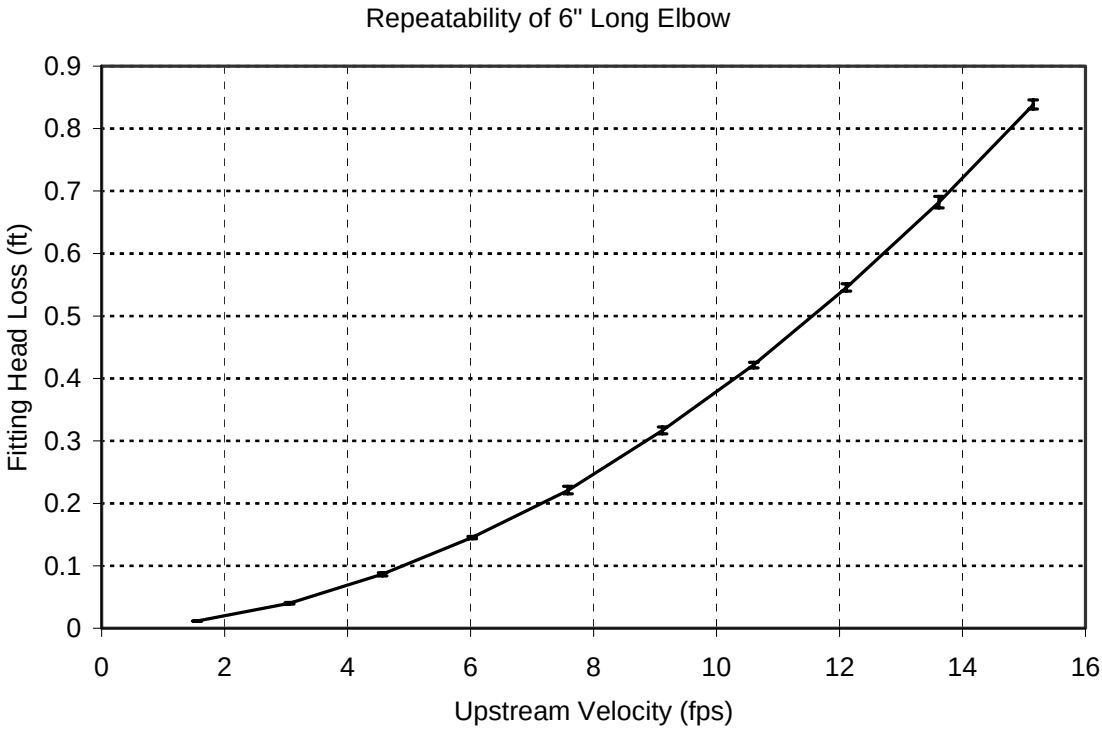

Figure 4.1. Fitting head loss for 5 tests on a 6-inch long elbow. The error bars show the range of measured values.

The repeatability of the resulting K-values of the 6-inch elbow was also assessed. Figure 4.2 illustrates the mean and the range of K-values obtained from the five tests versus the upstream velocities. It is evident from Figure 4.2 that the largest variation occurs at low flows. For velocities greater than 4 fps, the range of K-values is less than 2% of the mean. At low flows, where the velocities are quite small, the total loss and the pipe friction loss are very small and of comparable magnitude, causing the difference between the two yield a value for the fitting loss (Figure 4.1) of the same order of magnitude as the accuracy of the instrumentation resulting in a large uncertainty in *K*, as was evident in the uncertainty analysis section.

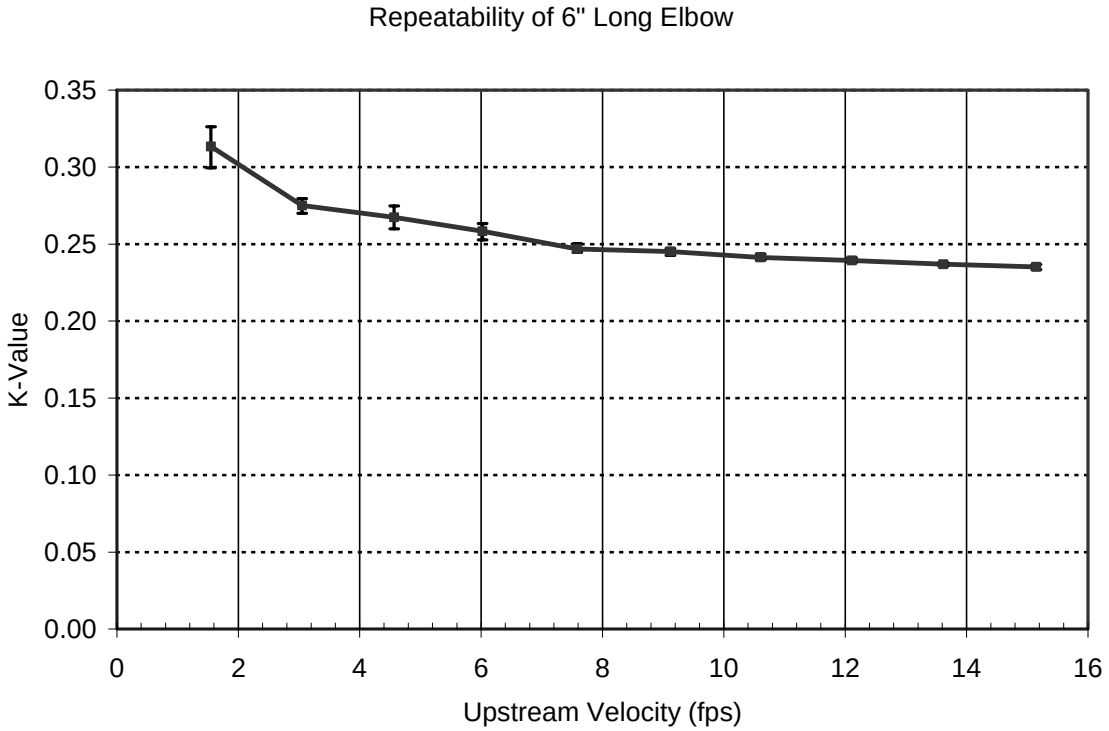

Figure 4.2. Average K-values for 5 tests on a 6-inch long elbow. The error bars show the range of measured values.

4.3. Elbows

Table 4.1 summarizes the loss coefficients obtained for 6, 8 and 10-inch elbows from the tests conducted at SAFL and from the past publications, including ASHRAE (1997).

Table 4.1. Summary of loss coefficients for elbows

Fitting	Past	SAFL		
		4 fps	**8 fps**	**12 fps**
6″ long radius elbow Weld	0.18-0.25	0.26	0.24	0.24
8″ long radius elbow Weld	0.16-0.26	0.22	0.20	0.19
10″ long radius elbow Weld	0.14-0.17	0.21	0.17	0.16
6×5″ reducing elbow (R/D = 1) Weld	------	0.36	0.33	0.33
8×6″ reducing elbow (R/D = 1) Weld	------	0.60	0.58	0.58
10×8″ reducing elbow (R/D = 1) Weld	------	0.34	0.30	0.30
5×6″ expanding elbow (R/D = 1) Weld	------	0.21	0.18	0.17
6×8″ expanding elbow (R/D = 1) Weld	------	0.17	0.14	0.13
8×10″ expanding elbow (R/D = 1) Weld	------	0.17	0.15	0.14

The past data are from Freeman (1892), Crane (1952), and Hydraulic Institute (1979). Prior to testing conducted at SAFL, no data had been collected for the reducing and expanding elbows.

The velocities in Table 4.1 refer to upstream velocities. Although K-values are smaller for expanding elbows than for reducing elbows for a given flow, the fitting head loss of expanding elbows is larger than that for reducing elbows. K-values obtained for all tested elbows are presented versus the Reynolds number in Attachment A.

4.3.1. Long Elbows

Figure 4.3 shows the average K-values of long elbows versus upstream velocity. The error bars show the range of K-values among manufacturers. All three sizes show higher values for *K* at lower velocities, and a leveling off at high velocities. K-values decrease as the size of elbow increases.

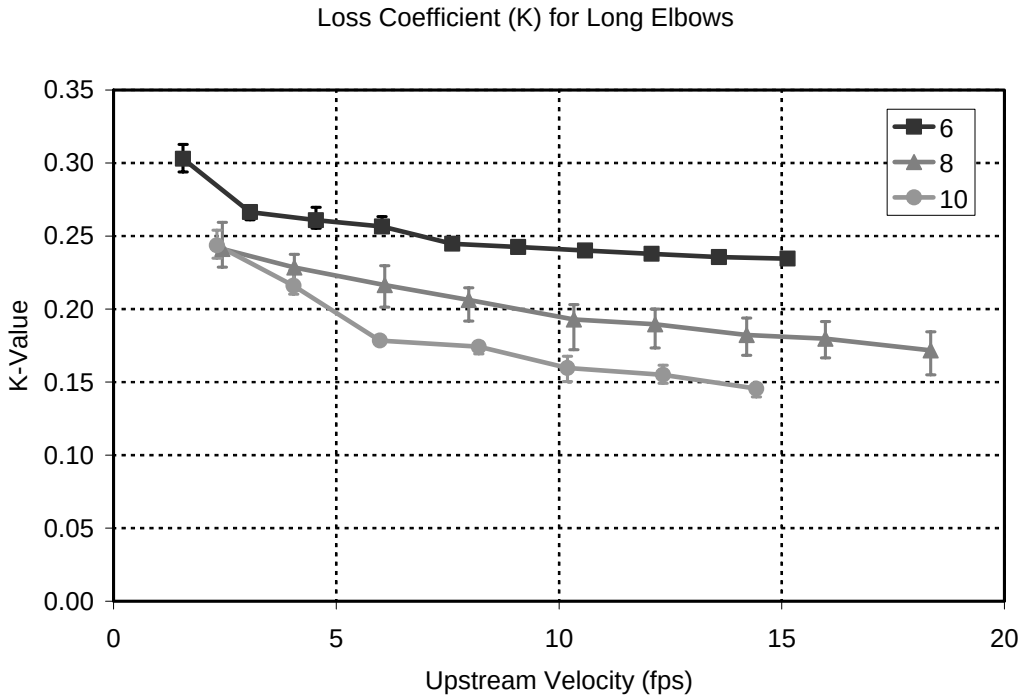

Figure 4.3. K-values of 6, 8 and 10-inch long radius elbows versus upstream velocities. Error bars show the range of measurements among the manufacturers.

The SAFL results are within the range of the K-values obtained by Rahmeyer (1999 and 2000), but slightly larger than those published in 2001ASHRAE Fundamentals. Figure 4.4 shows the 2001ASHRAE Fundamentals data and the SAFL and Rahmeyer data for upstream velocities of about 6 to 7 fps. A power function can be fit to the SAFL and Rahmeyer data explaining more than 95% of the variance. The results of these tests show that the 2001 ASHRAE Fundamentals data are slightly lower than those obtained by Rahmeyer (1999 and 2000) and SAFL.

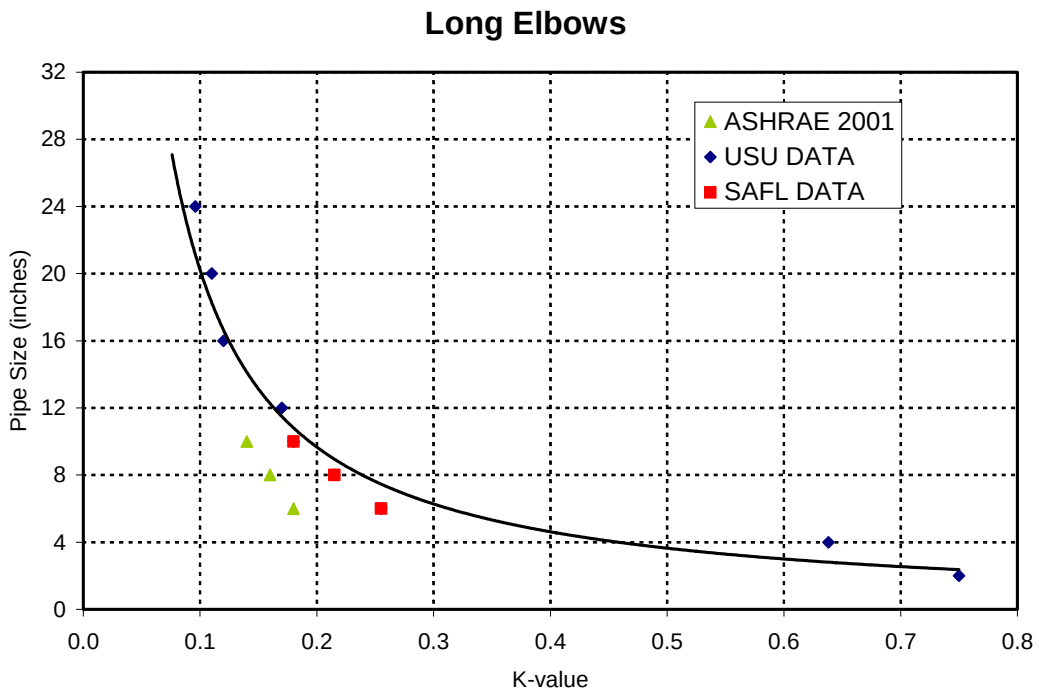

Figure 4.4. Fitting sizes versus K-values published in 2001ASHRAE Fundamentals, measured at Utah Water Research Laboratory (USU), and obtained in this study.

4.3.2. Expanding Elbows

Figure 4.5 illustrates the K-values obtained for 5×6, 6×8 and 8×10-inch long radius expanding elbows versus upstream velocities. The trends are very similar to those of the

long radius elbows (Figure 4.3). All three sizes show slightly higher values for *K* at lower velocities, and a leveling off at high velocities. The 8×10-inch expanding elbow has higher K-values than the 6×8-inch expanding elbow, showing that *K* does not simply decrease as the upstream or downstream size of the elbow increases. The results indicate that the K-value of expanding elbows varies with size and the percent expansion of the elbow.

Comparing expanding elbows with constant diameter elbows and concentric expansions, it is concluded that the loss coefficients of expanding elbows are slightly smaller than the sum of loss coefficients of long elbows and concentric expansions.

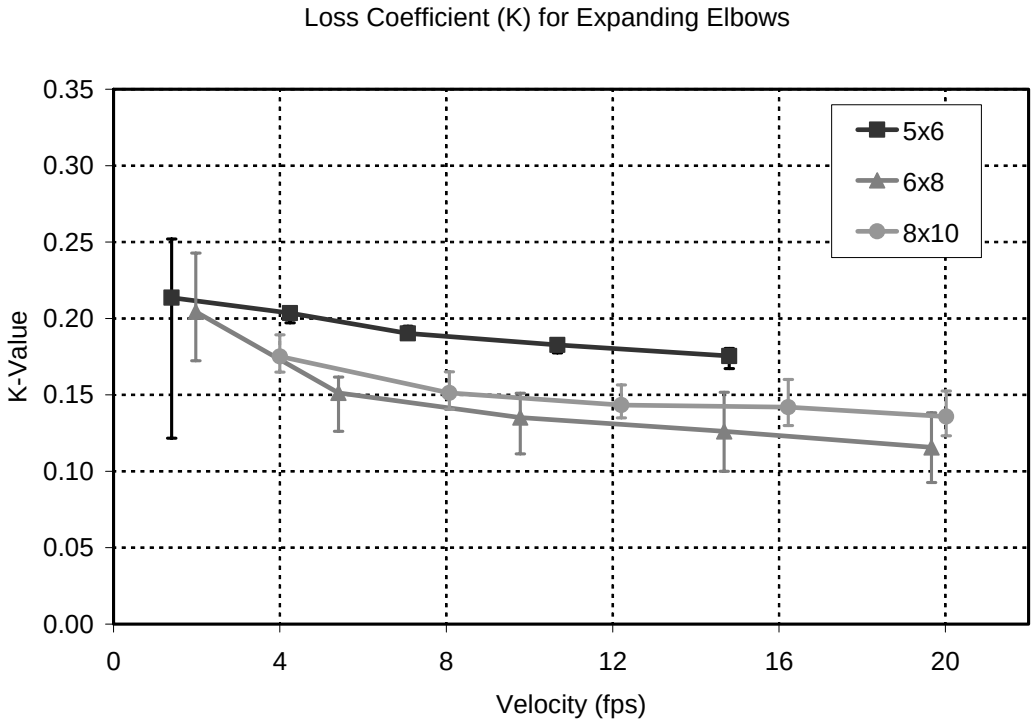

Figure 4.5. K-values of 5×6, 6×8 and 8×10-inch long radius expanding elbows versus upstream velocities. Error bars show the range of measurements among the manufacturers.

4.3.3. Reducing Elbows

Figures 4.6 shows the K-values obtained for 6×5, 8×6 and 10×8-inch long radius

reducing elbows versus upstream velocities. The trends are rather similar to those of the long radius elbows (Figure 4.3) and expanding elbows (Figures 4.5). All three sizes show significantly greater K-values at lower velocities, and a leveling off at high velocities. The 10×8-inch reducing elbow has significantly higher K-values than the 6×5-inch expanding elbow, indicating that the reducing elbow K-value is dependent on both size and the percent reduction of the elbow. The variety of the reducing elbows used in this study was too limited (only three types) to develop a relationship between the reducing elbow K-value and size and percent area reduction of the reducing elbow.

Comparing reducing elbows with constant diameter elbows and concentric reducers, it is concluded that the loss coefficients of 10×8-inch reducing elbows are relatively close to the sum of loss coefficients of 10-inch long elbows and 10×8-inch concentric reducers, while the loss coefficients of 8×6-inch reducing elbows are larger than the sum of loss coefficients of 8-inch long elbows and 8×6-inch concentric reducers.

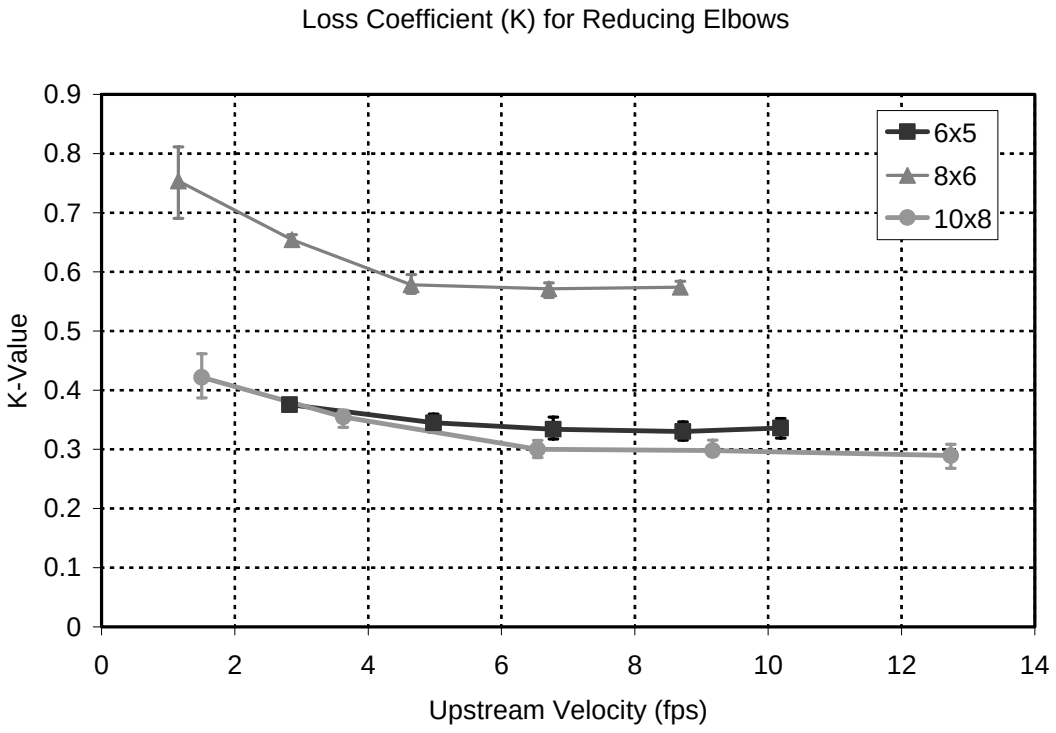

Figure 4.6. K-values of 5×6, 6×8 and 8×10-inch long radius expanding elbows versus upstream velocities. Error bars show the range of measurements among the manufacturers.

4.4. Tees

Table 4.2 summarizes the loss coefficients obtained for 6, 8 and 10-inch Tees from the tests conducted at SAFL, from the Hydraulic Institute (1979) and Miller (1990). There is a limited data available for reducing Tees. Therefore, most of the data obtained for reducing 6×6×5″, 8×8×6″ and 10×10×8″ are new with no reference for comparison. K-values obtained for all tested Tees are presented versus the Reynolds number in Attachment B.

The data in Table 4.2 are divided into three types of flows: 100% Branch, 100% Line and 100% Mix. The 100% Branch occurs when all the flow entering the straight section of a Tee flows through the branch, i.e. Q_2 in Figure 3.1 is zero. The 100% Line refers to no flow entering through the branch, i.e. Q_3 in Figures 3.1 and 3.2 is zero. The 100% Mix occurs when water only enters from the branch, i.e. Q_1 in Figure 3.2 is zero. In past publications, it was indicated that 100% Branch and 100% Mix flows should have the same head loss coefficients. However, the results obtained from this study show a significant difference between the two, primarily due to the different geometries of the two conditions. Test results from Utah Water Research Laboratory also indicate a difference between the 100% Branch and 100% Mix flow conditions.

4.4.1. Branching Tees

Figures 4.7 and 4.8 show the K-values obtained for the branching flow leg and the straight-thru flow leg of 6, 8, and 10-inch branching Tees. The K-value of the branching leg varies from 0.43 to 0.7 for the three sizes, with larger K-values for smaller size Tees. The branching K-value increases with decreasing flow and reaches minimum when 75% of the inflow exits through the branching leg.

Figure 4.8 gives the K-values in the straight-thru flow leg of the branching Tee. The maximum K-value is 0.13 for 100% of flow through the straight leg. The trend is more or less similar to the one for the branching leg, increasing for low and high flows through the straight leg. The results also show small negative K-values (-0.01 to -0.03) when 50% to 75% of water flows through the straight leg. Very small K-values, about 0.01 to

0.04, were obtained for 12 and 24-inch Tees by the Utah Water Research Laboratory (2001). Idelchik (1994) indicated a K-value of zero under these conditions. The SAFL test results, however, show a bias in giving very small negative numbers, especially when 75% of water flows through the straight leg.

Table 4.2. Summary of loss coefficients for Tees

Fitting	Past	SAFL
6″ Weld Tee, 100% Branch	0.62	0.56
6″ Weld Tee, 100% Line	0.12	0.12
6″ Weld Tee, 100% Mix	0.62	0.88
8″ Weld Tee, 100% Branch	0.58	0.53
8″ Weld Tee, 100% Line	0.10	0.08
8″ Weld Tee, 100% Mix	0.58	0.70
10″ Weld Tee, 100% Branch	0.53	0.52
10″ Weld Tee, 100% Line	0.09	0.06
10″ Weld Tee, 100% Mix	0.53	0.77
6×6×5″ Weld Reducing Tee, 100% Branch	0.87	0.78
6×6×5″ Weld Reducing Tee, 100% Line	-----	0.08
6×6×5″ Weld Reducing Tee, 100% Mix	1.4	0.83
8×8×6″ Weld Reducing Tee, 100% Branch	0.96	0.59
8×8×6″ Weld Reducing Tee, 100% Line	-----	0.06
8×8×6″ Weld Reducing Tee, 100% Mix	1.7	0.85
10×10×8″ Weld Reducing Tee, 100% Branch	0.92	0.78
10×10×8″ Weld Reducing Tee, 100% Line	-----	0.06
10×10×8″ Weld Reducing Tee, 100% Mix	1.5	0.77

A negative K-value is clearly unrealistic, implying a non-Bernoulli gain in Energy as the flow traverses the fitting. The impossibility of such an energy gain suggests an artifact in the testing procedure. Fitting head loss is determined indirectly by subtracting the estimated downstream pipe friction loss from the measured total pressure across the fitting and the pipe. As explained earlier, the inclusion of a downstream section of pipe in the fitting loss measurement is necessitated by the secondary flows and non-uniform velocities downstream of the fitting, thus rendering pressure measurement directly downstream of the fitting useless. Subsequently, any difference between the actual and assumed pipe friction loss becomes part of the total head loss caused by the fitting. It is hardly surprising that a pipe loss estimate based on data obtained for well developed,

uniform pipe flow might be in error due flow effects of the fitting, the very reason the downstream pipe was included in the first place. Unfortunately, there is no obvious solution to this dilemma. Should there actually be less friction head loss in the downstream pipe than the known flow rate would imply based on well developed flow conditions, the pipe loss will be overestimated and the fitting loss (and the associated K-value) underestimated? For K-values close to zero, such an underestimation could produce negative K-values and may indeed explain those shown here. Nevertheless, K-values are too small that for any practical purposes and can be assumed zero.

The K-values shown in Figures 4.7 and 4.8 are average values over a range of flows. The error bars show the range of K-values among the fittings tested from four manufacturers.

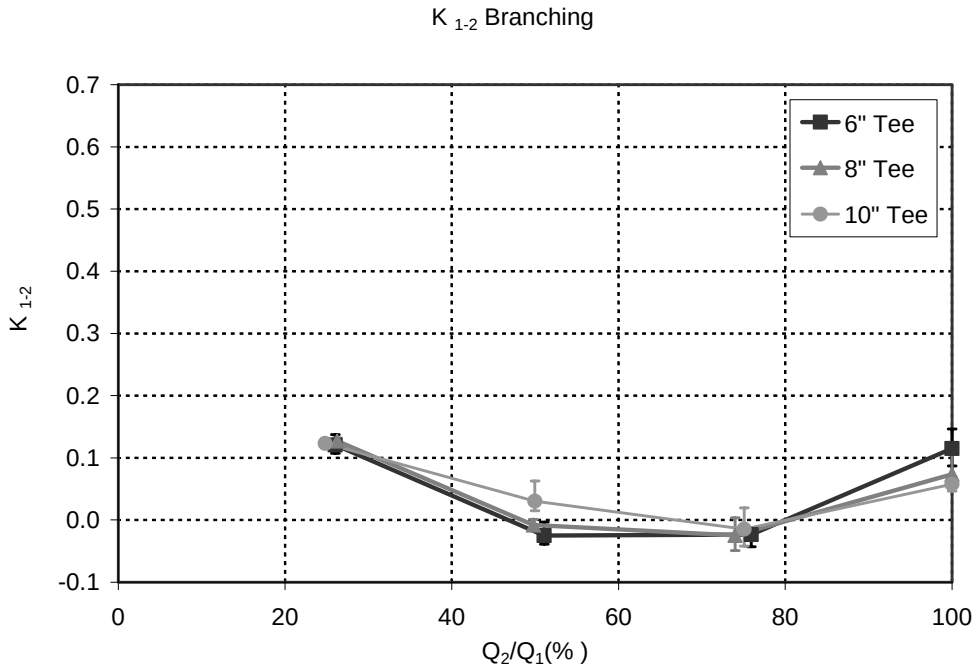

Figure 4.7. K-values of the branching leg of 6, 8, and 10-inch branching Tees versus the percentage flow through the branching leg. Error bars show the range of measurements among the manufacturers.

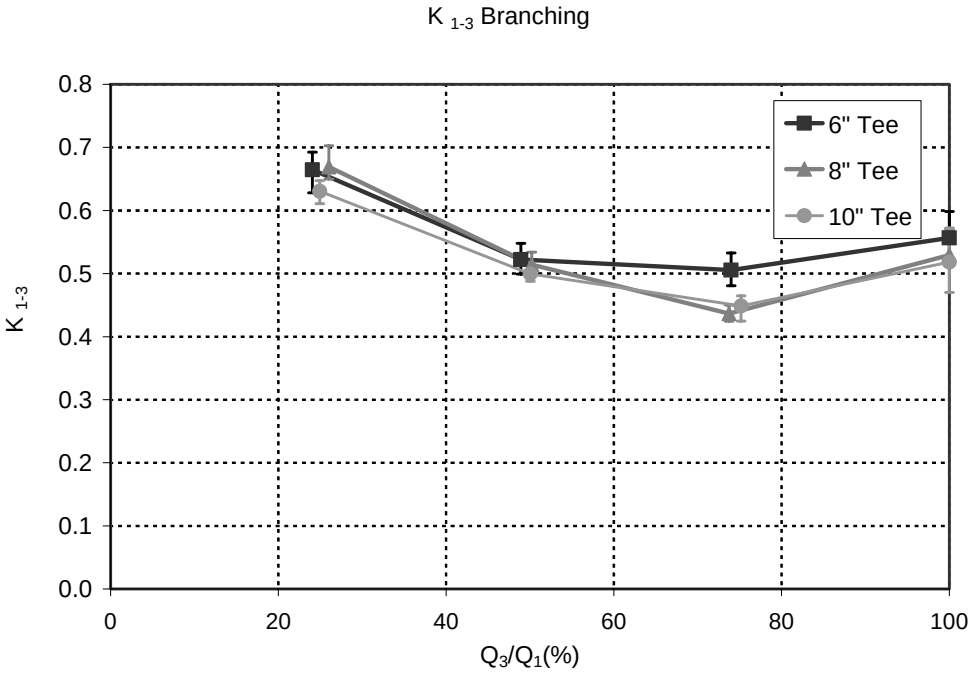

Figure 4.8. K-values of the straight-thru leg of 6, 8, and 10-inch branching Tees versus the percentage flow through the straight leg. Error bars show the range of measurements among the manufacturers.

4.4.2. Mixing Tees

Figures 4.9 and 4.10 demonstrate the K-values obtained for flows through the branching leg and the straight-thru leg of 6, 8, and 10-inch mixing Tees. The K-value of the branching leg (Figure 4.9) varies from 0.5 to 1.0 for the three sizes when more then 50% of the flow is through the branching leg of the Tee. When 25% of the total flow enters from the branching leg, the K-values become negative. The gain in energy occurs due to the mixing of lower flow from the branch leg with high energy flow from the straight leg. Similar phenomena were experienced at Utah Water Research Laboratory while testing the 12 and 16-inch Tees.

The K-values of the straight leg in a mixing Tee span a large range, from over 1 at 25% flow to about 0.12 when 100% of water flows through the straight leg. The results are in general agreement with the results of Utah Water Research Laboratory.

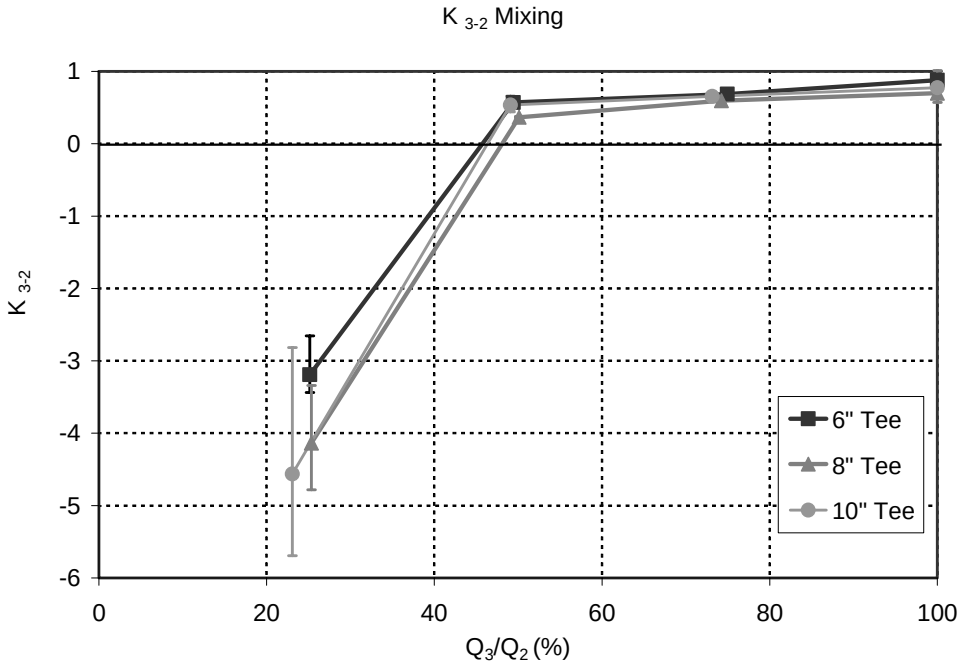

Figure 4.9. K-values of the branching leg of 6, 8, and 10-inch mixing Tees versus the percentage flow through the branching leg. Error bars show the range of measurements among the manufacturers.

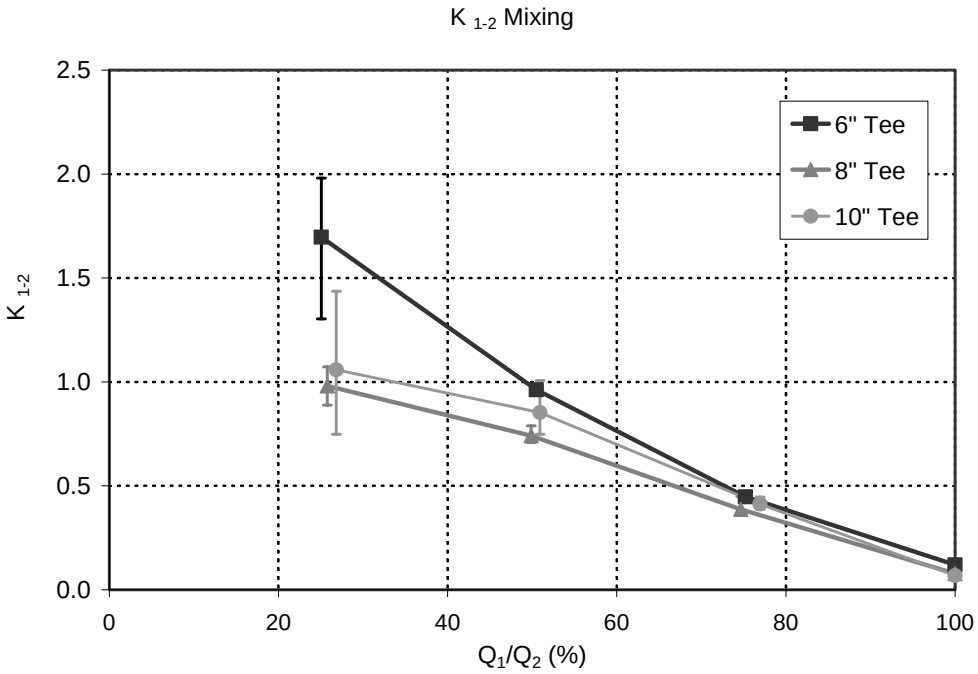

Figure 4.10. K-values of the straight leg of 6, 8, and 10-inch mixing Tees versus the percentage flow through the straight leg. Error bars show the range of measurements among the manufacturers.

4.4.4. Reducing Branching Tees

Figures 4.11 and 4.12 show the K-values obtained for the branching flow leg and the straight-thru flow leg, respectively, of 6×6×5, 8×8×6, and 10×10×8-inch branching Tees. The branching leg of these Tees functions rather like a reducing elbow. The K-value of the branching leg (Figure 4.11) varies from 0.3 to 0.85 for the three sizes. The K-values vary with size and the percent of flow in the branching leg of the Tee. The K-values approach their minimum as 50% or 75% of flow exits through the branch, and reach maximum when 100% of flow exits through the branch.

Figure 4.12 gives the K-values in the straight-thru flow leg of the branching Tee. The maximum K-value occurs when 25% of flow exits through the straight leg. Similar to regular branching Tees, very small negative K-values were exhibited for the medium range flows exiting through the straight leg. The data are nearly identical to those obtained for simple branching Tees (Figure 4.7).

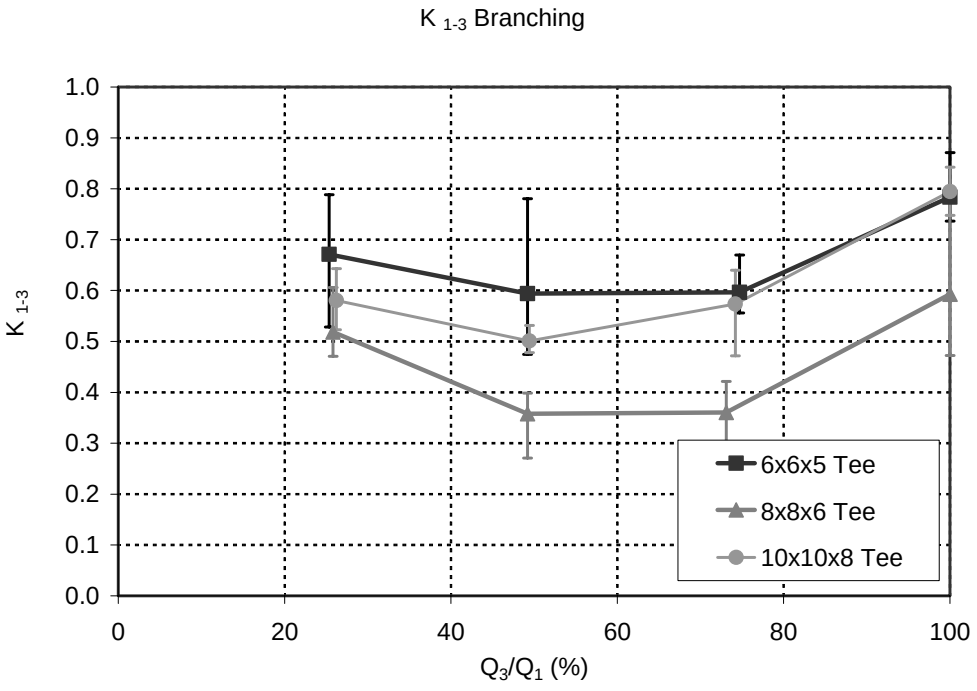

Figure 4.11. K-values of the branching leg of 6×6×5, 8×8×6, and 10×10×8 inch branching Tees versus the percentage flow through the branching leg. Error bars show the range of measurements among the manufacturers.

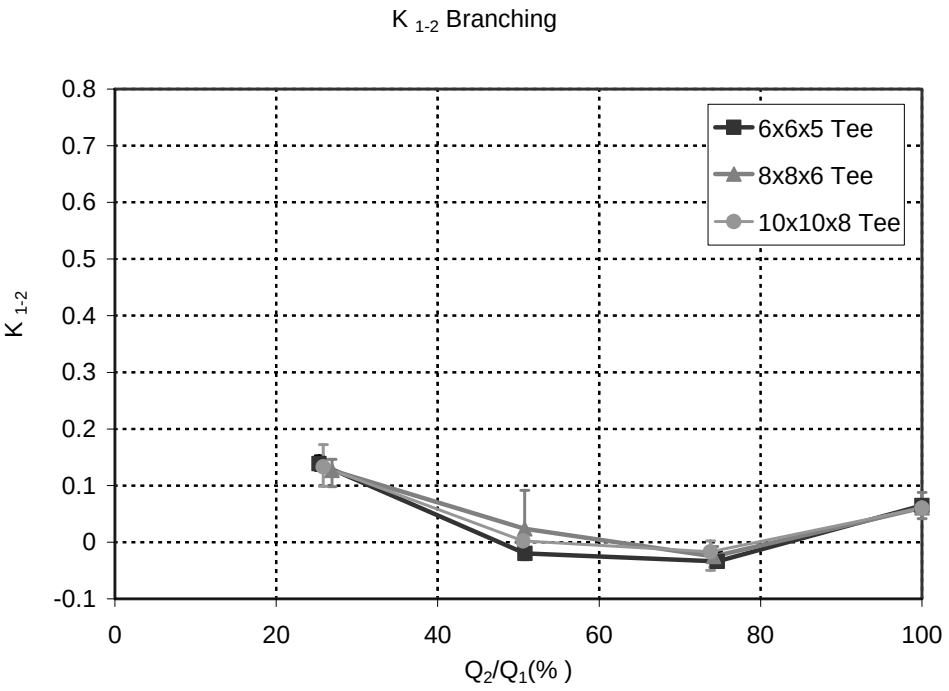

Figure 4.12. K-values of the straight leg of 6×6×5, 8×8×6, and 10×10×8-inch branching Tees versus the percentage flow through the straight leg. Error bars show the range of measurements among the manufacturers.

4.4.5. Expanding Mixing Tees

Figures 4.13 and 4.14 illustrate the K-values obtained for the branching flow leg and the straight-thru flow leg, respectively, of 6×6×5, 8×8×6, and 10×10×8-inch mixing Tees. The branching leg of these Tees functions rather like an expanding elbow. The K-value of the branching leg (Figure 4.13) varies from 0.3 to 1 for the three sizes, when 50% or greater flow enters the fitting through the branch. For a mixing percentage of 25% and lower, the K-values become negative, similar to regular mixing Tees. The K-values vary with size and the percent expansion in the mixing leg of the Tee.

Figure 4.14 gives the K-values in the straight-thru flow leg of the mixing Tee. Similar to simple Tee, K-values varied from more than 1 at 25% mixing to less than 0.1 with 100% of the water traversing the straight leg.

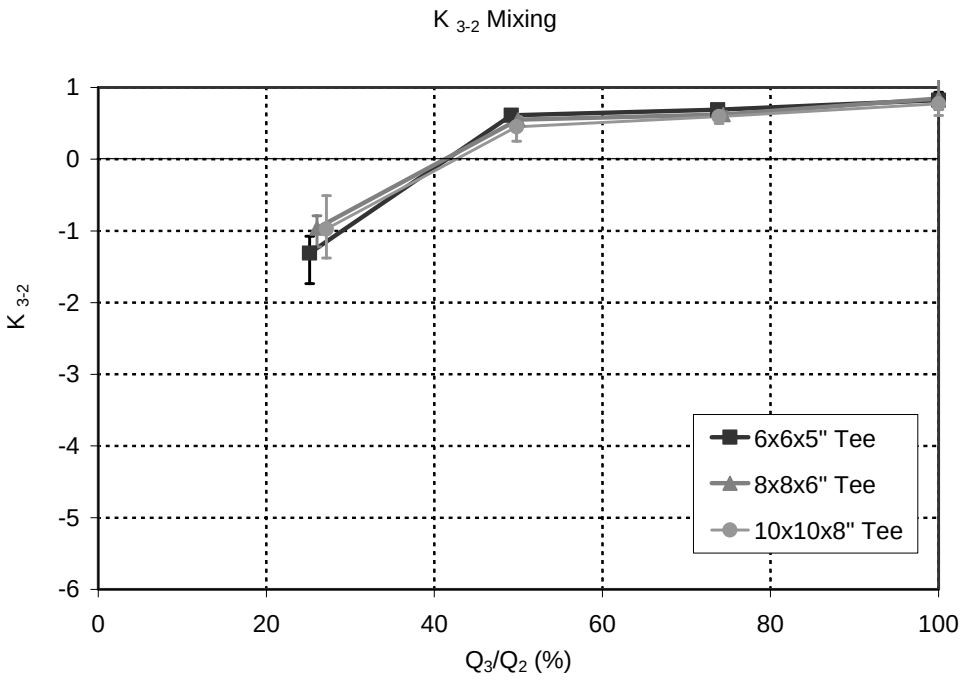

Figure 4.13. K-values of the branching leg of 6×6×5, 8×8×6, and 10×10×8 inch mixing Tees versus the percentage flow through the branching leg. Error bars show the range of measurements among the manufacturers.

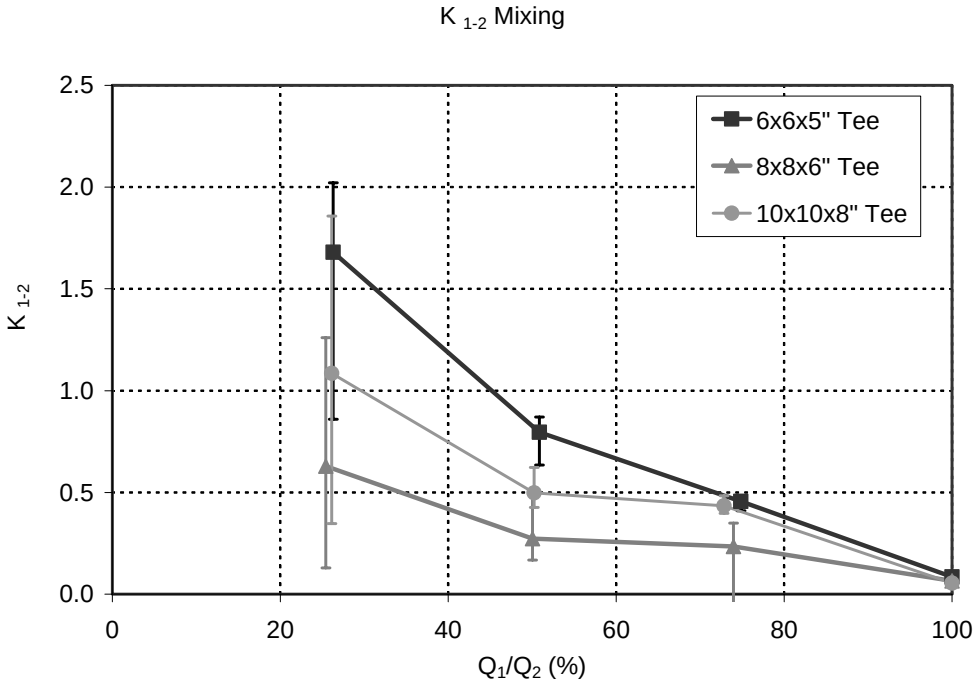

Figure 4.14. K-values of the straight leg of 6×6×5, 8×8×6, and 10×10×8 inch mixing Tees versus the percentage flow through the straight leg. Error bars show the range of measurements among the manufacturers.

4.5. Reducers and Expansions

Table 4.3 summarizes the loss coefficients obtained for 6, 8 and 10-inch reducers and expansions. There is no previous data available for the reducers and expansions listed in the table. Therefore, there are no previous data for comparison. The velocities shown in the last three columns represent the upstream velocities. The values marked by asterisks were extrapolated from the tests. The extrapolations were necessitated by available head limitation as explained earlier.

Table 4.3. Summary of loss coefficients for reducers and expansions

Fitting	Past	SAFL		
		4 fps	**8 fps**	**12 fps**
6×4″ concentric reducer, Weld	------	0.62	0.54*	0.53*
8×6″ concentric reducer, Weld	------	0.31	0.28	0.26*
10×8″ concentric reducer, Weld	------	0.16	0.14	0.14
4×6″ concentric expansion, Weld	------	0.28	0.28	0.29
6×8″ concentric expansion, Weld	------	0.15	0.12	0.11
8×10″ concentric expansion, Weld	------	0.11	0.09	0.08

4.5.1. Reducers

Figure 4.15 illustrates the K-values obtained for 6×4, 8×6 and 10×8-inch concentric reducers versus upstream velocities. The results show a decrease and a leveling off of k-value with increasing velocity. K-value is nearly independent of velocity for the 10×8 concentric reducer. The results indicate a strong dependence of the K-value on size of the reducer.

4.5.2. Expansions

Figures 4.16 illustrates the K-values obtained for 4×6, 6×8 and 8×10-inch concentric expansions versus upstream velocities. The results show that the expansions K-values vary moderately at low velocities and level off at high velocities. Even though the K-values of expansions are smaller than the K-values of reducers, the fitting head loss of expansions are larger than the fitting head loss of reducers for a given flow (Figure 4.17). This is a by-product of using the upstream velocity to define the K-value.

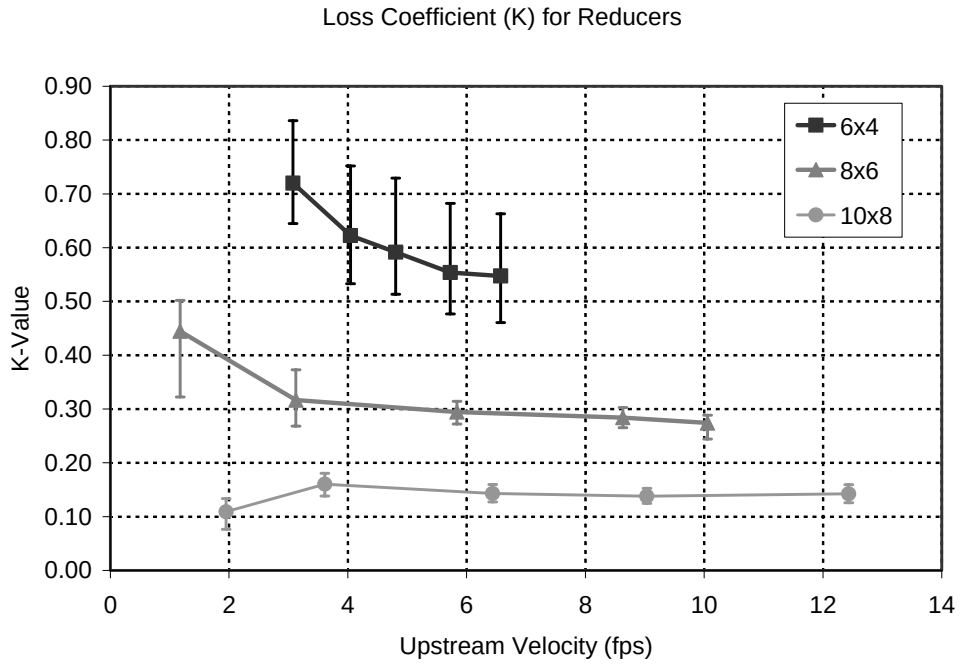

Figure 4.15. K-values of 6×4, 8×6, and 10×8-inch concentric reducers versus upstream velocities. Error bars show the range of measurements among the manufacturers.

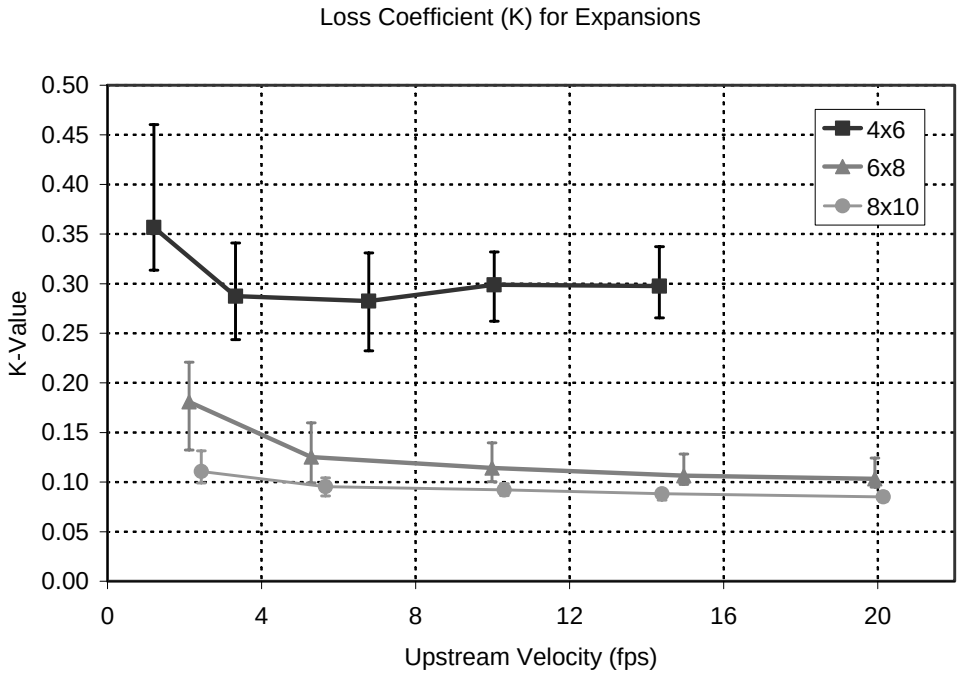

Figure 4.16. K-values of 4×6, 6×8, and 8×10-inch concentric expansions versus upstream velocities. Error bars show the range of measurements among the manufacturers.

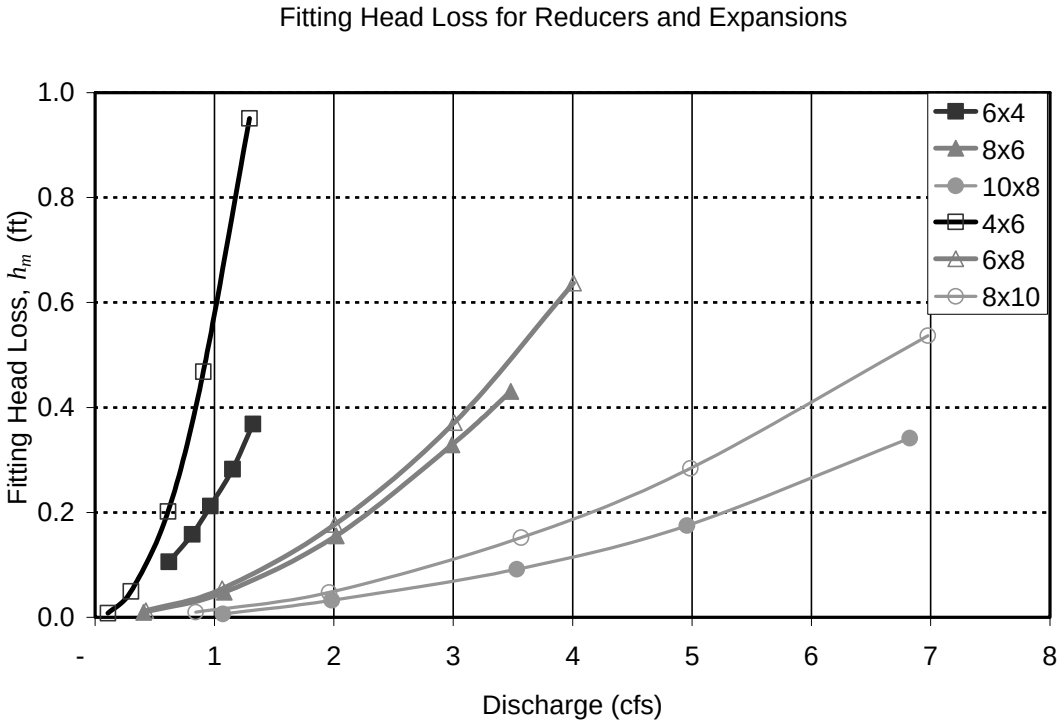

Figure 4.17. Comparison of the fitting head loss of 4×6, 6×8, and 8×10-inch concentric expansions with the fitting head loss of 6×4, 8×6, and 10×8-inch concentric reducers for a given flow.

5. Uncertainty Analysis

Uncertainty is a property of testing that depends on all contributing measurements. The analysis of uncertainties is a vital part of any scientific experiment. To determine the potential effects of errors associated with the measurement of all the parameters affecting the K-values as described in section 3, an uncertainty analysis was conducted. In this analysis, we examined the uncertainties in the estimation of the fitting head loss, h_m, and then that in the K-value calculations.

Pressure and flow were measured using the pressure transducer and the orifice flow meters. However, the orifice flow meters were calibrated using the SAFL weigh tanks, stop watch and pressure transducers. For the parameters which were measured repeatedly, e.g. pressure and flow, the error was estimated at the 95% confidence level using the standard deviation of the measurements. For the parameters which were measured only once, e.g. time and pipe length, the accuracy of the instrument was assumed to be the measurement error at the 95% confidence level.

The errors associated with all the above parameters propagate when estimating the fitting head loss and the K-value. To determine the uncertainty in the estimate of the fitting head loss, equation 3.4 can be rearranged as follows

$$h_m = h_1(\Delta P) - h_2(Q, D_1, D_2) - h_3(L_1, L_2, Q) \tag{5.1}$$

where h_1 is the head associated with the pressure differential between points 1 and 2, h_2 is the difference between the velocity heads and h_3 is the sum of friction head losses.

$$h_1 = \left(\frac{P_1 - P_2}{\gamma} \right) \tag{5.2}$$

$$h_2 = \frac{Q^2}{2g} \left(\frac{1}{A_2^2} - \frac{1}{A_1^2} \right) \tag{5.3}$$

$$h_3 = \sum_i L_i \, f_i(Q) \tag{5.4}$$

Since h_3 is based on measurements in straight pipe before testing the fitting, one can assume that the errors associated with h_1, h_2 and h_3 are independent of each other, and the errors associated with the fitting head loss, h_m, can be expressed as follows:

$$\delta h_m = \sqrt{\delta h_1^{\,2} + \delta h_2^{\,2} + \delta h_3^{\,2}} \tag{5.5}$$

In equation 5.5, δh_1, δh_2 and δh_3 are the uncertainties associated with the differential pressure measured by the transducer, the change in the velocity head and the friction loss through the pipes, respectively. The error associated with h_1 is stated by the manufacturer to be 0.25% of the full scale. It was actually determined to be better than 0.1% of the full scale range as a result of the auto-calibration component of the test procedure. The error associated with h_2 is a function of the errors in measuring the pipe diameters and the flow, and it can be estimated as

$$\delta h_2 = \left|\frac{\partial h_2}{\partial D_1}\right| \delta D_1 + \left|\frac{\partial h_2}{\partial D_2}\right| \delta D_2 + \left|\frac{\partial h_2}{\partial Q}\right| \delta Q \tag{5.6}$$

The error associated with h_3 is a function of the pipe length and the flow as follows

$$\delta h_3 = \left|\frac{\partial h_3}{\partial L_1}\right| \delta L_1 + \left|\frac{\partial h_3}{\partial L_2}\right| \delta L_2 + \left|\frac{\partial h_3}{\partial Q}\right| \delta Q \tag{5.7}$$

By determining the errors associated with measuring D_1, D_2, L_1, L_2 and Q at the 95% confidence level and by estimating the values of the partial differential of h_2 and h_3 with respect to D_1, D_2, L_1, L_2 and Q, one can determine the potential error associated with h_2 and h_3 and subsequently the uncertainty in estimating the fitting head loss, δh_m. Consequently, using equation 3.1, the uncertainties in estimating the head loss coefficient, K, of a given fitting can be determined as follows.

$$\delta K = \left|\frac{\partial K}{\partial h_m}\right| \delta h_m + \left|\frac{\partial K}{\partial D_1}\right| \delta D_1 + \left|\frac{\partial K}{\partial Q}\right| \delta Q \tag{5.8}$$

Tables 5.1 to 5.7 give the uncertainties associated with each parameter for 6, 8 and 10-inch elbows, a 6x4-inch reducer and a 4x6-inch expansion, and a 6-inch branching Tee,

respectively, under all flow conditions. The results show that the error associated with flow, $\delta Q/Q$, is about 1% and decreases as flow increases. Only at low flows, e.g. 0.3 cfs, $\delta Q/Q$ exceeds 2% and even becomes 13% for a 4x6-inch concentric expansion. The repeatability testing produced a range of K-values which was smaller than the calculated uncertainty in the estimate, lending support to this uncertainty analysis.

The errors associated with flow and pressure measurements produced uncertainties in estimating the fitting head loss, $\delta h_m/h_m$, and the K-value exceeding 2%. The greatest uncertainties occur at low flows, due to small pressure differential values, a fact supported by the repeatability testing. At low flows, where the velocities are small, the total head loss and the pipe friction loss are very small and of comparable magnitude, causing the difference between the two to yield a value for the fitting loss, h_m, of the same order of magnitude as the accuracy of the instrumentation resulting in a large uncertainty in the K-value. For example in Table 5.5 for a 4x6-inch expansion, at a flow of 0.11 cfs the fitting head loss is 0.007 ft and the error associated with the fitting head loss is 0.005 ft, resulting in 97% uncertainty in the estimate of the K-value.

Tables 5.6 and 5.7 give the uncertainties for the K-values of the branching and straight legs of a 6-inch branching Tee with 50% flow through branches. As was presented in section 5, the tests showed negative K-values for the straight leg when 50% of the flow exited through the straight leg. The K-values were very small, i.e. -0.03. The potential error associated with the K-value is about 0.04 resulting in more than 100% uncertainty. Under such circumstances, introducing uncertainty as a percentage of the parameter value becomes meaningless. For this specific case, the K-value is very small and can be assumed to be zero for design purposes.

The results presented in Tables 5.1 to 5.7 were obtained by assuming no error in measuring the pipe diameter and length. The error in pipe length does not affect the 6-inch elbow, but it does affect the 8 and 10-inch elbows. The effect of pipe diameter, however, is more substantial. A 0.002 ft error in measuring the 6-inch pipe diameter increases the uncertainties in the K-value by 14%, i.e. by about 0.03. The same error in measuring the 8-inch pipe diameter increases the uncertainties in the K-value by 20%, i.e.

by about 0.01.

The results of the analysis can be summarized as follows:

- For elbows and reducers, the main source of uncertainty is the friction loss. Using the Darcy-Weisbach equation would further adversely affect the uncertainty in the estimate of the K-value.
- For expansions and Tees with a 50% flow through the branch, the main source of error is the change in the velocity head.
- The uncertainty in the estimate of the K-value decreases as flow increases.
- The uncertainty in the estimate of the K-value decreases as the size of the fitting increases.
- In most cases and at higher flows, the K-value varies by less than 0.04.
- Except for a few cases, the variability in the K-values obtained for the fittings from the manufacturers was larger than the uncertainties in the estimate of the K-value.

Table 5.1. Results of the error analysis conducted on 6-inch long elbows.

Q (cfs)	h (ft)	h_m (ft)	$\delta Q/Q$	δh_3 (ft)	δh_m (ft)	K	δK
0.304	0.030	0.011	2.43%	0.001	0.001	0.299	0.045
0.598	0.101	0.037	1.41%	0.002	0.002	0.261	0.025
0.896	0.214	0.081	1.15%	0.003	0.004	0.255	0.019
1.202	0.372	0.146	1.07%	0.005	0.009	0.256	0.022
1.507	0.556	0.216	1.05%	0.008	0.009	0.241	0.016
1.800	0.777	0.310	1.07%	0.011	0.011	0.242	0.015
2.096	1.033	0.418	1.10%	0.014	0.015	0.241	0.015
2.388	1.312	0.536	1.12%	0.019	0.020	0.238	0.015
2.695	1.638	0.673	1.13%	0.023	0.024	0.235	0.015
2.994	1.996	0.831	1.18%	0.030	0.031	0.235	0.015

Q Discharge
h Measured pressure differential
h_m Fitting head loss
δQ Error associated with flow
δh_3 Error associated with the friction head loss
δh_m Uncertainty associated with estimating the fitting head loss
δK Uncertainty associated with estimating the K-value.

Table 5.2. Results of the error analysis conducted on 8-inch long elbows.

Q (cfs)	h (ft)	h_m (ft)	$\delta Q/Q$	δh_3 (ft)	δh_m (ft)	K	δK
0.881	0.071	0.026	0.77%	0.001	0.002	0.257	0.023
1.426	0.170	0.063	0.51%	0.001	0.003	0.239	0.012
2.153	0.362	0.136	0.59%	0.003	0.006	0.226	0.012
2.745	0.563	0.210	0.59%	0.004	0.005	0.215	0.008
3.591	0.898	0.323	0.54%	0.006	0.012	0.193	0.009
4.226	1.224	0.451	0.52%	0.008	0.009	0.195	0.006
4.870	1.582	0.581	0.45%	0.009	0.017	0.189	0.007
5.503	1.983	0.734	0.60%	0.015	0.027	0.187	0.009
6.330	2.516	0.904	0.46%	0.017	0.038	0.174	0.009

Q Discharge
h Measured pressure differential
h_m Fitting head loss
δQ Error associated with flow
δh_3 Error associated with the friction head loss
δh_m Uncertainty associated with estimating the fitting head loss
δK Uncertainty associated with estimating the K-value.

Table 5.3. Results of the error analysis conducted on 10-inch long elbows.

Q (cfs)	h (ft)	h_m (ft)	$\delta Q/Q$	δh_3 (ft)	δh_m (ft)	K	δK
1.087	0.037	0.014	1.67%	0.001	0.001	0.232	0.025
2.274	0.146	0.058	1.08%	0.002	0.003	0.212	0.016
3.327	0.286	0.107	1.17%	0.004	0.005	0.183	0.013
4.435	0.486	0.180	0.78%	0.005	0.006	0.174	0.008
5.463	0.711	0.260	0.92%	0.008	0.014	0.166	0.012
6.546	0.972	0.341	0.69%	0.009	0.016	0.152	0.009
7.628	1.284	0.447	0.74%	0.012	0.017	0.146	0.008

Q Discharge
h Measured pressure differential
h_m Fitting head loss
δQ Error associated with flow
δh_3 Error associated with the friction head loss
δh_m Uncertainty associated with estimating the fitting head loss
δK Uncertainty associated with estimating the K-value.

Table 5.4. Results of the error analysis conducted on a 6x4-inch reducer.

Q (cfs)	h (ft)	h_m (ft)	$\delta Q/Q$	δh_3 (ft)	δh_m (ft)	K	δK
0.629	1.264	0.134	1.38%	0.013	0.022	0.880	0.032
0.822	2.114	0.202	1.23%	0.019	0.035	0.778	0.030
0.955	2.824	0.258	1.12%	0.023	0.041	0.738	0.025
1.151	4.038	0.337	1.07%	0.032	0.057	0.662	0.024
1.346	5.484	0.449	1.09%	0.043	0.078	0.646	0.024

Table 5.5. Results of the error analysis conducted on a 4x6-inch expansion.

Q (cfs)	h (ft)	h_m (ft)	$\delta Q/Q$	δh_2 (ft)	δh_m (ft)	K	δK
0.106	-0.006	0.007	13.50%	0.005	0.005	0.333	0.322
0.300	-0.058	0.053	2.67%	0.007	0.008	0.310	0.061
0.616	-0.267	0.214	1.37%	0.016	0.016	0.296	0.031
0.920	-0.583	0.501	1.34%	0.035	0.035	0.311	0.030
1.294	-1.198	0.968	1.04%	0.053	0.055	0.303	0.024

Q Discharge
h Measured pressure differential
h_m Fitting head loss
δQ Error associated with flow
δh_2 Error associated with the change in velocity head
δh_3 Error associated with the friction head loss
δh_m Uncertainty associated with estimating the fitting head loss
δK Uncertainty associated with estimating the K-value.

Table 5.6. Results of the error analysis conducted on a 6-inch branching Tee (K_{13}) at 50% flow.

Q (cfs)	h (ft)	h_m (ft)	$\delta Q/Q$	δh_2 (ft)	δh_m (ft)	K	δK
0.298	-0.001	0.019	3.05%	0.003	0.003	0.551	0.123
1.013	-0.030	0.196	1.09%	0.013	0.013	0.498	0.045
1.598	-0.111	0.481	1.05%	0.031	0.031	0.491	0.042
2.304	-0.304	0.994	1.09%	0.065	0.068	0.488	0.044
2.994	-0.486	1.614	1.20%	0.122	0.122	0.469	0.047

Table 5.7. Results of the error analysis conducted on a 6-inch branching Tee (K_{12}) at 50% flow.

Q (cfs)	h (ft)	h_m (ft)	$\delta Q/Q$	δh_2 (ft)	δh_m (ft)	K	δK
0.298	-0.020	-0.001	3.05%	0.003	0.004	-0.043	0.112
1.013	-0.243	0.001	1.09%	0.013	0.026	0.001	0.067
1.598	-0.630	-0.028	1.05%	0.031	0.036	-0.029	0.037
2.304	-1.287	-0.069	1.09%	0.067	0.083	-0.034	0.042
2.994	-2.324	-0.136	1.20%	0.122	0.135	-0.040	0.041

Q Discharge
h Measured pressure differential
h_m Fitting head loss
δQ Error associated with flow
δh_2 Error associated with the change in velocity head
δh_m Uncertainty associated with estimating the fitting head loss
δK Uncertainty associated with estimating the K-value.

6. Characterization of Fittings

For each type, size and manufacturer, one fitting was sliced at its mid-plane. The dimensions of the sliced fittings were then measured[1].

The inlet and outlet diameter of all fitting tested were checked by a caliper accurate to 0.001 inch. The inlet and outlet diameters and wall thicknesses of all fittings were measured in both X and Y directions. Average values are shown in Tables 6.1 to 6.3. In general, the wall thickness of all long elbows, Tees and concentric reducers were constant along the center line, but for reducing elbows and reducing Tees, the wall thickness varied slightly. From the tables, it is evident that the radius at the shoulder of the fittings, R, varied significantly among the vendors.

In most cases, the inlet and outlet internal diameters (I.D.) of the fittings were machined to meet the nominal dimensions and to match the upstream and downstream pipe ID. The internal surface transition, Tc, of the fittings is given in two classes:

a smooth transition
b sharp transition

The transitions of reducing elbows and reducing Tees were sharp which causes additional local head loss.

The internal surface roughness of the fittings was characterized. The internal surface of all fittings was painted and thus difficult to characterize. Therefore, roughness classification was qualitative and comparative as follows:

1 smooth surface with no casting imperfections, scabs and sand scale.
2 smooth surface with a few imperfections.
3 rough and sharp transition of the surface or wavy.

The Tees have different shape configurations (shown in Figure 6.1) and fall into three

[1] All samples used to characterize the geometry and roughness were marked with a label cross-referenced to results in the report, packed in corrosion-protective packing materials, and prepared for long-term storage. They will ultimately be stored at a location designated by TC 6.1.

categories:

1 Tees with a spherical shape.

3 Tees with a cylindrical shape.

2 Tees with shapes Between a cylindrical and a spherical shape.

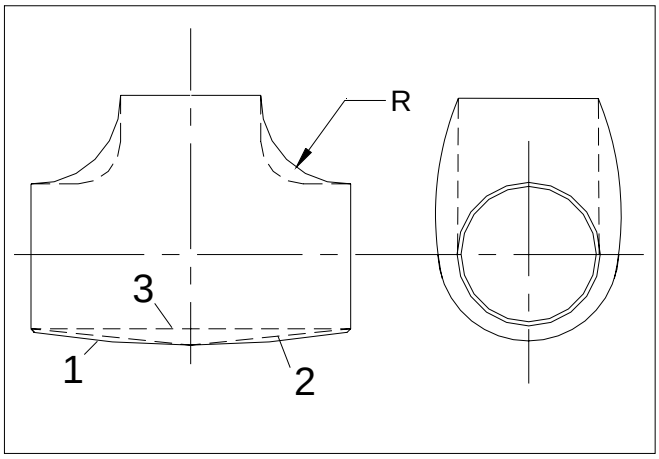

Figure 6.1. Different shapes for the Tee fittings

To visualize the disparity among manufacturers, the photos of concentric reducers have been provided in Appendix D.

Table 6.1. Dimensions and characteristics of 6-inch fittings

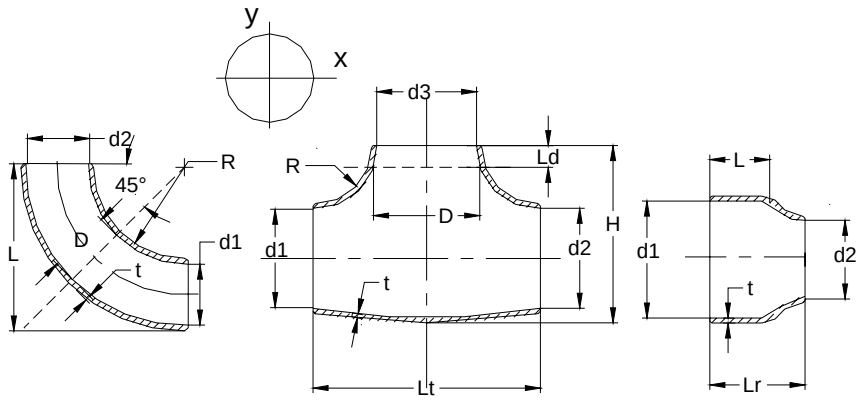

Rank = comparison index of the surface roughness among the manufacturers with 1 being smooth and 4 being rough

Rc = roughness index

Tc = transition index

6" Fitting									
		Dimensions (in)							
		x	y	x	y	x	y	x	y
Vendor		**C**		**B**		**A**		**D**	
Elbow	d1	6.012	6.02	6.051	6.017	6.072	6.009	6.048	6.074
	d2	6.066	6.062	6.026	6.038	6.03	6.058	6.062	6.03
	R	5.76		5.634		5.585		5.71	
	D	6.027		6.037		5.92		6.056	
	t	0.320		0.310		0.35		0.303	
	Rc	2		1		2		2	
	Rank	2		1		4		3	
	Tc	a		a		a		a	
Vendor		**G**		**B**		**A**		**F**	
Reducing Elbow	d1	6.076		6.076		5.91		6.05	
	d2	5.072		5.06		4.97		5.05	
	D	6.038		6.027		5.536		6.026	
	t	0.31		0.33		0.35		0.31	
	Rc	1		2		1		2	
	Rank	1		3		2		4	
	Tc	b		b		b		b	

6" Fitting continued									
Vendor		**C**		**B**		**A**		**D**	
Tees	d1	5.87	5.970	5.848	5.91	5.855	5.995	5.995	5.877
	d2	5.848	5.910	5.84	5.997	5.85	5.90	5.945	5.935
	d3	5.935	6.018	5.997	5.998	5.957	5.928	6.093	6.085
	R	2.499		2.395				2.477	
	Ld	1		1		1		1	
	Lt	11.27		11.25		11.13		11.28	
	D	6.136		6.088				6.117	
	t	0.384		0.51		0.36		0.36	
	Rc	2		1		3		2	
	Rank	2		1		4		3	
	Tc	b		b		b		b	
Vendor		**C**		**B**		**A**		**H**	
Reducing Tee	d1	5.89		5.86		5.99		5.93	
	d2	5.99		5.98		6.05		5.93	
	d3	4.95		4.93		5.01		4.92	
	R	-----		-----		-----		-----	
	Ld	1		1		1		1	
	Lt	11.25		11.25		11.38		11.25	
	D	4.99		5.12		5.05			
	t	0.328		0.435		0.340		0.360	
	Rc	3		2		3			
	Rank	3		1		4		*	
	Tc	b		b		b			
Vendor		**C**		**B**		**A**		**D**	
Reducer	d1	6.05		6.046		6.024		6.12	
	d2	3.99		3.843		3.77		3.8	
	L	0.77		0.4		0.75		0.69	
	Lr	5.55		5.51		5.51		5.54	
	t	0.32		0.289		0.308		0.289	
	Rc	3		1		2		2	
	Rank	4		1		2		3	
	Tc	b		b		b		b	

Table 6.2. Dimensions and characteristics of 8-inch fittings

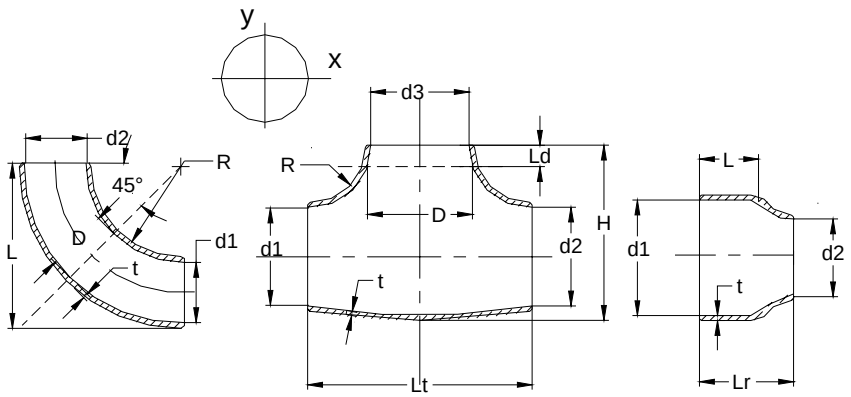

Rank = comparison index of the surface roughness among the manufacturers with 1 being smooth and 4 being rough

Rc = roughness index

Tc = transition index

8" Fittings									
	Dimension (in)								
		x	y	x	y	x	y	x	y
Vendor		**C**		**B**		**A**		**D**	
Elbow	d1	8.075	7.988	7.85	7.95	7.835	7.935	7.903	7.89
	d2	8.014	8.057	7.93	7.975	7.976	7.894	7.948	7.97
	R	7.462		7.427		7.688		7.711	
	D	7.956		7.933		7.828		7.951	
	t	0.337		0.372		0.367		0.328	
	Rc	2		2		2		2	
	Rank	2		3		4		1	
	Tc	b		a		b		a	
Vendor		**F**		**B**		**A**		**G**	
Reducing elbow		x	y	x	y	x	y	x	y
	d1	7.978	7.903	7.983	7.902	7.825	7.857	7.99	7.948
	d2	5.97	5.908	5.95	5.957	5.945	5.925	5.96	5.937
	D	7.693		7.66		6.912		7.659	
	t	0.43		0.45		0.37		0.428	
	Rc	2		3		3		3	
	Rank	1		2		4		3	
	Tc	b		b		b		a	

8" Fittings continued									
Vendor		**C**		**B**		**A**		**D**	
Tee	d1	7.782	7.81	7.678	7.776	7.8	7.903	7.8	7.868
	d2	7.783	7.805	7.628	7.8	7.795	7.938	7.705	7.8
	d3	7.995	7.964	7.92	7.988	7.91	8.025	7.86	7.958
	R	2.949		2.822		2.913		2.994	
	Ld	1.5		1.5		1.5		1.5	
	Lt	14		14		13.94		14.1	
	D	8.174		8.23		8.205		8.154	
	t	0.427		0.486		0.421		0.41	
	Rc	2		3		1		2	
	Rank	3		4		1		2	
	Tc	b		b		b		b	
Vendor		**C**		**B**		**A**		**H**	
Reducing Tee	d1	7.648	7.848	7.673	7.87	7.79	7.765	7.876	7.97
	d2	7.775	7.855	7.86	7.785	7.84	7.845	7.9	7.908
	d3	5.986	6.003	5.922	5.965	5.865	5.943	6.02	5.995
	R	------		------		------		------	
	Ld	1.5		1.5		1.5		1.5	
	Lt	14.0		14.0		13.94		14.12	
	D	6.33		6.084		6.112			
	t	0.391		0.359		0.339		0.296	
	Rc	2		2		2			
	Rank	3		1		2		*	
	Tc	b		b		b			
Vendor		**C**		**B**		**A**		**D**	
Reducer	d1	8.015	7.976	8.069	7.99	7.989	7.97	8.054	8.011
	d2	6.008	5.97	5.963	5.969	6.144	6.129	5.903	5.99
	L	0.64		0.97		0.93		0.49	
	Lr	6.11		6.00		6.01		6.02	
	t	0.335		0.315		0.347		0.299	
	Rc	3		2		2		2	
	Rank	4		1		3		2	
	Tc	b		b		b		b	

Table 6.3. Dimensions and characteristics of 10-inch fittings

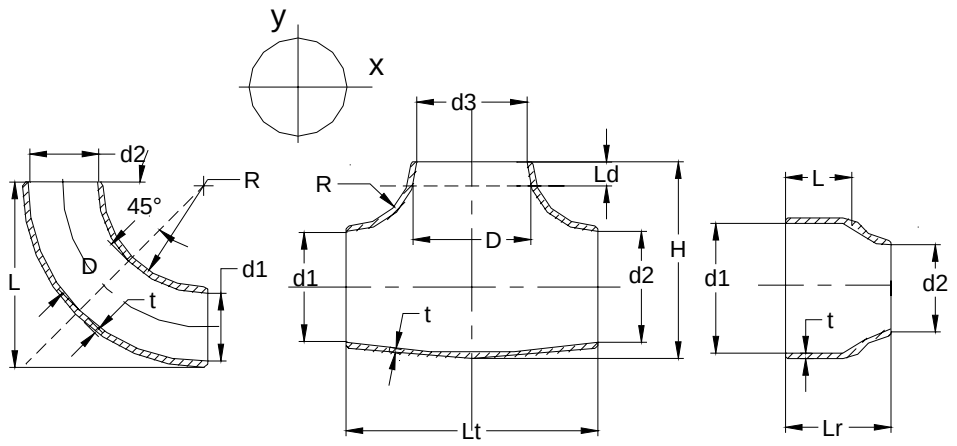

Rank = comparison index of the surface roughness among the manufacturers with 1 being smooth and 4 being rough

Rc = roughness index

Tc = transition index

10" Fittings									
		Dimension (in)							
		x	y	x	y	x	y	x	y
Vendor		**C**		**B**		**A**		**D**	
Elbow	d1	9.995	10.11	10.01	10	9.995	9.988	10.04	9.97
	d2	9.945	10.07	9.97	10.03	10.03	9.905	9.96	10.01
	R	9.694		9.724		9.579		9.716	
	D	9.941		9.944		9.842		9.883	
	t	0.36		0.359		0.42		0.412	
	Rc	1		1		2		2	
	Rank	2		1		3		4	
	Tc	b		a		b		b	
Vendor		**G**		**B**		**A**		**F**	
Reducing Elbow	d1	9.865	9.978	9.945	9.875	10.02	9.95	10.01	9.903
	d2	7.982	7.894	7.94	7.87	7.975	7.935	7.896	7.872
	D	9.87		9.97		9.943		9.798	
	t	0.442		0.41		0.511		0.512	
	Rc	2		1		2		2	
	Rank	3		1		4		2	
	Tc	b		b		b		b	

10" Fittings continued									
Vendor		**C**		**B**		**A**		**D**	
Tees	d1	9.85	9.915	9.865	9.964	9.801	9.855	9.833	9.808
	d2	9.81	9.815	9.865	9.972	9.793	9.868	9.838	9.825
	d3	9.83	9.945	9.938	9.98	9.812	10.08	9.897	9.897
	R	3.342		3.37		3.404		3.394	
	Ld	2		2		2		2	
	Lt	16.92		16.89		17.18		17.11	
	D	10.62		10.52		10.62		10.59	
	t	0.554		0.635		0.515		0.507	
	Rc	2		2		2		3	
	Rank	2		1		3		4	
	Tc	b		b		b		b	
Vendor		**C**		**B**		**A**		**H**	
Reducing Tee	d1	9.635	9.874	9.668	9.675	9.878	9.925	9.845	9.847
	d2	9.617	9.868	9.75	9.803	9.913	9.928	9.878	9.845
	d3	7.875	7.925	7.975	7.968	7.941	7.925	7.868	7.968
	R	------		-----		------		-----	
	Ld	2		2		2		2	
	Lt	17.14		16.94		17.1			
	D	8.443		8.683					
	t	0.602	0.55	0.568	0.647	0.458	0.456	0.453	0.425
	Rc	3		2		2		*	
	Rank	3		1		2			
	Tc	b		b		b			
Vendor		**C**		**B**		**A**		**D**	
Reducer	d1	9.993	9.992	10.01	10.02	10.01	10.02	10.03	9.958
	d2	7.93	7.916	7.93	7.922	7.94	7.92	7.718	7.7
	L	N/A		N/A		N/A		N/A	
	Lr	7.06		7.02		7.01			
	t	0.38		0.397		0.38		0.397	
	Rc	2		2		2			
	Rank	2		3		1		*	
	Tc	b		b		b			

7. Summary and Conclusion

The head loss coefficients, K-value, of 6, 8 and 10-inch wrought butt welded steel fittings were determined by testing 60 fittings from seven manufacturers at St. Anthony Falls Laboratory. The fittings included 90^{o} long elbows, reducing and expansion elbows, Tees, reducing Tees, concentric reducers and expansions. A total of 1,256 tests were conducted in this study. An uncertainty analysis was conducted to determine the accuracy and repeatability of the test set-up and instrumentation. Except for under very low flows, the error in estimating the K-value was often less than 0.04 for most fittings. The results also showed that in most cases, the variability of the K-values among manufacturers was more than the uncertainties in the estimate of the K-value.

The results of the testing show that the K-value of long elbows as a function of upstream velocity is smallest for larger pipe fittings and increases as the pipe fitting size decreases. For expanding and reducing elbows, the percent of expansion and reduction, respectively, has a significant effect on K-value.

For mixing flows in Tees and reducing Tees, the K-value of the branching leg becomes negative when less than 25% of the total flow enters from the branching leg. This phenomenon has also been observed and documented by Rahmeyer (2001) and indicated by Idelchik (1994) and Miller (1990). For branching flows in Tees, the K-value of the straight leg is very similar to those in reducing Tees. However, for branching flows in reducing Tees, the K-value of the branching leg varies with size and the percent reduction in flow area.

The K-values of reducers and expansions show a weak dependence on upstream velocity. They are dependent on both the fitting size, and the percent reduction and expansion of the flow area. For a given flow, the fitting head loss of an expansion is larger than the fitting head loss of the same size reducer.

8. Recommendations

For ASHRAE publications, the recommended K-values for 6, 8 and 10-inch fittings are summarized in Tables 8.1 to 8.7. The K-values are given either for specific upstream velocities (for long elbows, reducing and expanding elbows, concentric reducers and concentric expansions), or for specific flow ratios (Tees, reducing Tees and expanding Tees). Some of the K-values presented in these tables (denoted with a star) are out of the tested ranges, and thus are extrapolated from the measured data using the best fit. In order to show the range of a recommended K-value, one standard deviation of the measured K-value as a percentage of the K-value is displayed and denoted by S_k.

Table 8.1. Loss coefficients of long elbows at specific velocities

V_1 (fps)	6"		8"		10"	
	K	S_K	K	S_K	K	S_K
2	0.29	3%	0.25	7%	0.24	4%
3	0.27	3%	0.24	7%	0.24	4%
5	0.26	2%	0.22	6%	0.19	3%
7	0.25	2%	0.21	6%	0.17	3%
10	0.24	1%	0.19	5%	0.16	3%
13	0.24	1%	0.19	5%	0.15	4%
17	0.23	1%	0.18	4%	0.14	4%
20	0.23	1%	0.18	4%	0.14	4%

Table 8.2. Loss coefficients of expanding elbows at specific velocities

Expanding Elbows	5" x 6"		6" x 8"		8" x 10"	
% change	20%		33%		25%	
V_1 (fps)	K	S_K	K	S_K	K	S_K
2	0.21	29%	0.20	16%	0.19*	7%
3	0.21	2%	0.18	16%	0.18	7%
5	0.20	2%	0.16	11%	0.17	7%
7	0.19	2%	0.14	11%	0.16	7%
10	0.18	2%	0.13	12%	0.15	7%
13	0.18	2%	0.13	16%	0.14	10%
16	0.18*	3%	0.12	16%	0.14	10%
20	0.17*	3%	0.11*	16%	0.14	10%

Table 8.3. Loss coefficients of reducing elbows at specific velocities

Reducing Elbows	**6" x 5"**		**8" x 6"**		**10" x 8"**	
% Change	**17%**		**25%**		**20%**	
V_1 (fps)	**K**	**S_K**	**K**	**S_K**	**K**	**S_K**
2	0.40*	1%	0.70	2%	0.40	4%
3	0.37	2%	0.65	2%	0.37	4%
4	0.36	3%	0.60	2%	0.34	4%
6	0.34	5%	0.58	2%	0.31	4%
8	0.33	5%	0.58	2%	0.30	4%
10	0.33	5%	0.57*	2%	0.30	4%
12	0.33*	5%	0.57*	2%	0.30	7%

Table 8.4. Loss coefficients of Tees at specific flow ratios

	6" mixing Q_1/Q_2		**6" mixing Q_3/Q_2**		**8" mixing Q_1/Q_2**		**8" mixing Q_3/Q_2**		**10" mixing Q_1/Q_2**		**10" mixing Q_3/Q_2**	
QR	**K_{1-2}**	**S_K**	**K_{3-2}**	**S_K**	**K_{1-2}**	**S_K**	**K_{3-2}**	**S_K**	**K_{1-2}**	**S_K**	**K_{3-2}**	**S_K**
25%	1.70	19%	-3.19	11%	0.98	8%	-4.13	16%	1.06	31%	-4.56	30%
50%	0.96	4%	0.57	8%	0.74	5%	0.37	3%	0.85	14%	0.54	21%
75%	0.45	9%	0.69	5%	0.39	11%	0.60	4%	0.41	6%	0.65	4%
100%	0.12	5%	0.88	12%	0.08	28%	0.70	30%	0.06	26%	0.77	18%

	6" branching Q_2/Q_1		**6" branching Q_3/Q_1**		**8" branching Q_2/Q_1**		**8" branching Q_3/Q_1**		**10" branching Q_2/Q_1**		**10" branching Q_3/Q_1**	
QR	**K_{1-2}**	**S_K**	**K_{1-3}**	**S_K**	**K_{1-2}**	**S_K**	**K_{1-3}**	**S_K**	**K_{1-2}**	**S_K**	**K_{1-3}**	**S_K**
25%	0.12	11%	0.66	4%	0.13	5%	0.67	4%	0.12	4%	0.63	3%
50%	0		0.52	4%	0		0.51	4%	0.03	70%	0.50	3%
75%	0		0.51	4%	0		0.44	4%	0		0.45	4%
100%	0.12	22%	0.56	6%	0.08	34%	0.53	5%	0.06	18%	0.52	10%

Table 8.5. Loss coefficients of reducing Tees at specific flow ratios

	6x5" mixing Q_1/Q_2		6x5" mixing Q_3/Q_2		8x6" mixing Q_1/Q_2		8x6" mixing Q_3/Q_2		10x8" mixing Q_1/Q_2		10x8" mixing Q_3/Q_2	
QR	K_{1-2}	S_K	K_{3-2}	S_K	K_{1-2}	S_K	K_{3-2}	S_K	K_{1-2}	S_K	K_{3-2}	S_K
25%	1.68	33%	-1.31	24%	0.63	92%	-0.96	19%	1.09	57%	-0.97	46%
50%	0.80	14%	0.61	7%	0.27	55%	0.55	4%	0.50	19%	0.45	37%
75%	0.46	7%	0.69	4%	0.23	87%	0.62	4%	0.43	9%	0.60	14%
100%	0.08	21%	0.82	10%	0.06	31%	0.85	24%	0.06	15%	0.77	14%

	6x5" branching Q_2/Q_1		6x5" branching Q_3/Q_1		8x6" branching Q_2/Q_1		8x6" branching Q_3/Q_1		10x8" branching Q_2/Q_1		10x8" branching Q_3/Q_1	
QR	K_{1-2}	S_K	K_{1-3}	S_K	K_{1-2}	S_K	K_{1-3}	S_K	K_{1-2}	S_K	K_{1-3}	S_K
25%	0.14	9%	0.67	16%	0.13	17%	0.52	12%	0.13	23%	0.58	9%
50%	0		0.59	22%	0.02	200%	0.36	17%	0.00		0.50	5%
75%	0		0.60	9%	0		0.36	18%	0		0.57	13%
100%	0.06	12%	0.78	8%	0.06	32%	0.59	24%	0.06	13%	0.79	6%

Table 8.6 Loss coefficients of expansions at specific velocities

Expansion	**4" x 6"**		**6" x 8"**		**8" x 10"**	
% Change	**50%**		**33%**		**25%**	
V_1 (fps)	**K**	**S_K**	**K**	**S_K**	**K**	**S_K**
2	0.32	6%	0.18	2%	0.11	1%
3	0.29	1%	0.16	1%	0.11	1%
5	0.28	1%	0.13	1%	0.10	1%
7	0.28	1%	0.12	1%	0.09	1%
10	0.30	1%	0.11	1%	0.09	1%
13	0.30	1%	0.11	1%	0.09	1%
17			0.10	1%	0.09	1%
20			0.10	1%	0.09	1%

Table 8.7. Loss coefficients of reducers at specific velocities

Reducers	**6" x 4"**		**8" x 6"**		**10" x 8"**	
% change	**33%**		**25%**		**20%**	
V_1 (fps)	**K**	**S_K**	**K**	**S_K**	**K**	**S_K**
2	0.82*	12%	0.37	17%	0.11	24%
3	0.73	12%	0.32	15%	0.15	15%
4	0.62	15%	0.30	6%	0.16	13%
6	0.55	17%	0.29	6%	0.15	10%
8	0.54*	18%	0.29	6%	0.14	10%
10	0.54*	18%	0.27	8%	0.14	10%
12	0.53*	18%	0.26*	8%	0.14	11%

References

ASHRAE, 1997. *1997 ASHRAE Handbook Fundamentals*, I.P. Eddition. Atlanta, GA.

Crane Co., 1952. *Crane valves and fittings*. Crane Co., Chicago, IL.

Crane Co., 1979. Flow of fluids through valves and fittings and pipe. *Technical paper no. 410*.

Freeman, J. R., 1941. *Experiments upon the flow of water in pipe and pipe fittings*. ASME, New York, NY.

Giesecke, F. E., and Badgett, W. H., 1932. Supplementary friction heads in one-inch cast iron Tees. *ASHVE Transactions*, 38:111.

Hydraulic Institute, 1979. *Hydraulic Institute Engineering Data Book*. 1st Edition, Cleveland, Ohio.

Idelchik, I. E., 1994. *Handbook of hydraulic resistance*. 3rd edition (translated). CRC Press, Inc., Boca Raton, FL.

Miller, D. S., 1990. *Internal flow systems: Design and performance prediction*. 2nd edition. Gulf Publishing Company, Huston, TX.

Pigott, R. J. S., 1950. Pressure losses in tubing, pipe and fittings. *Transactions of ASME*. 7:679-689.

Rahmeyer, W. J., 1999a. Pressure loss coefficients of threaded and forged weld pipe fittings for ells, reducing ells and pipe reducers. *ASHRAE Transaction Research*. 105(2):334-354.

Rahmeyer, W. J., 1999b. Pressure loss coefficients of threaded and forged weld pipe Tees. *ASHRAE Transaction Research*. 105(2):355-385.

Appendix A. K-values of all tested long elbows

In this attachment the K-values obtained for all tested long elbows are plotted versus the Reynolds number. The Reynolds number has been calculated using the velocity and geometry upstream of the fitting.

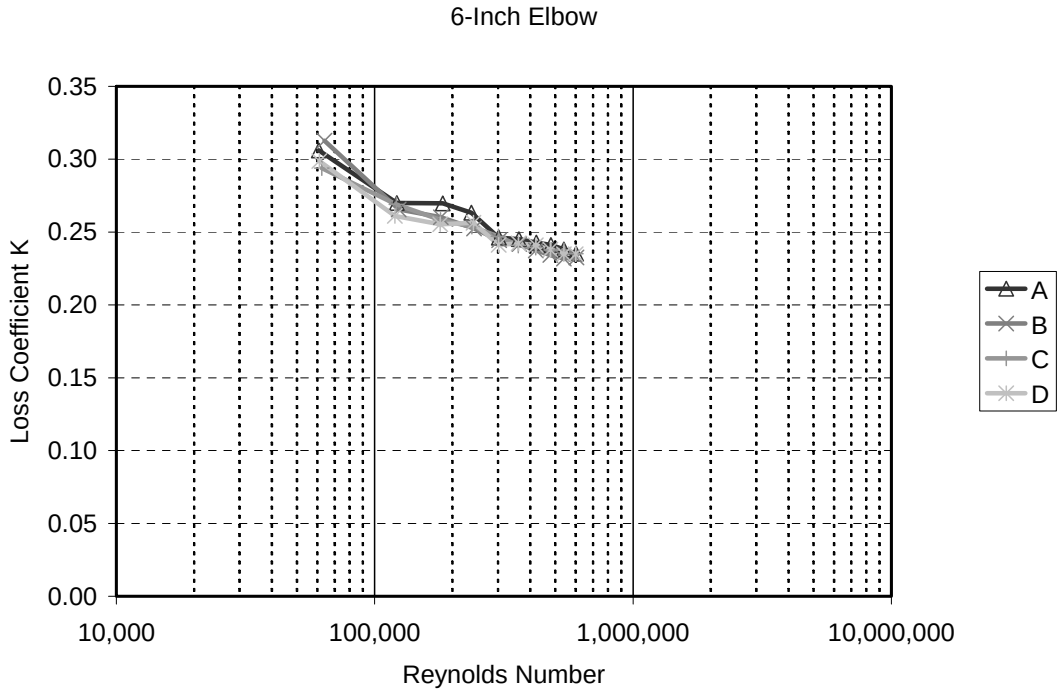

Figure A.1. K-values of 6-inch long elbows from four manufacturers versus the Reynolds number.

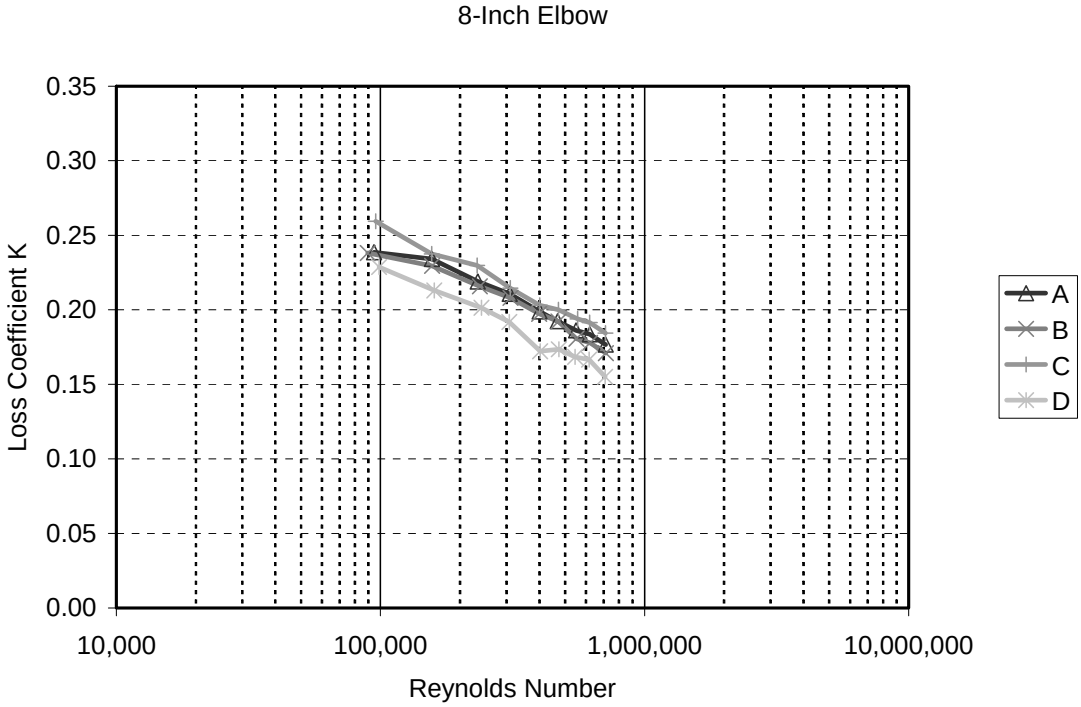

Figure A.2. K-values of 8-inch long elbows from four manufacturers versus the Reynolds number

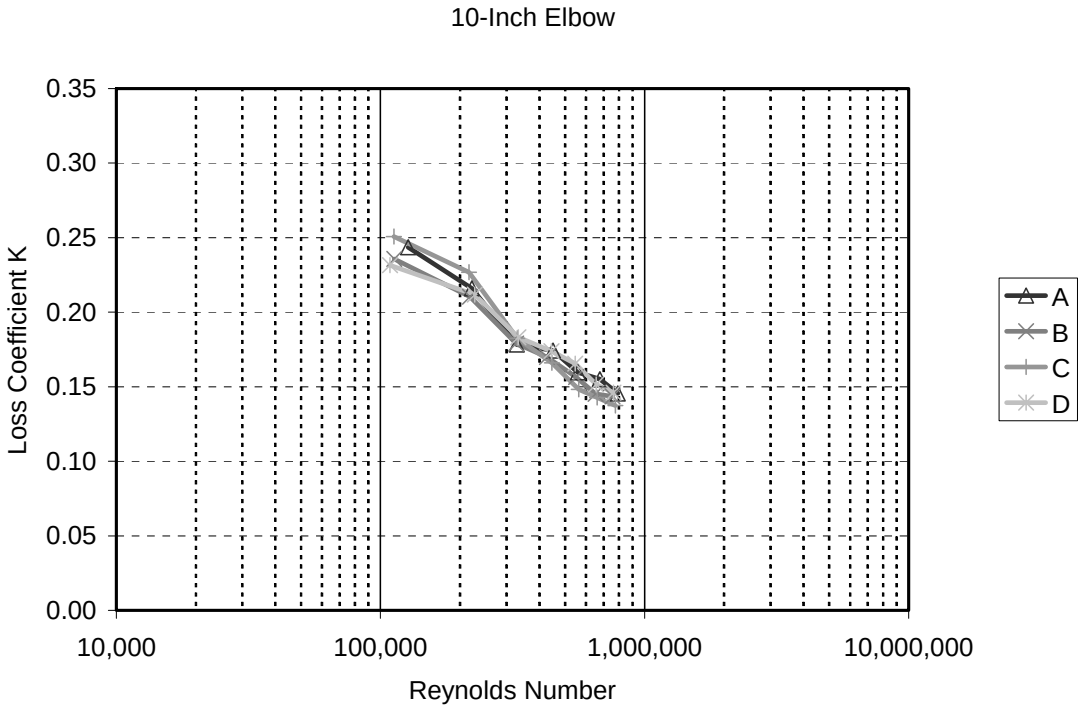

Figure A.3. K-values of 10-inch long elbows from four manufacturers versus the Reynolds number

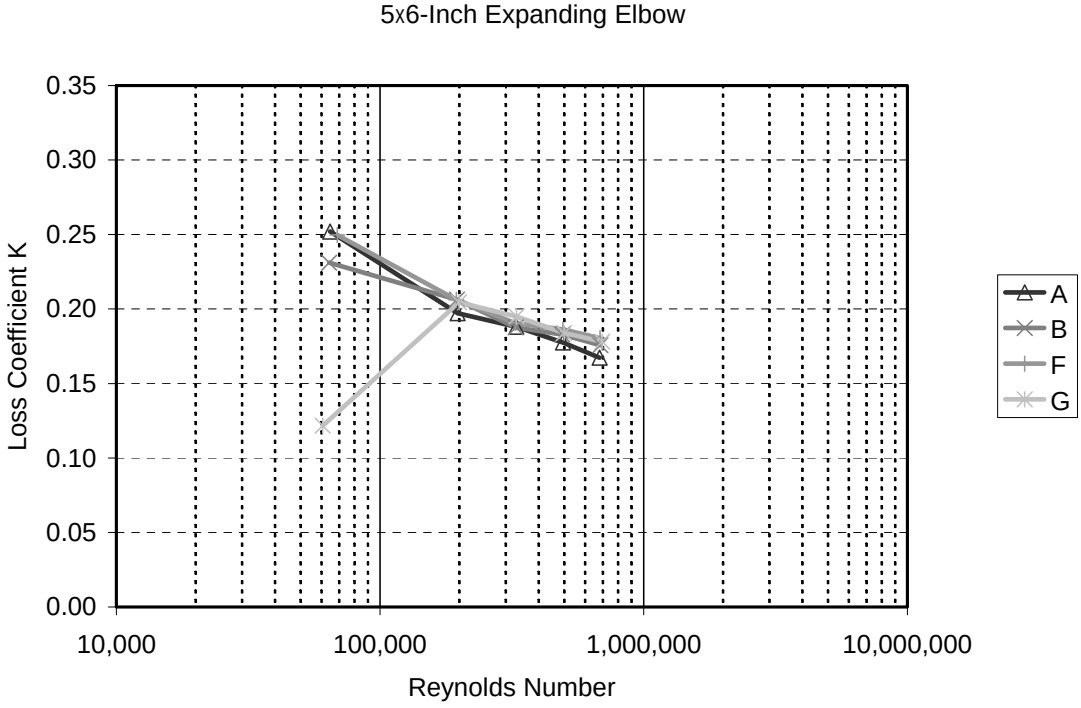

Figure A.4. K-values of 5×6-inch expanding elbows from four manufacturers versus the Reynolds number.

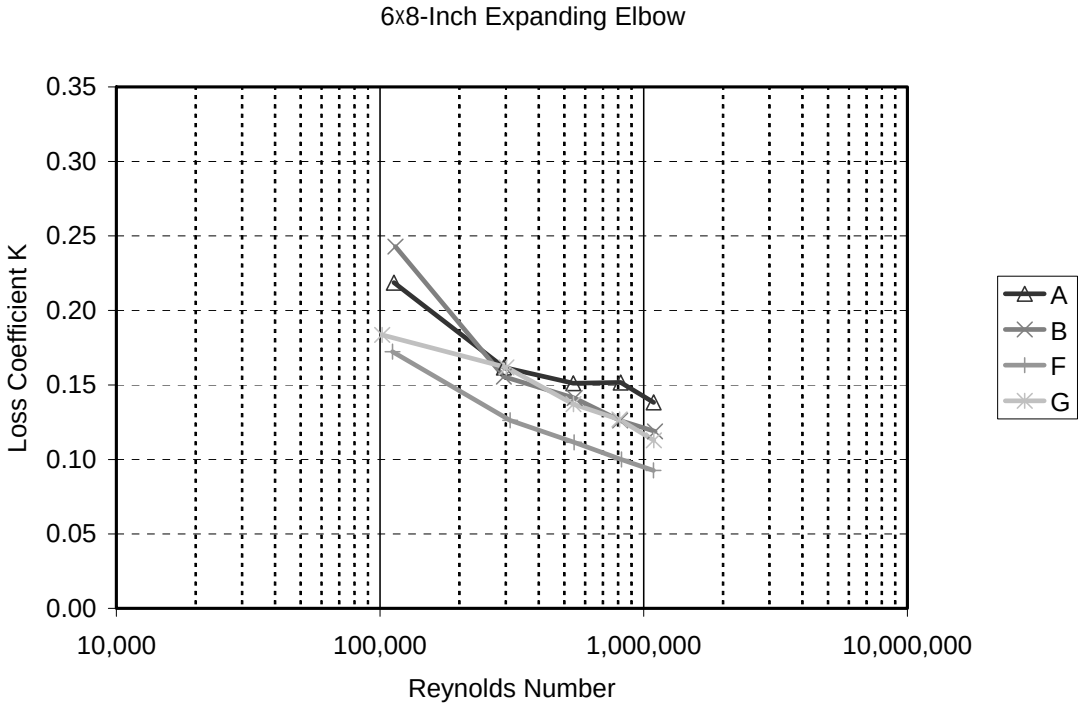

Figure A.5. K-values of 6×8-inch expanding elbows from four manufacturers versus the Reynolds number.

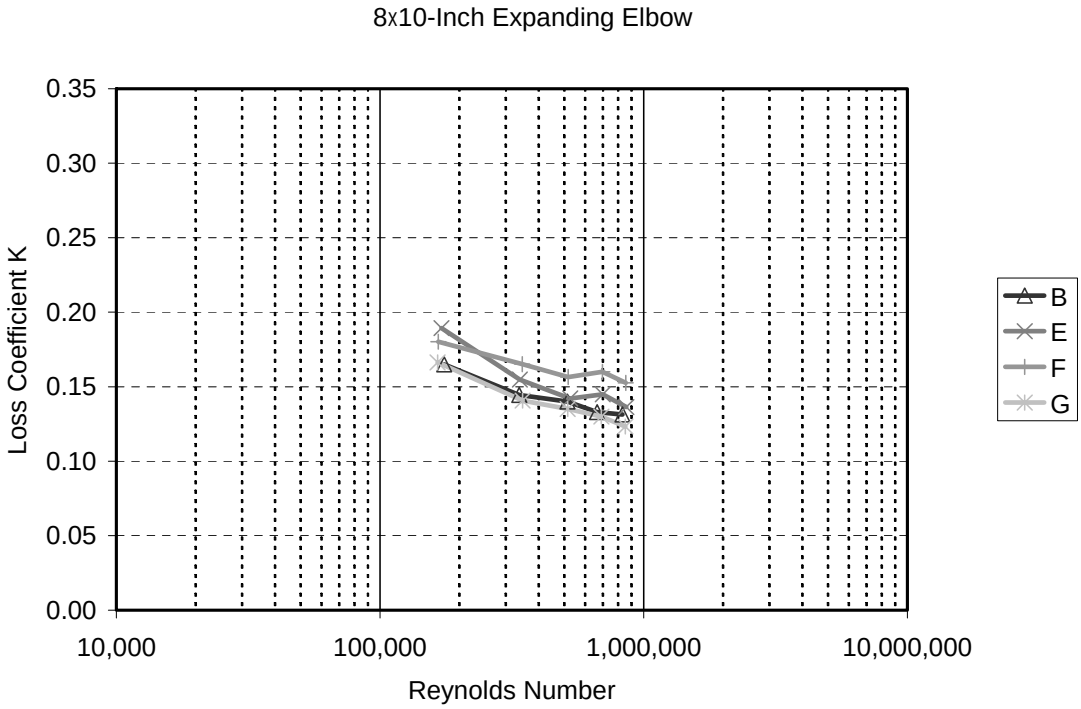

Figure A.6. K-values of 8×10-inch expanding elbows from four manufacturers versus the Reynolds number.

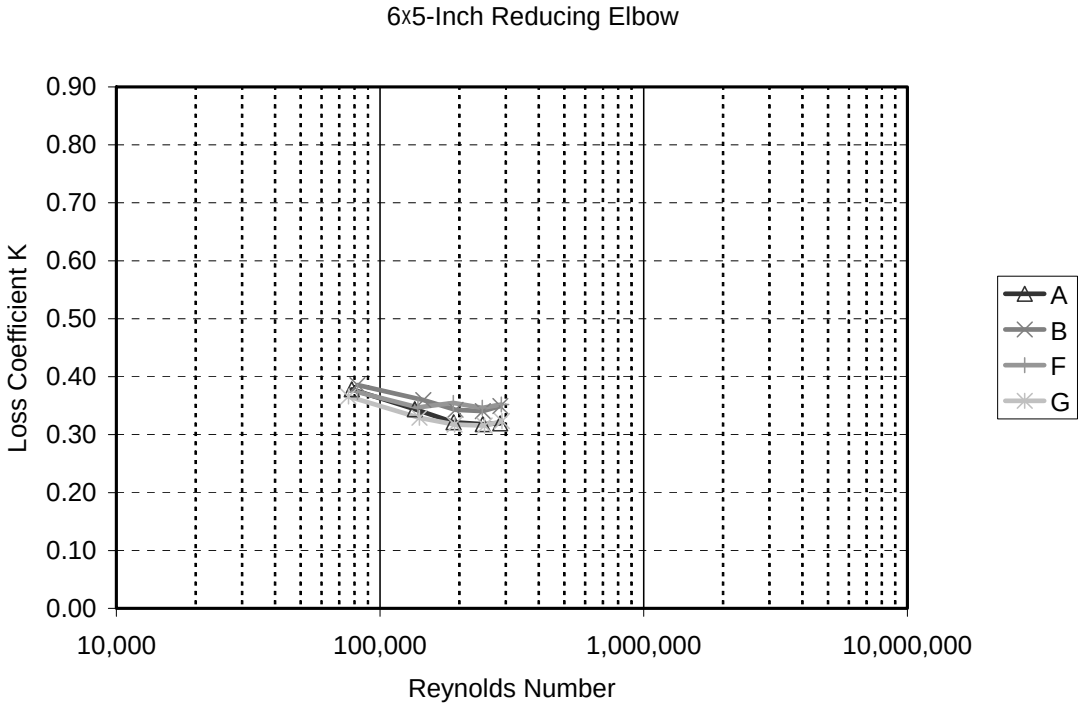

Figure A.7. K-values of 6×5-inch reducing elbows from four manufacturers versus the Reynolds number.

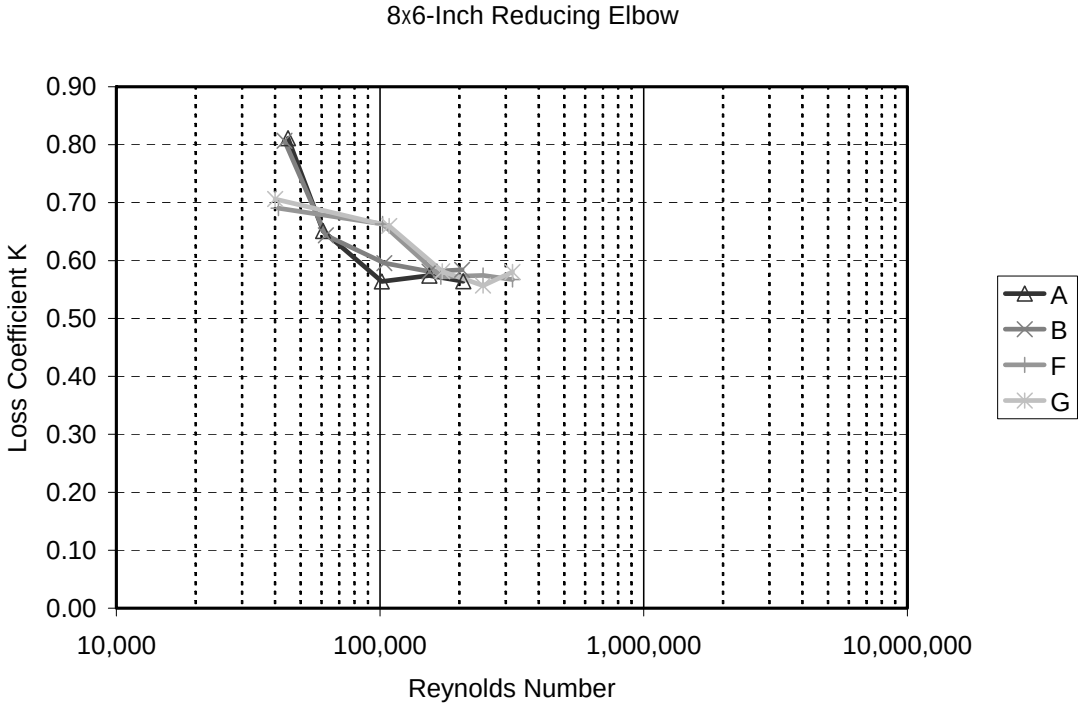

Figure A.8. K-values of 8×6-inch reducing elbows from four manufacturers versus the Reynolds number.

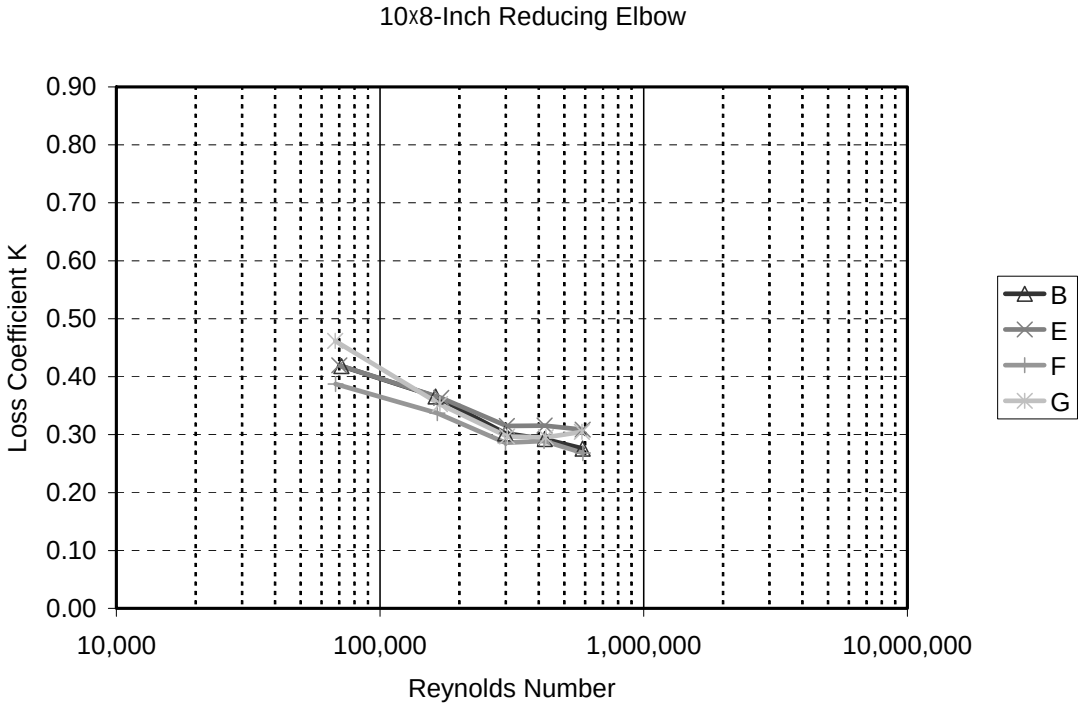

Figure A.9. K-values of 10×8-inch reducing elbows from four manufacturers versus the Reynolds number.

Appendix B. K-values of all tested Tees

In this attachment the K-values obtained for all tested Tees are plotted versus the percentage of flow through the fitting. In order to evaluate the effect of flow rate on K-value, the K-values of 50% flow through the fittings plotted against the upstream velocity are also illustrated.

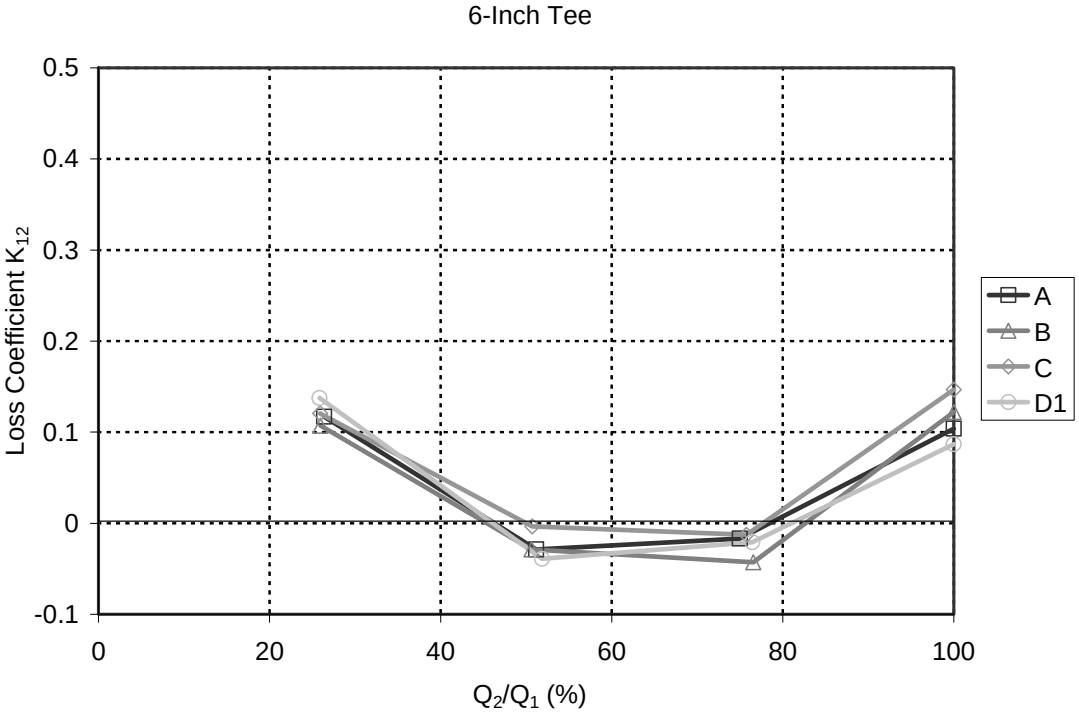

Figure B.1. K-values for the flow through the straight leg of the 6-inch branching Tees from four manufacturers.

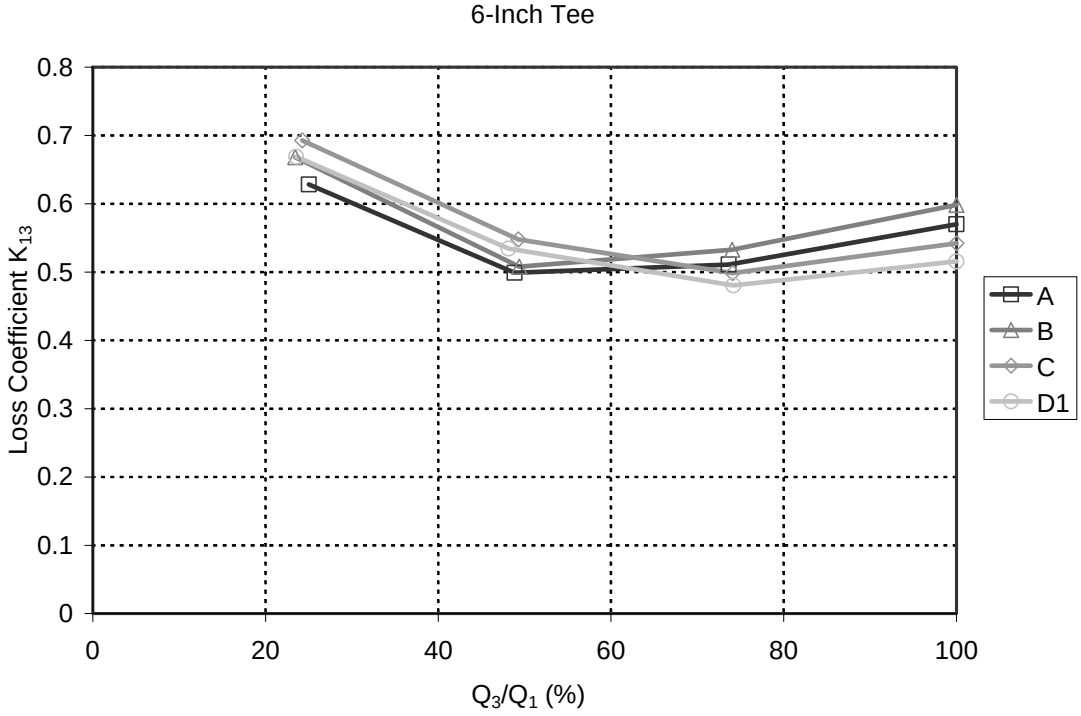

Figure B.2. K-values for the flow through the branching leg of the 6-inch branching Tees from four manufacturers.

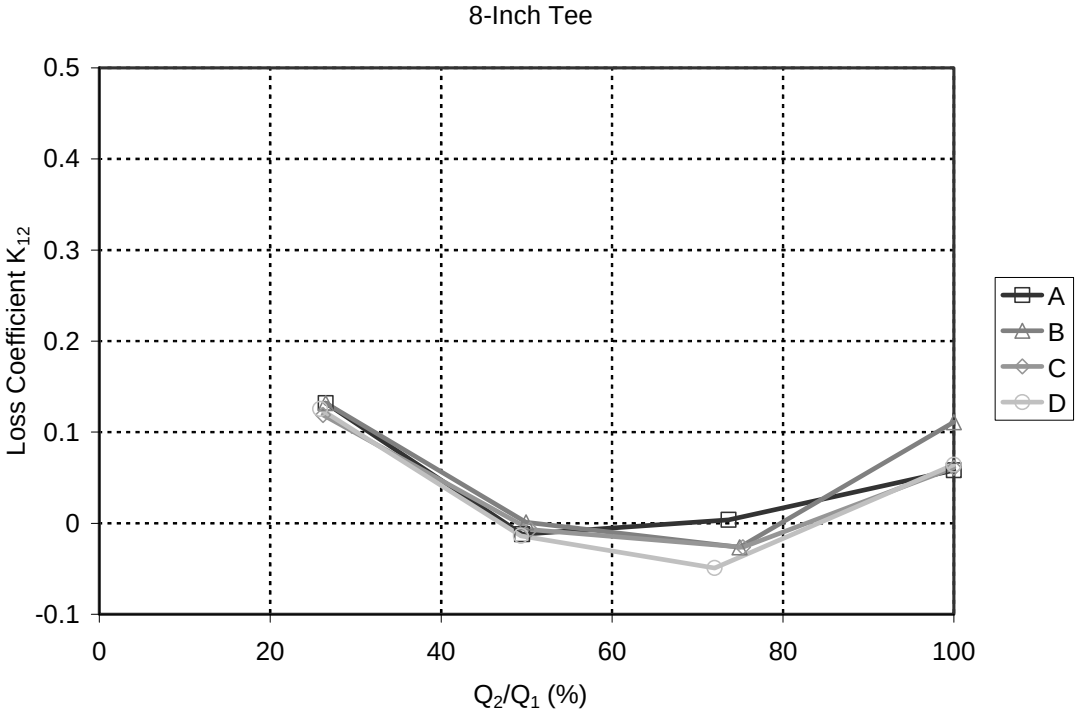

Figure B.3. K-values for the flow through the straight leg of the 8-inch branching Tees from four manufacturers.

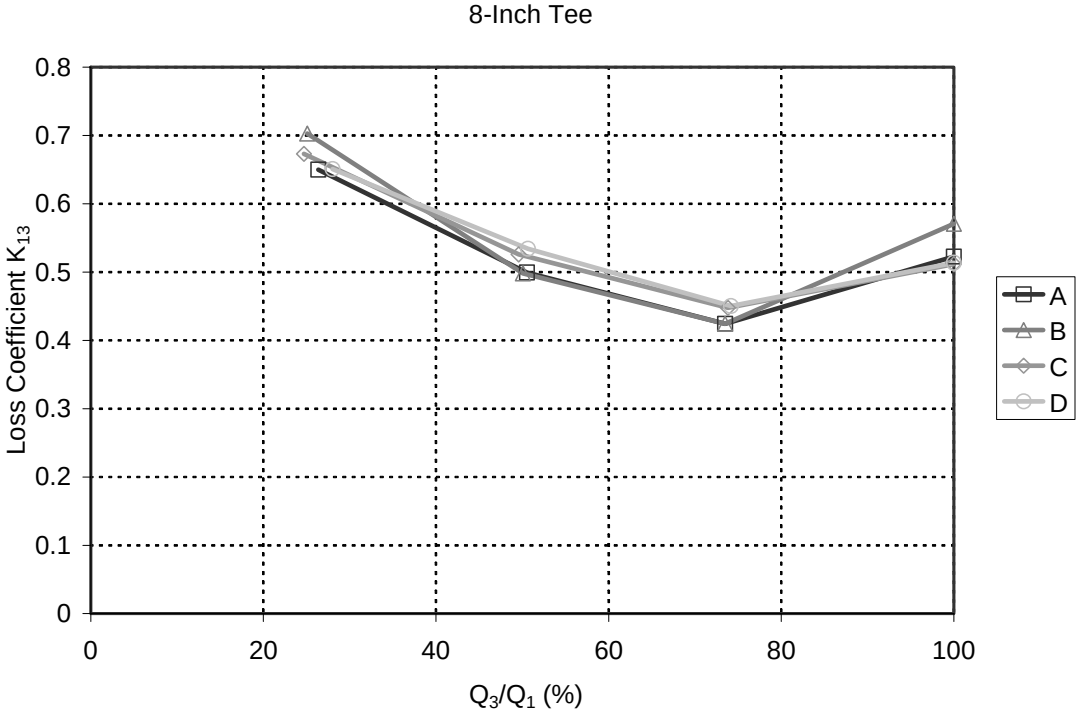

Figure B.4. K-values for the flow through the branching leg of the 8-inch branching Tees from four manufacturers.

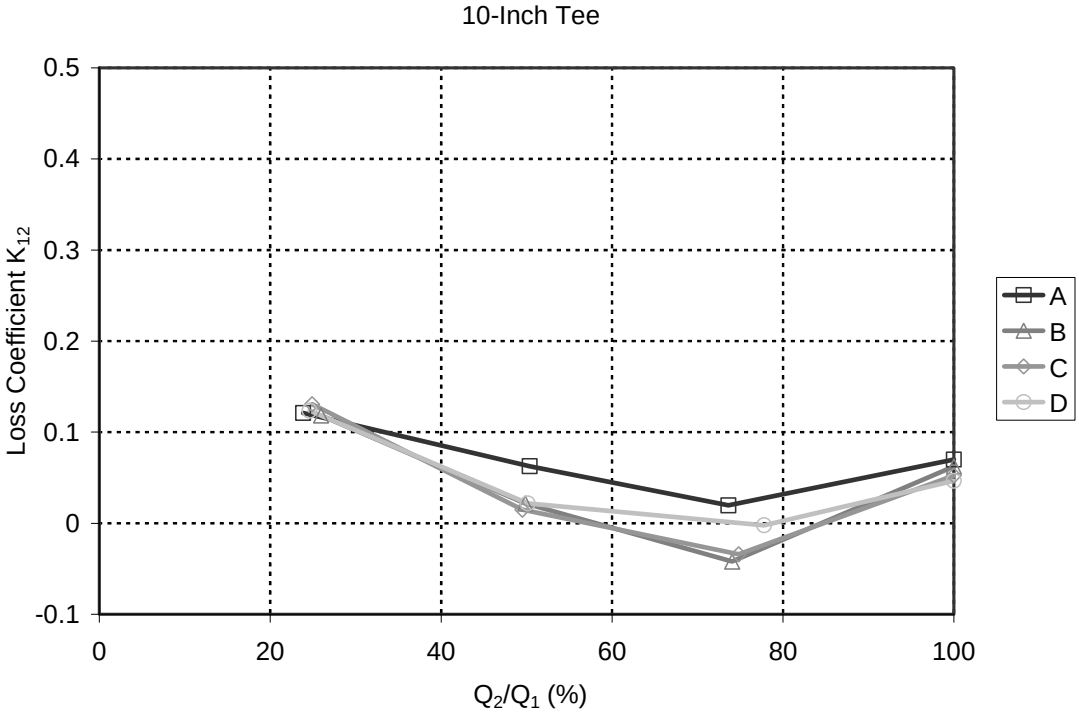

Figure B.5. K-values for the flow through the straight leg of the 10-inch branching Tees from four manufacturers.

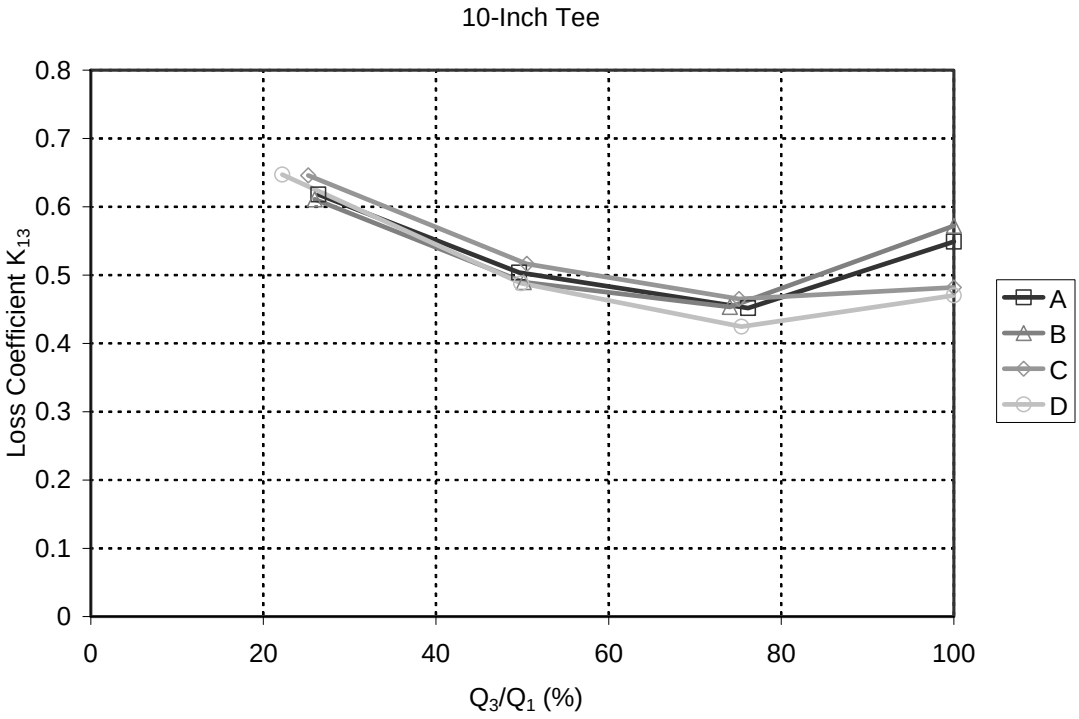

Figure B.6. K-values for the flow through the branching leg of the 10-inch branching Tees from four manufacturers.

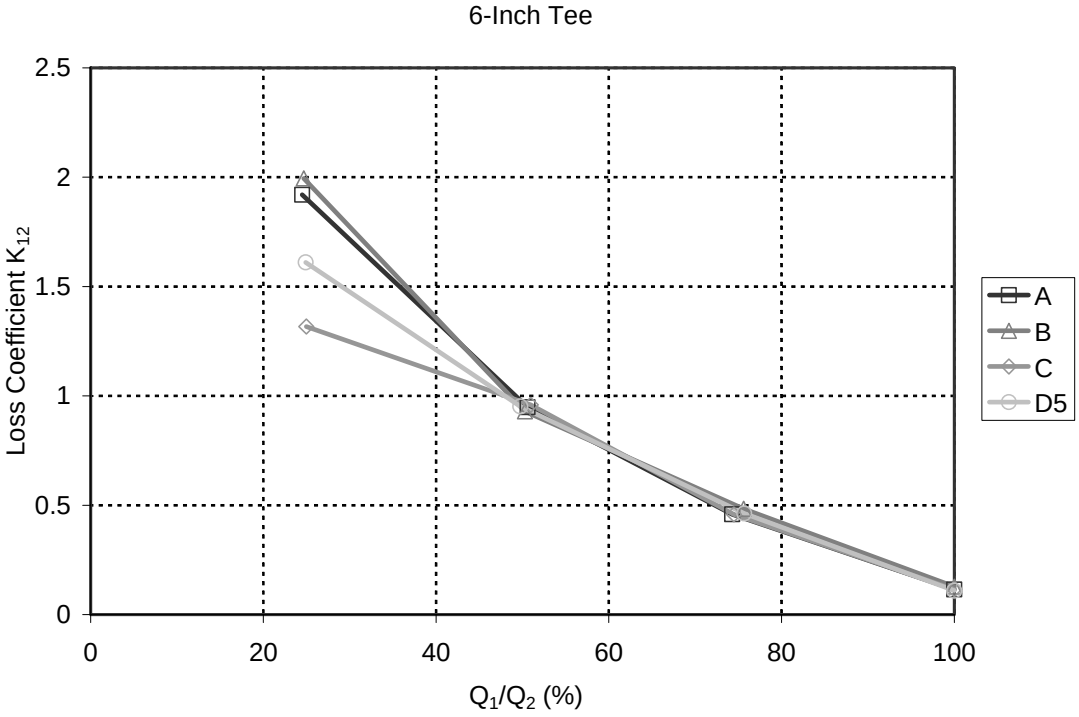

Figure B.7. K-values for the flow through the straight leg of the 6-inch mixing Tees from four manufacturers.

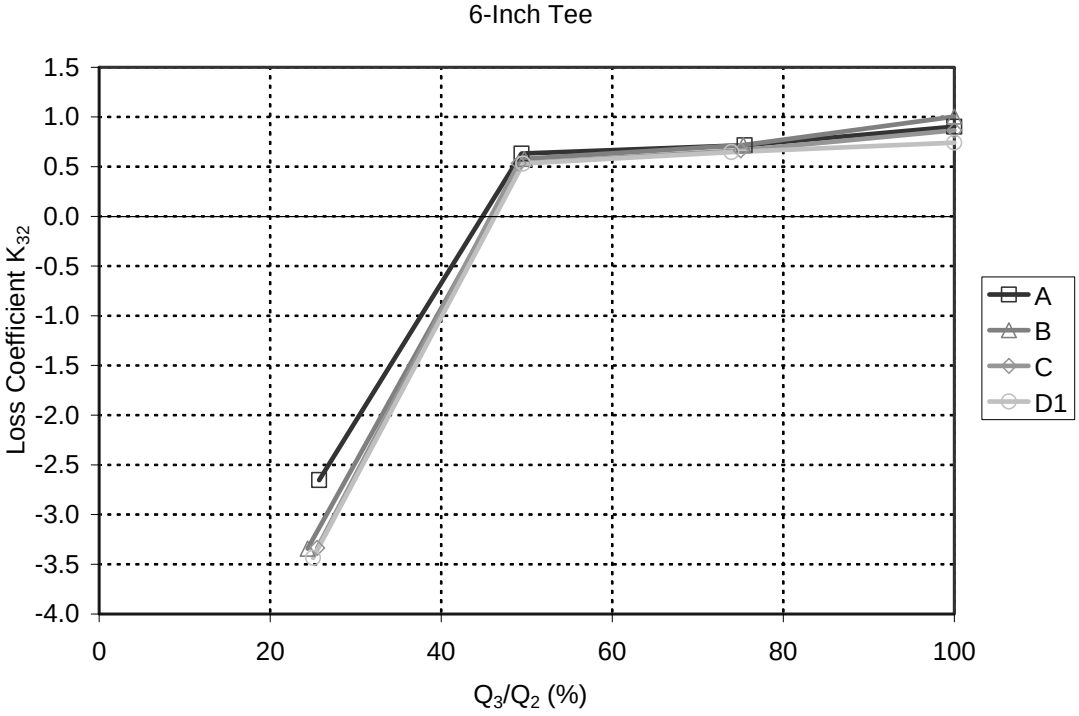

Figure B.8. K-values for the flow through the branching leg of the 6-inch mixing Tees from four manufacturers.

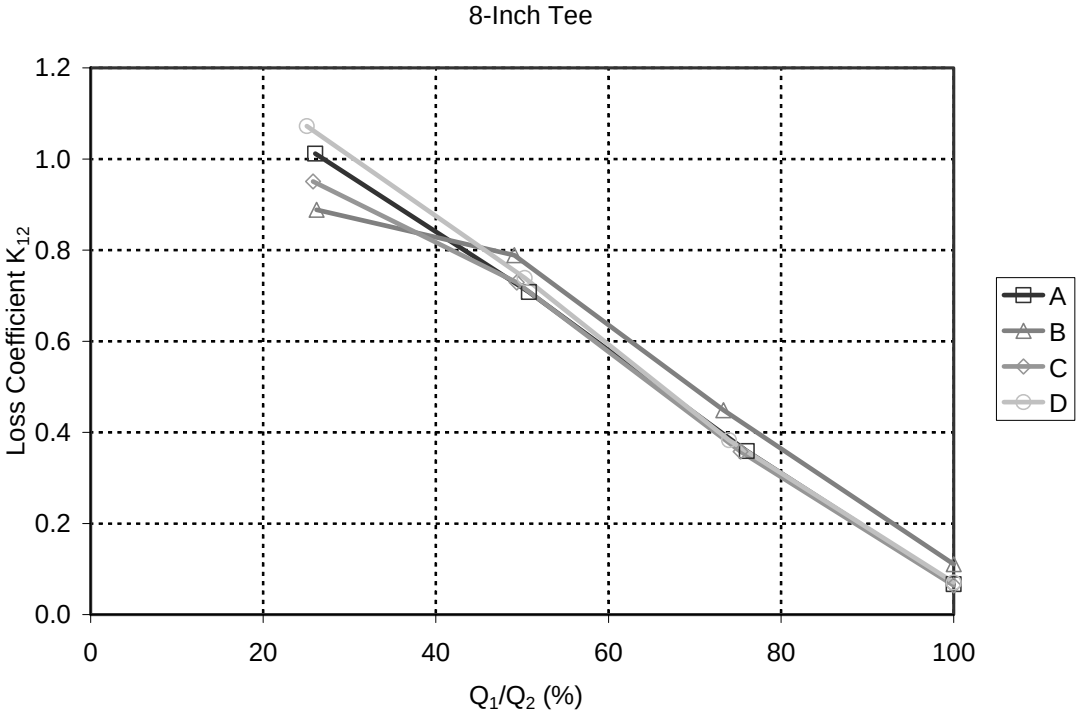

Figure B.9. K-values for the flow through the straight leg of the 8-inch mixing Tees from four manufacturers.

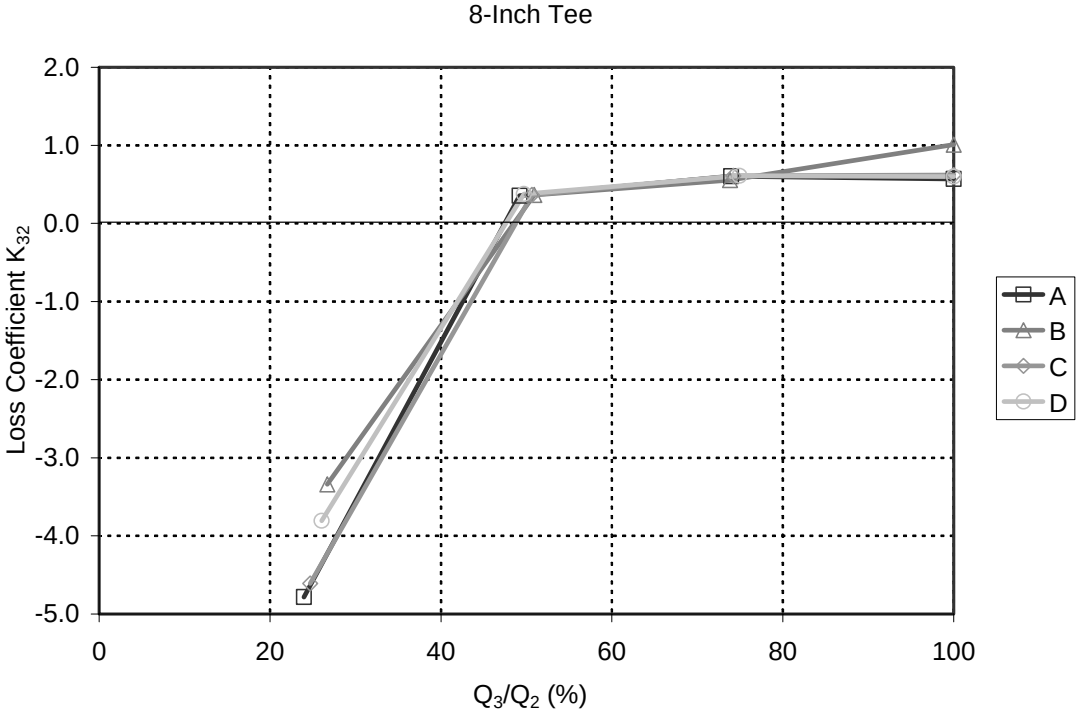

Figure B.10. K-values for the flow through the branching leg of the 8-inch mixing Tees from four manufacturers.

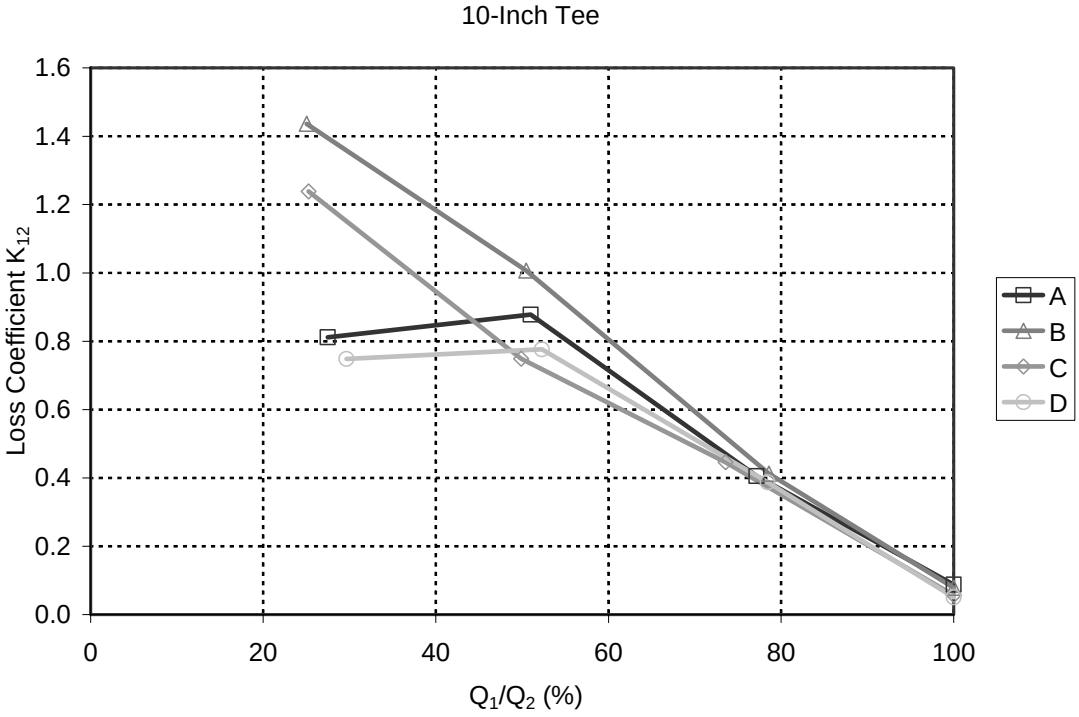

Figure B.11. K-values for the flow through the straight leg of the 10-inch mixing Tees from four manufacturers.

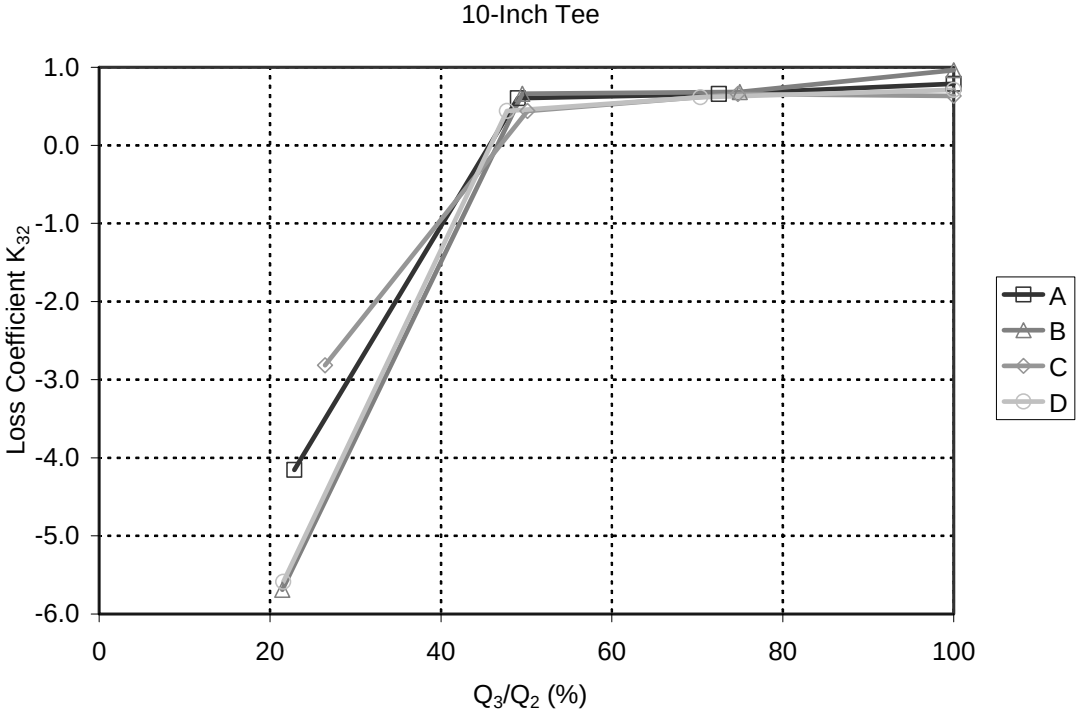

Figure B.12. K-values for the flow through the branching leg of the 10-inch mixing Tees from four manufacturers.

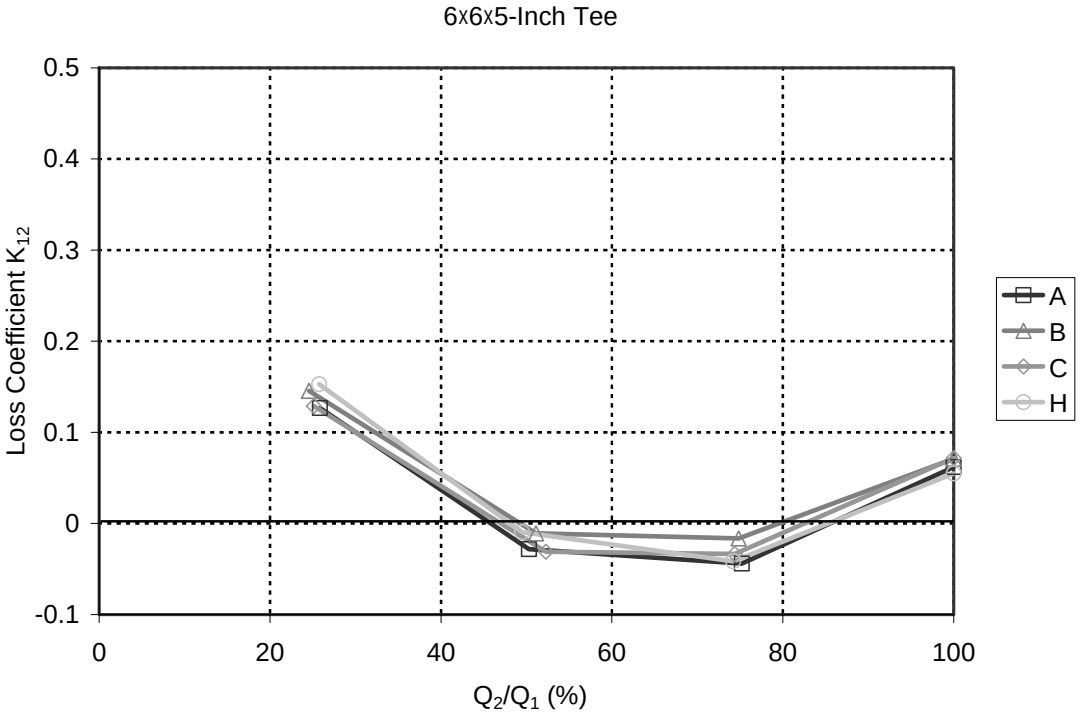

Figure B.13. K-values for the flow through the straight leg of the 6×6×5-inch branching Tees from four manufacturers.

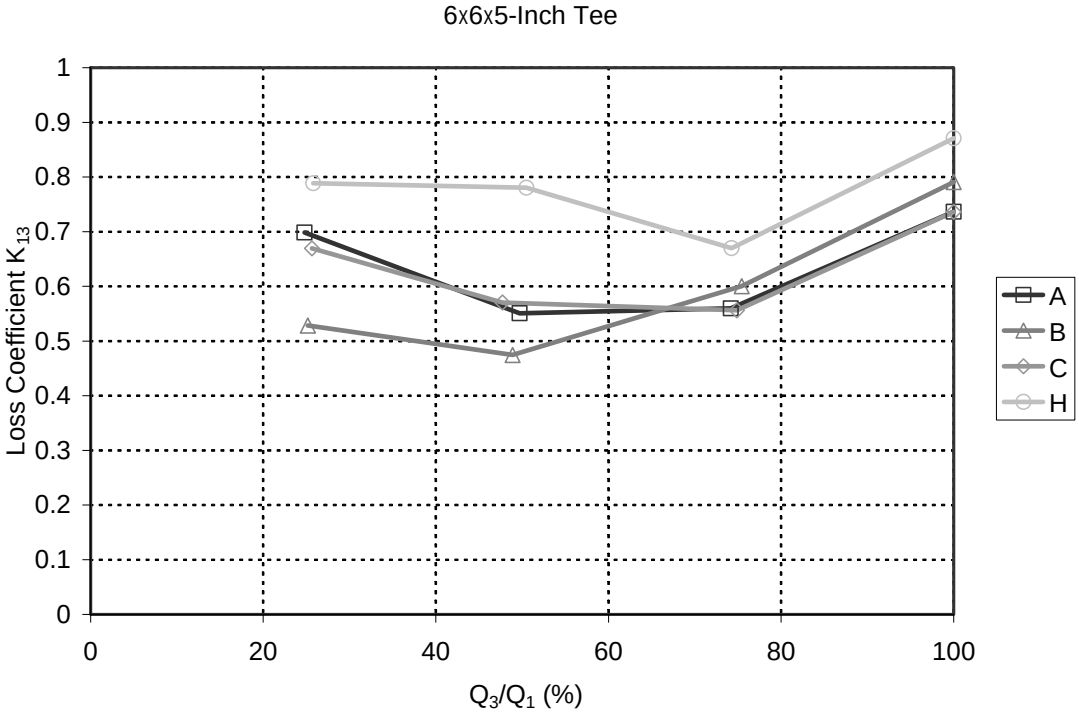

Figure B.14. K-values for the flow through the branching leg of the 6×6×5-inch branching Tees from four manufacturers.

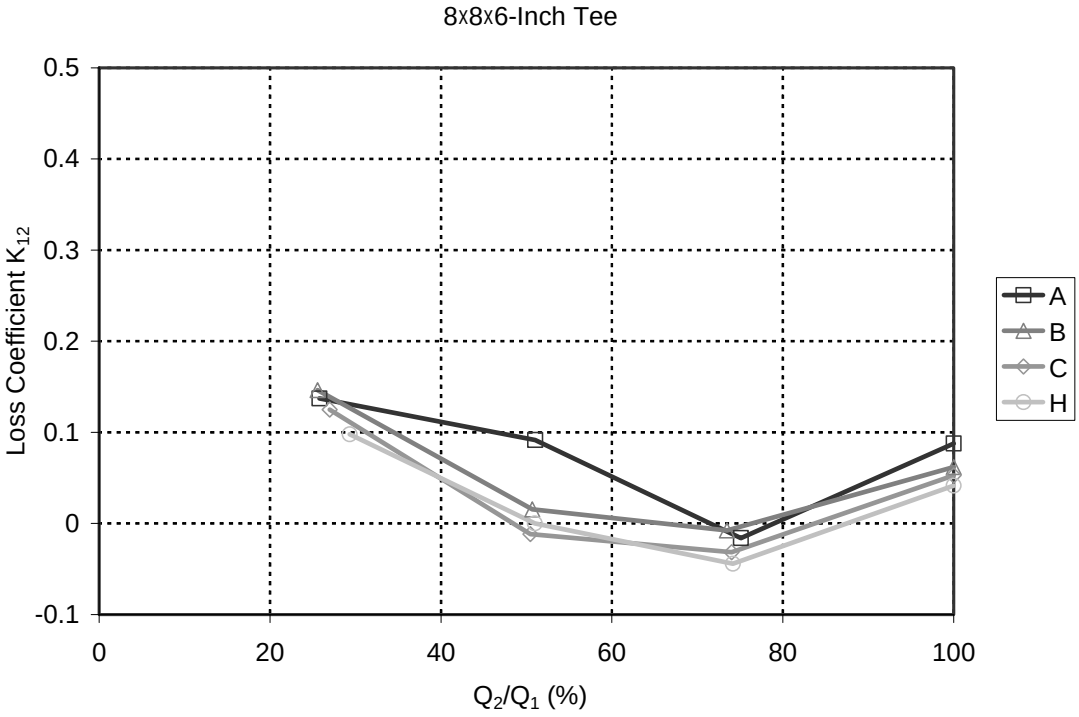

Figure B.15. K-values for the flow through the straight leg of the 8×8×6-inch branching Tees from four manufacturers.

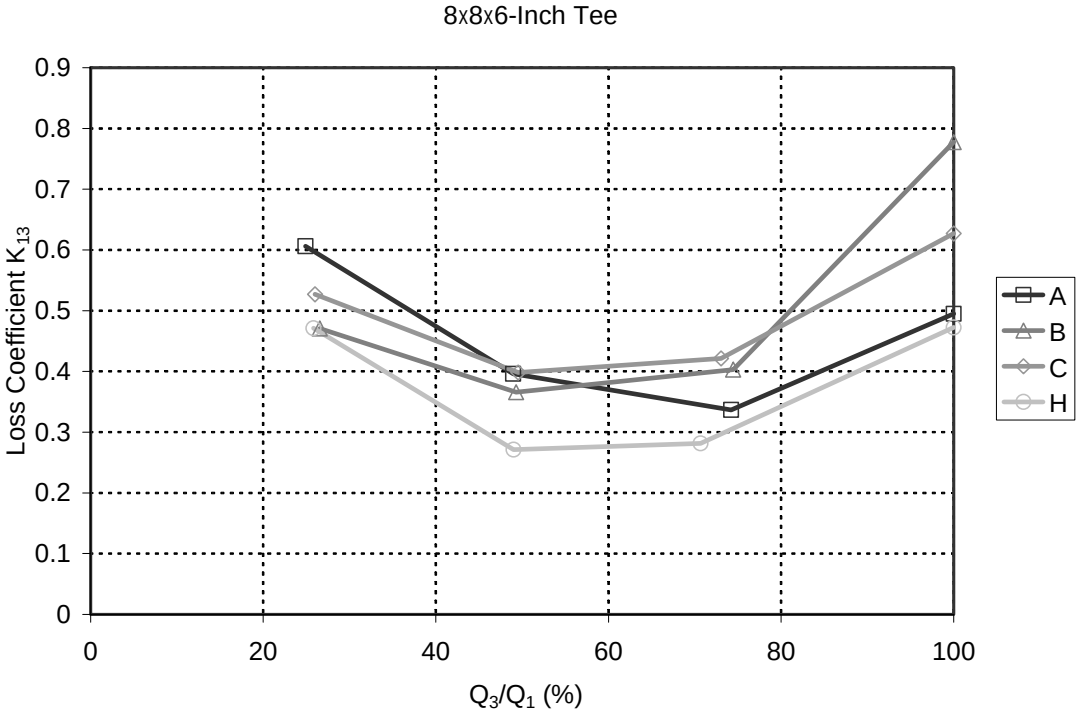

Figure B.16. K-values for the flow through the branching leg of the 8×8×6-inch branching Tees from four manufacturers.

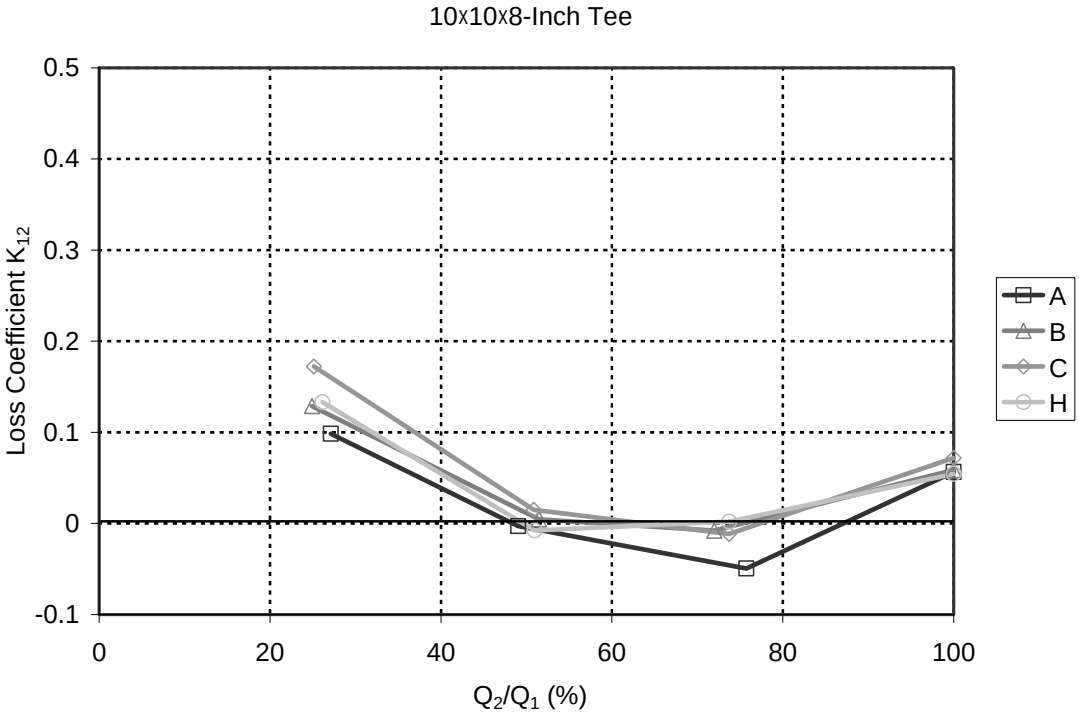

Figure B.17. K-values for the flow through the straight leg of the 10×10×8-inch branching Tees from four manufacturers.

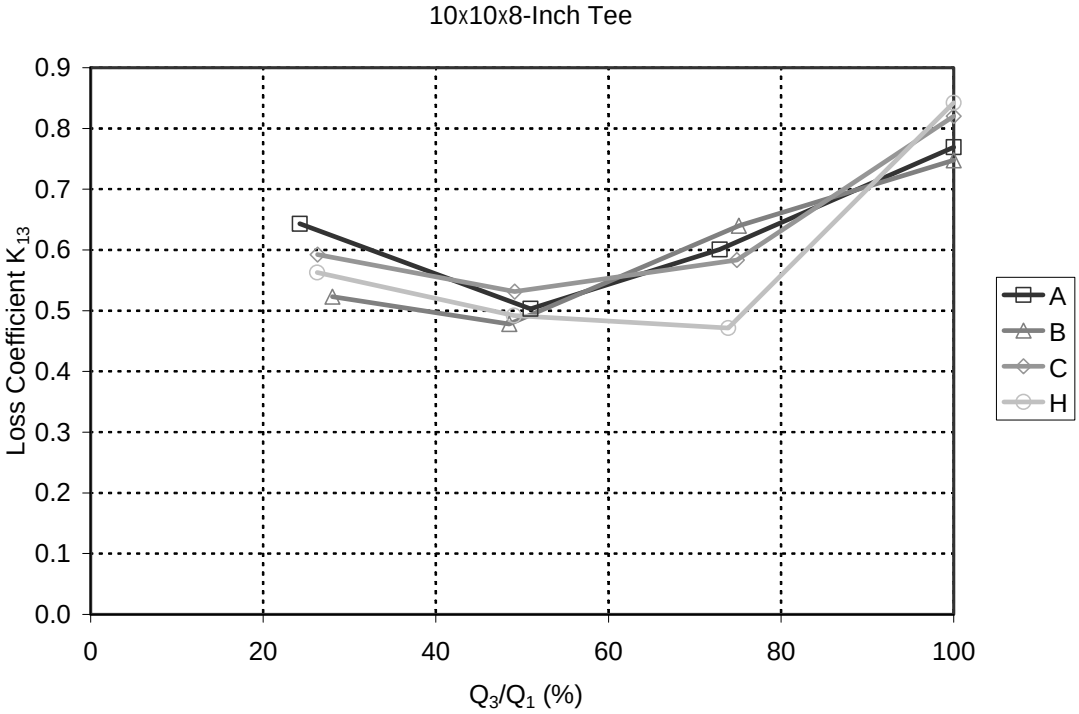

Figure B.18. K-values for the flow through the branching leg of the 10×10×8-inch branching Tees from four manufacturers.

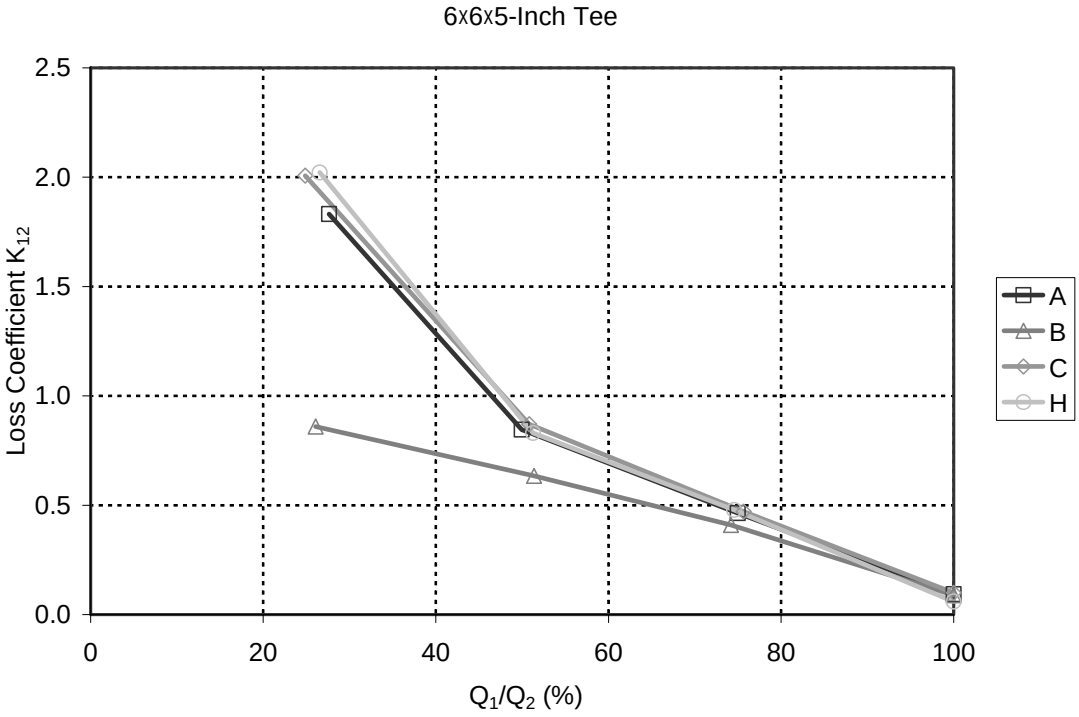

Figure B.19. K-values for the flow through the straight leg of the 6×6×5-inch mixing Tees from four manufacturers.

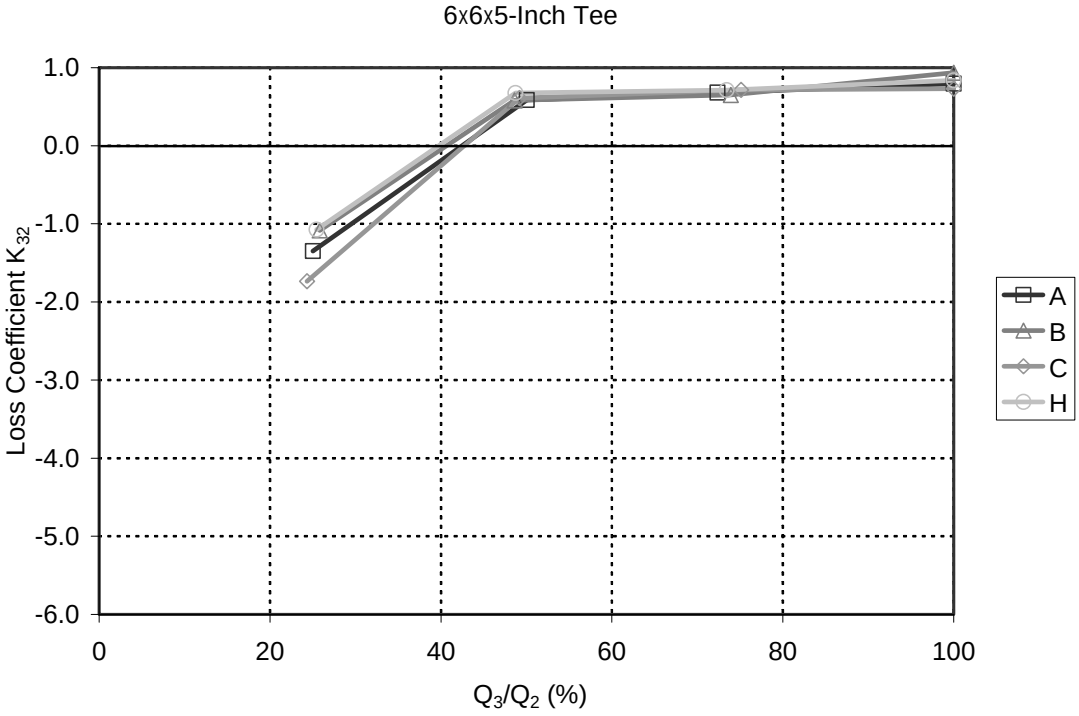

Figure B.20. K-values for the flow through the branching leg of the 6×6×5-inch mixing Tees from four manufacturers.

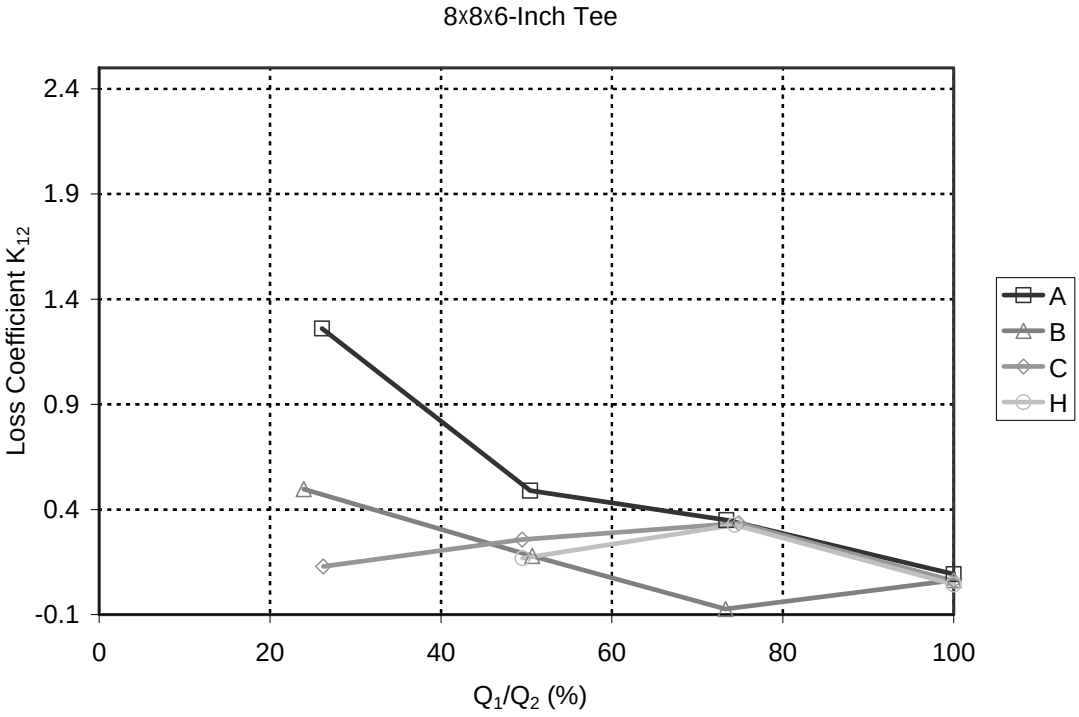

Figure B.21. K-values for the flow through the straight leg of the 8×8×6-inch mixing Tees from four manufacturers.

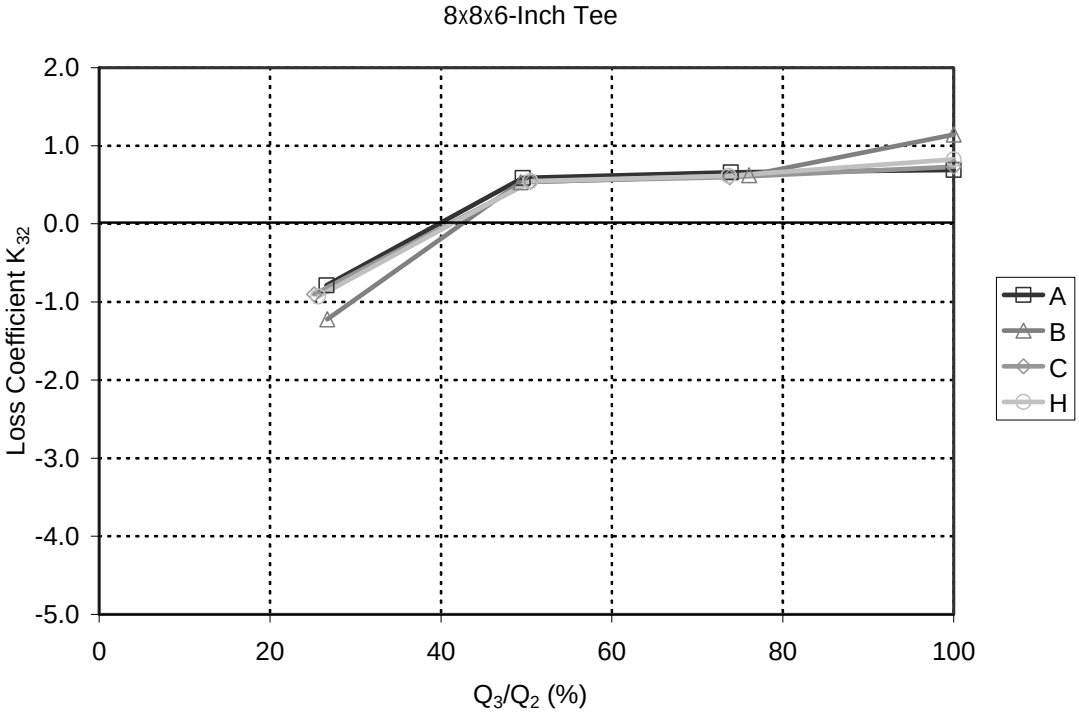

Figure B.22. K-values for the flow through the branching leg of the 8×8×6-inch mixing Tees from four manufacturers.

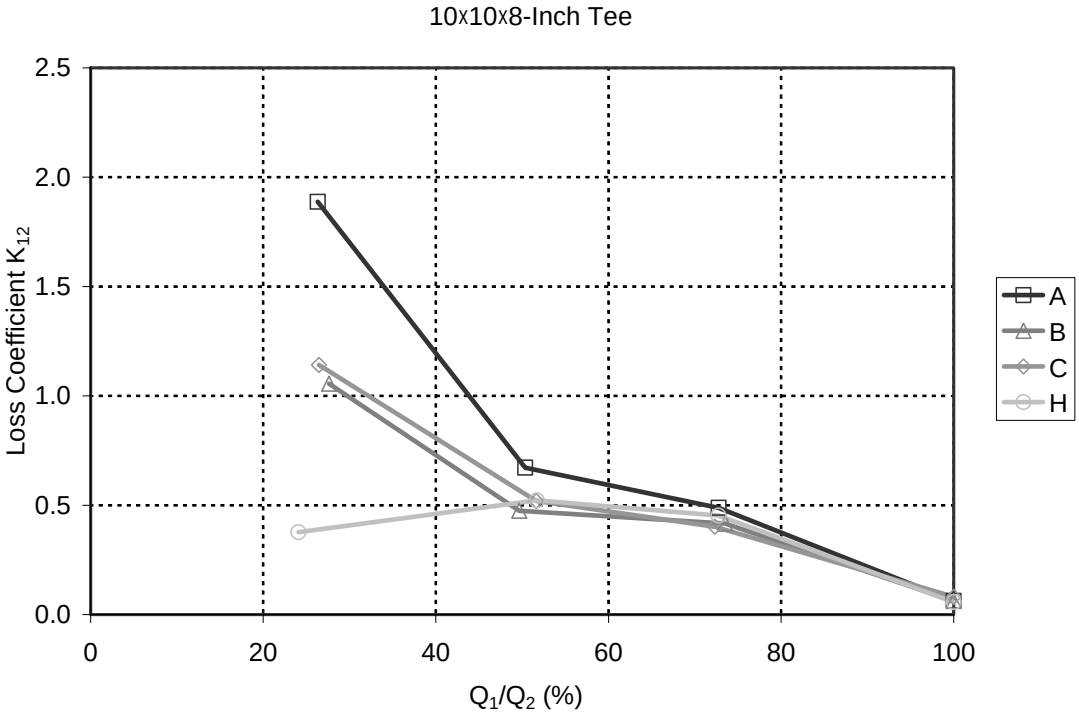

Figure B.23. K-values for the flow through the straight leg of the 10×10×8-inch mixing Tees from four manufacturers.

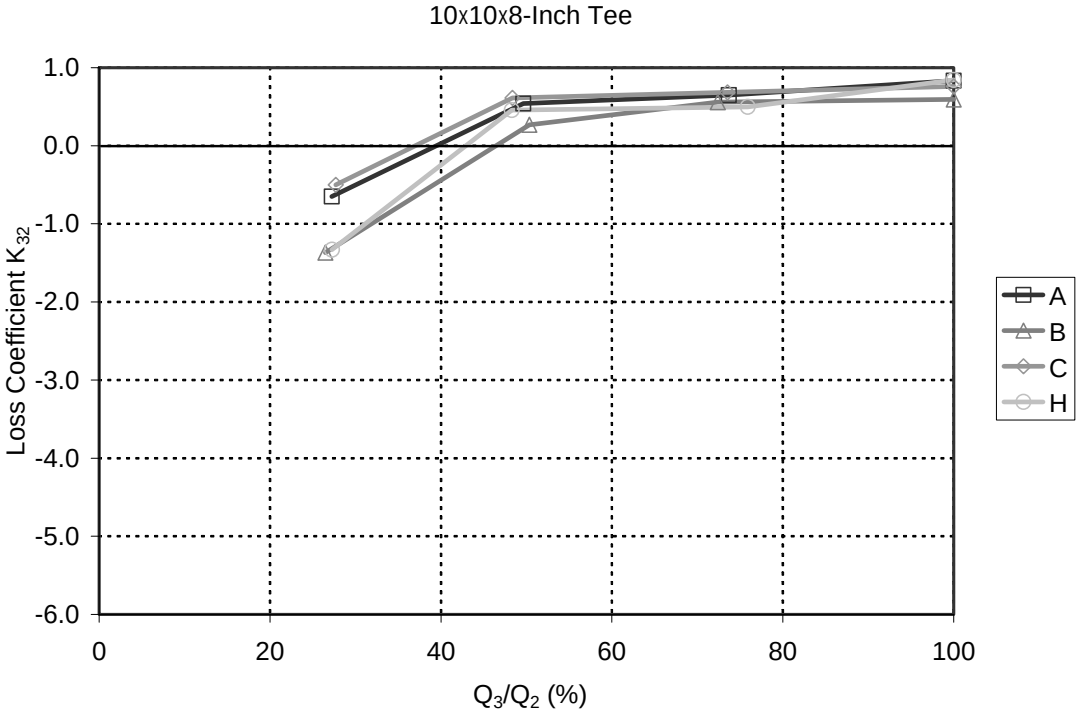

Figure B.24. K-values for the flow through the branching leg of the 10×10×8-inch mixing Tees from four manufacturers.

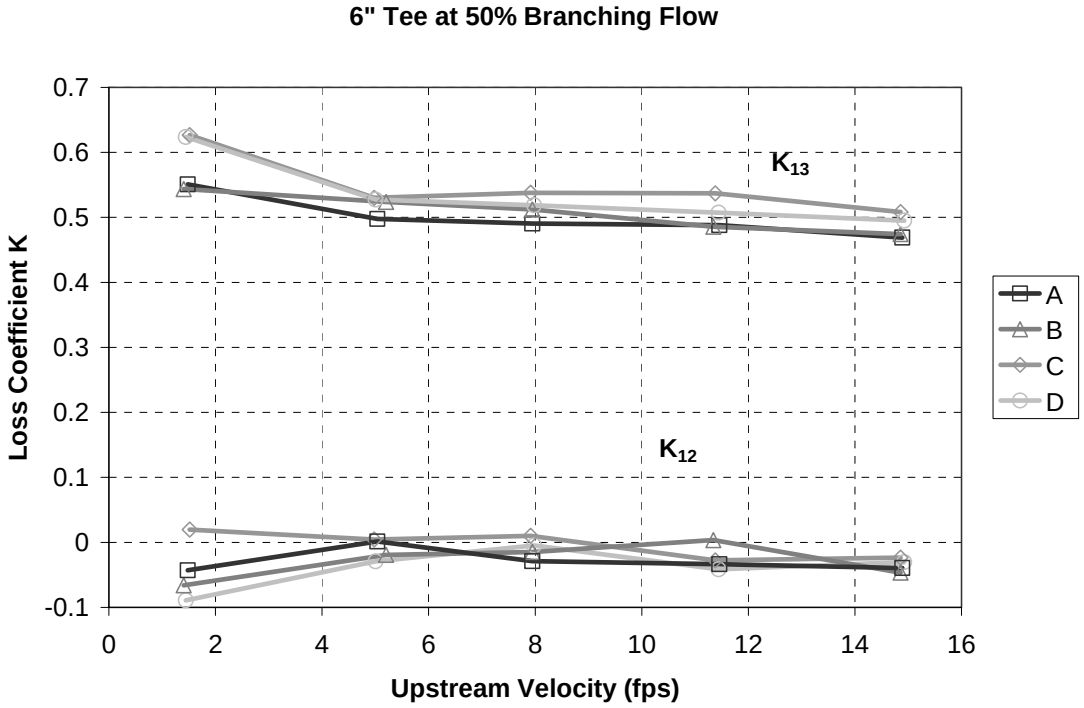

Figure B.25. K-values for the 6-inch branching flow Tees at 50% flow from four manufacturers.

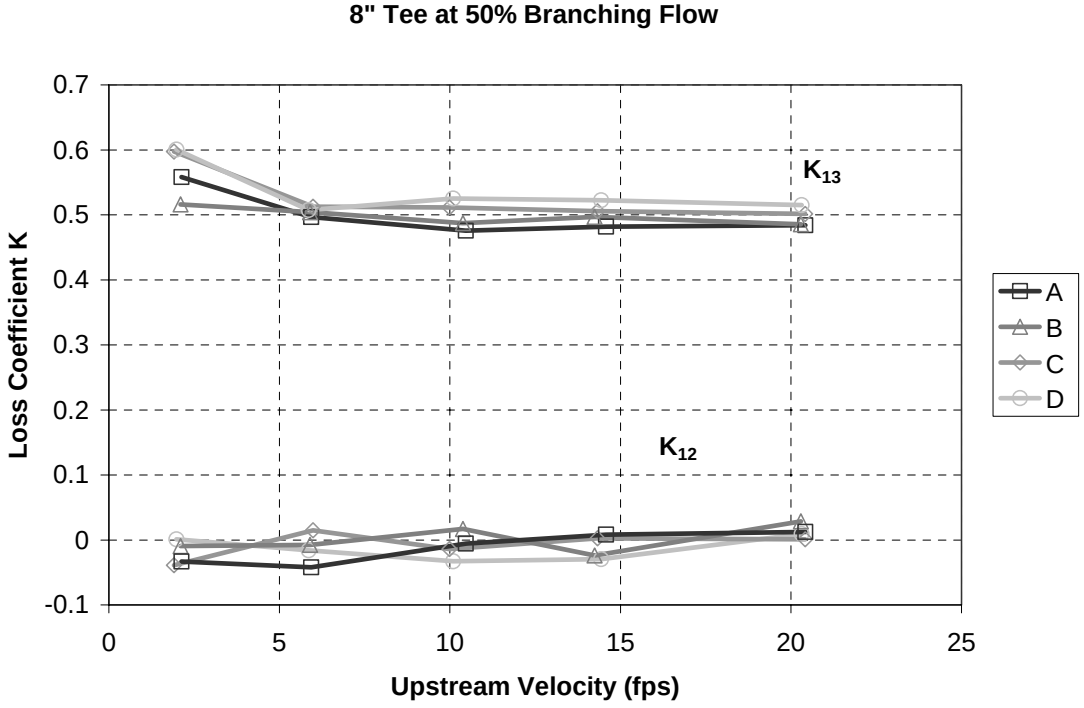

Figure B.26. K-values for the 8-inch branching flow Tees at 50% flow from four manufacturers.

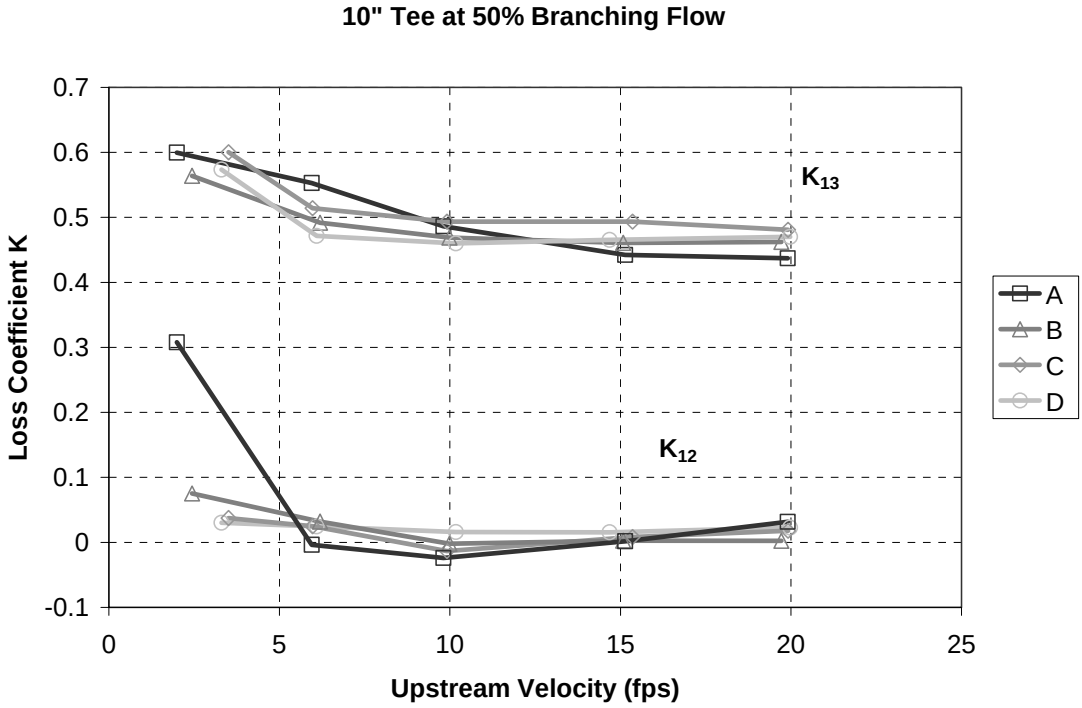

Figure B.27. K-values for the 10-inch branching flow Tees at 50% flow from four manufacturers.

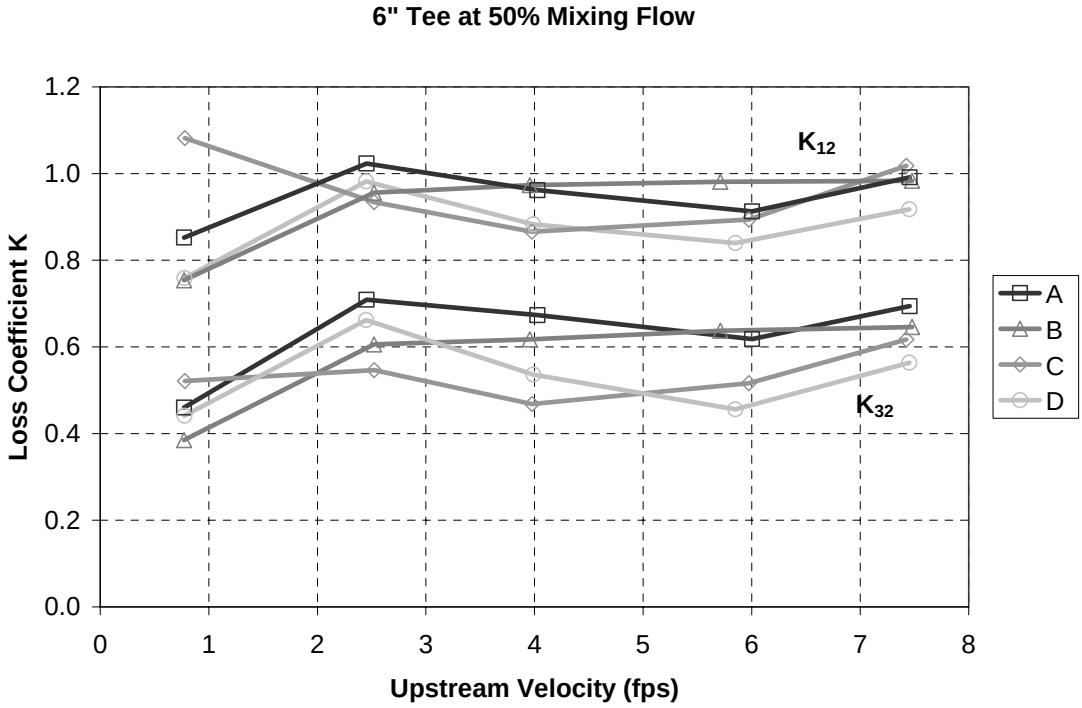

Figure B.28. K-values for the 6-inch mixing flow Tees at 50% flow from four manufacturers.

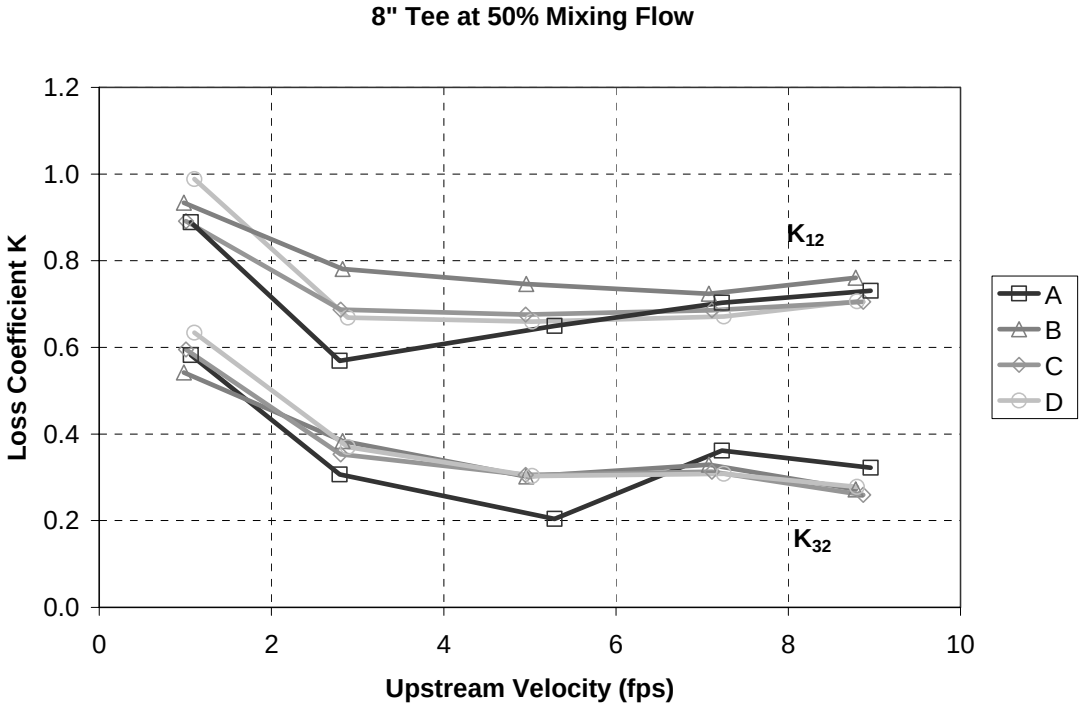

Figure B.29. K-values for the 8-inch mixing flow Tees at 50% flow from four manufacturers.

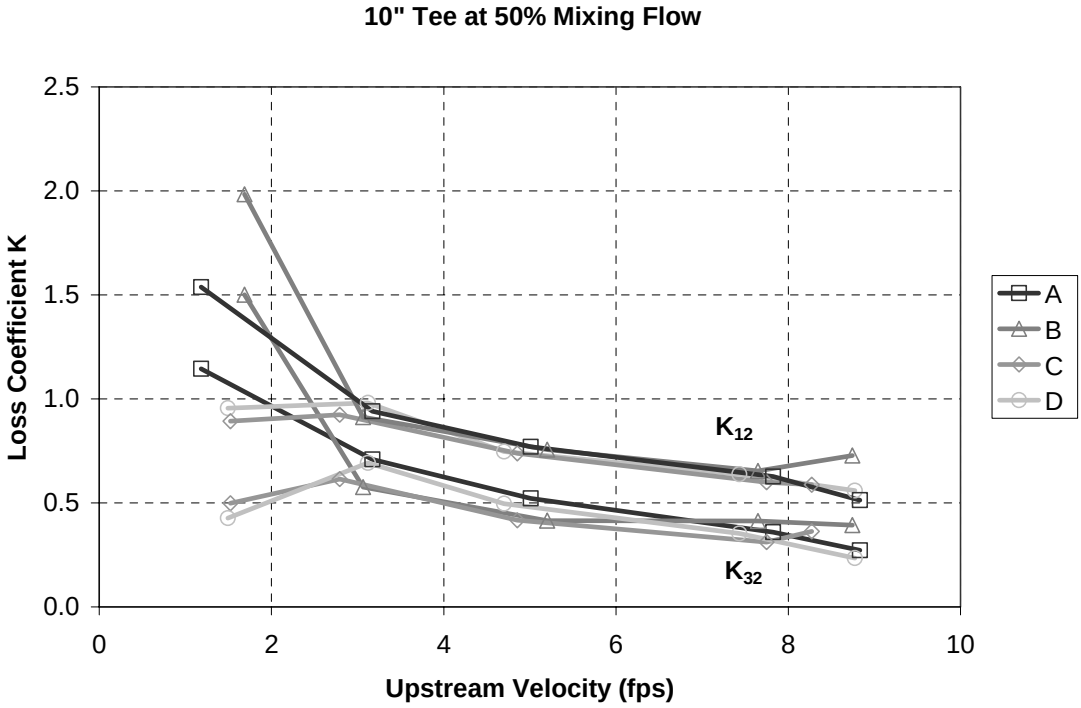

Figure B.28. K-values for the 10-inch mixing flow Tees at 50% flow from four manufacturers.

Appendix C. K-values of all tested concentric reducers and expansions

In this attachment the K-values obtained for all tested reducers and expansions are plotted versus the Reynolds number. The Reynolds number has been calculated using the velocity and geometry upstream of the fitting.

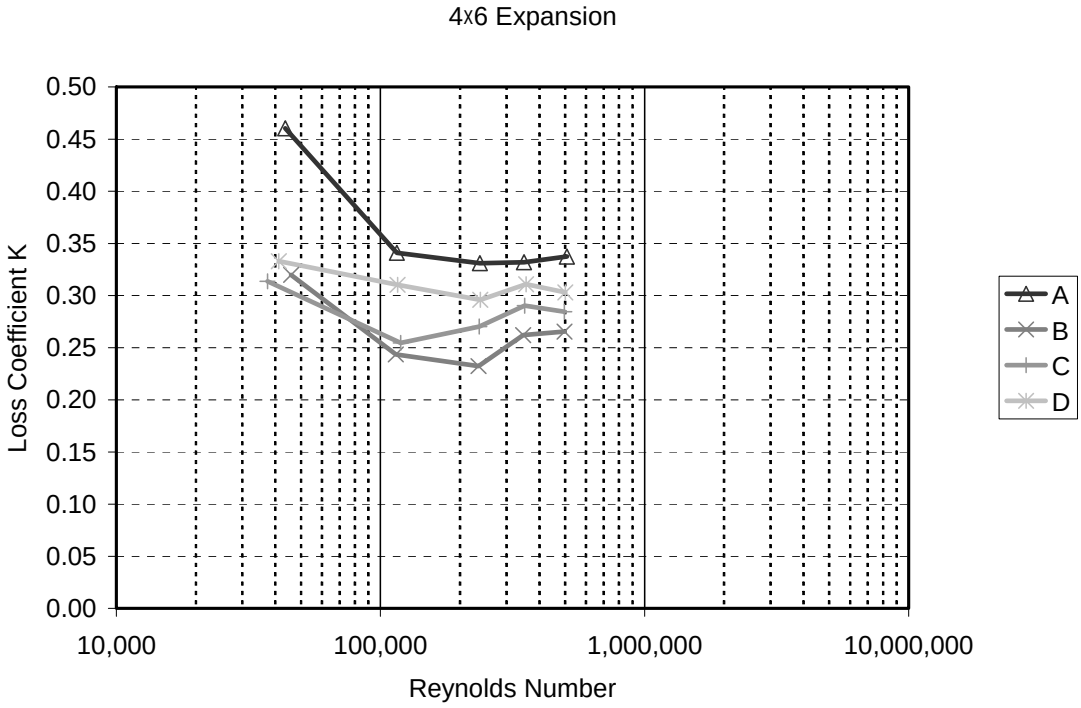

Figure C.1 K-values of 4×6-inch concentric expansions from four manufacturers versus the Reynolds number.

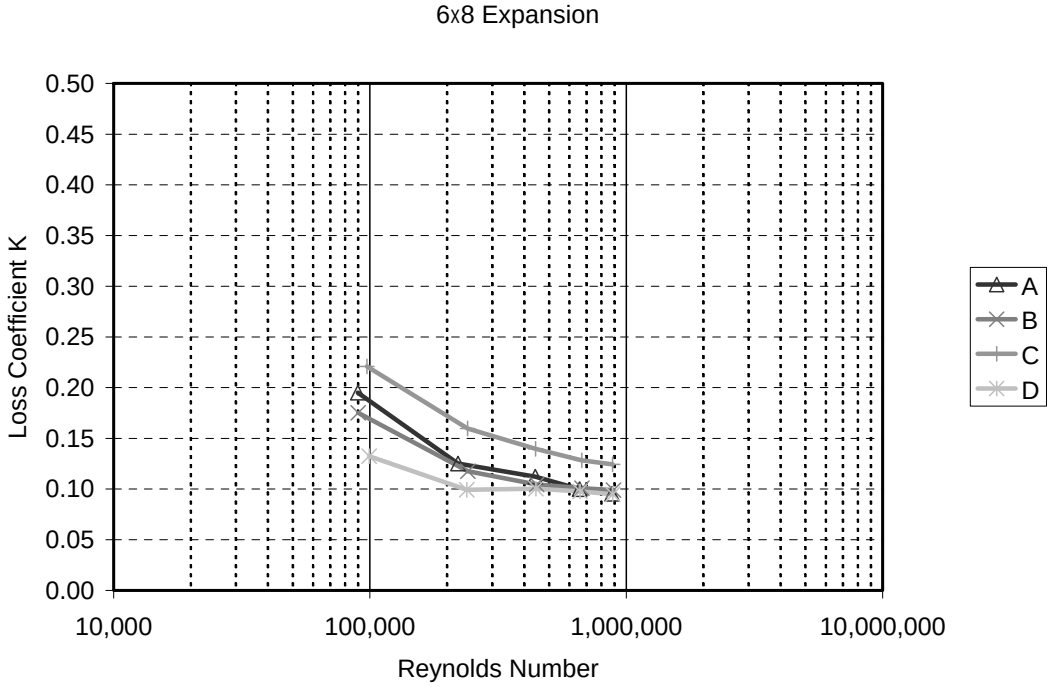

Figure C.2 K-values of 6×8-inch concentric expansions from four manufacturers versus the Reynolds number.

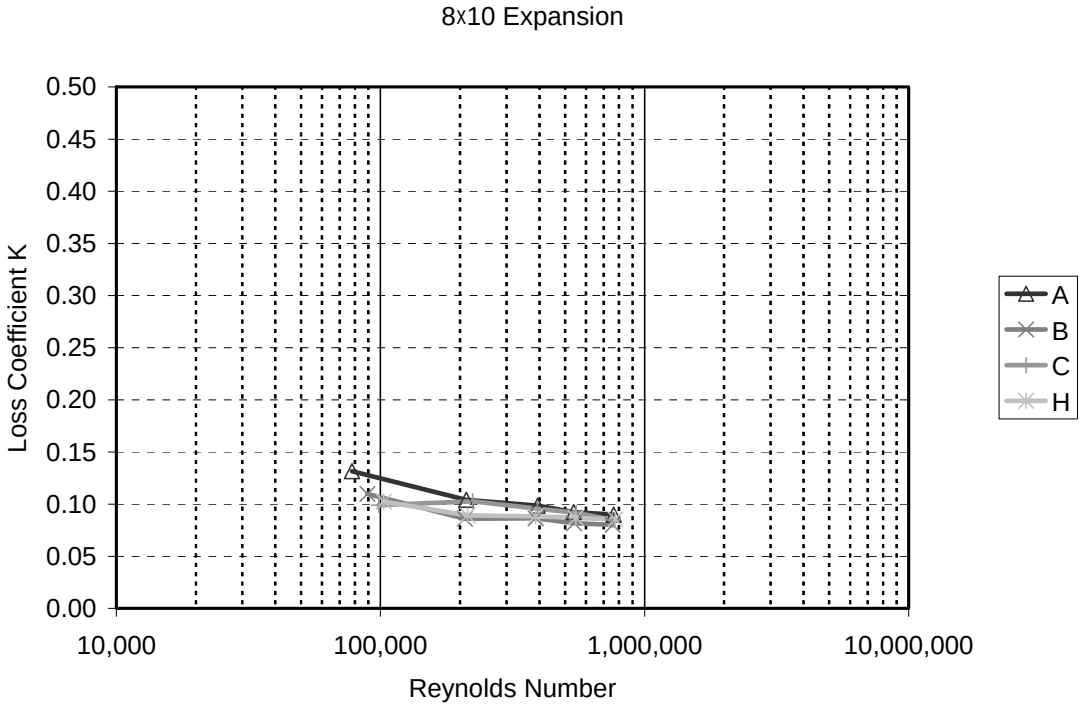

Figure C.3 K-values of 8×10-inch concentric expansions from four manufacturers versus the Reynolds number.

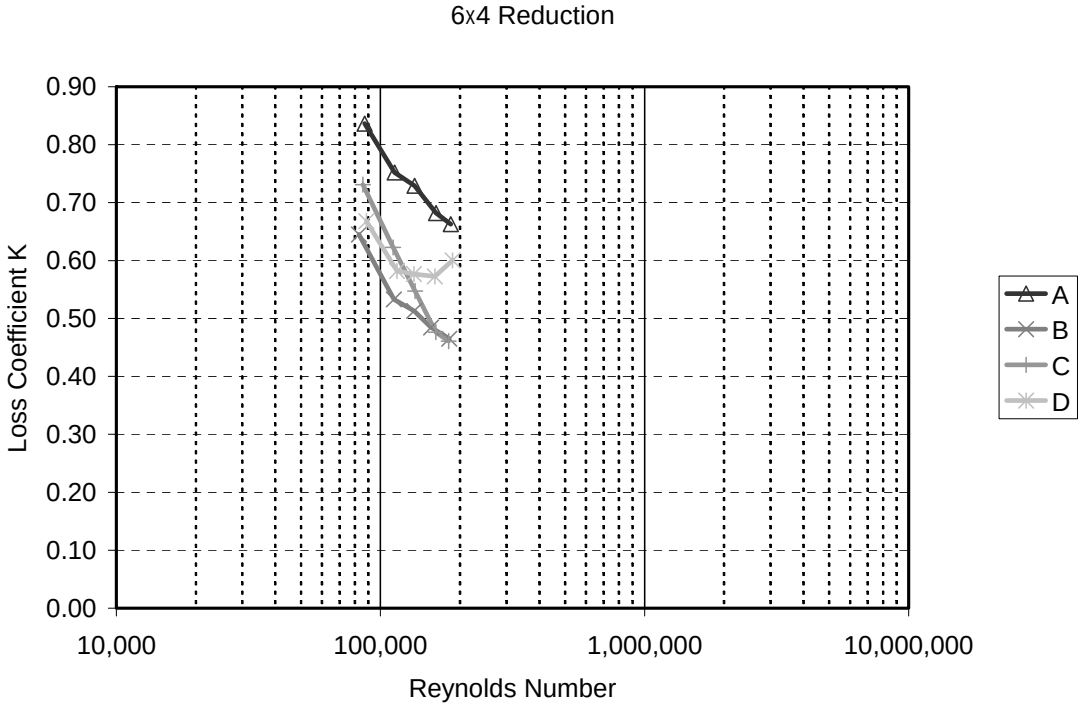

Figure C.4 K-values of 6×4-inch concentric reducers from four manufacturers versus the Reynolds number.

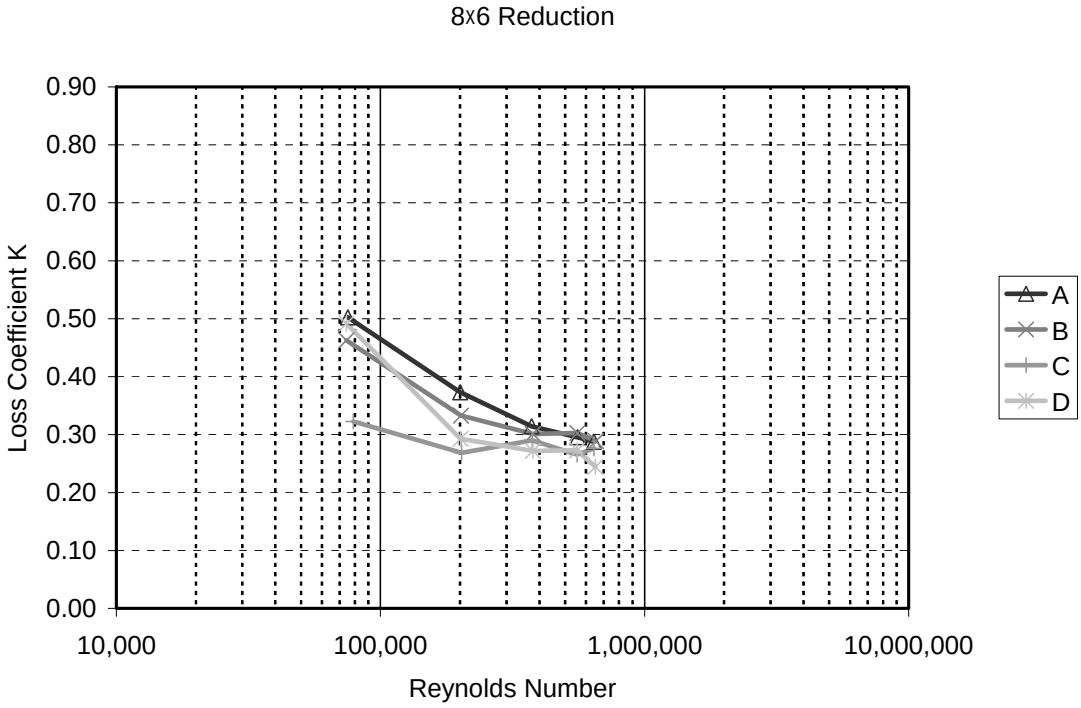

Figure C.5 K-values of 8×6-inch concentric reducers from four manufacturers versus the Reynolds number.

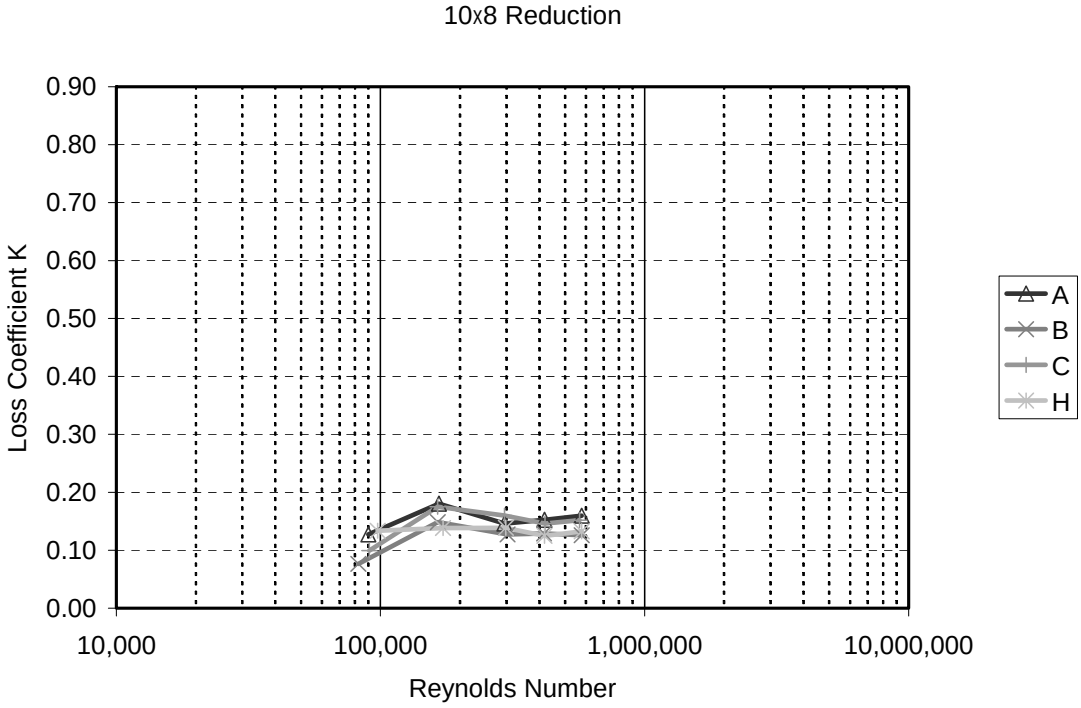

Figure C.6 K-values of 10×8-inch concentric reducers from four manufacturers versus the Reynolds number.

Appendix D. Photos of the sliced reducers tested

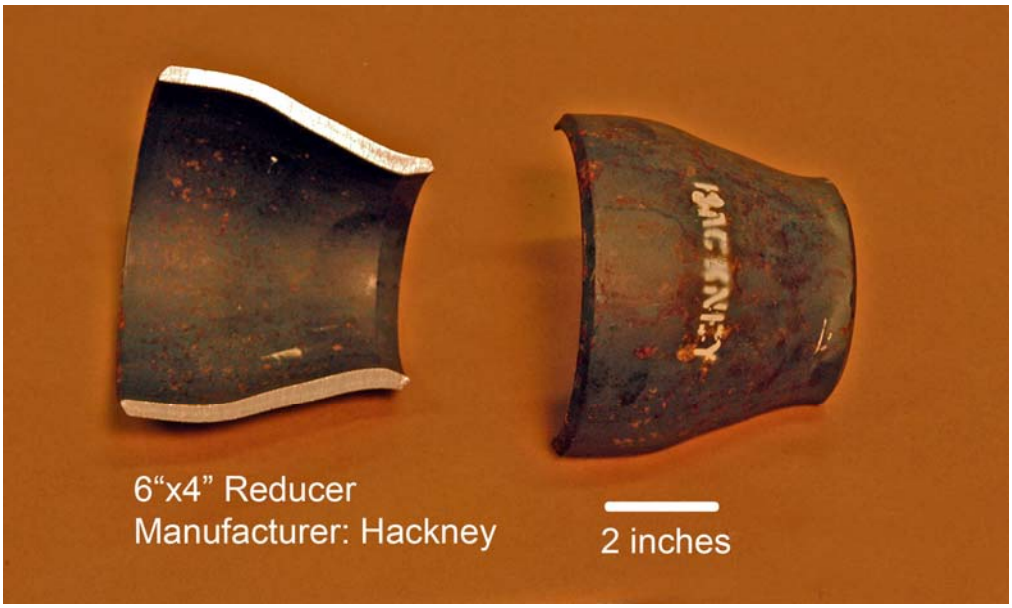

Figure D.1 Scaled photo of 6x4-inch concentric reducer manufactured by Hackney.

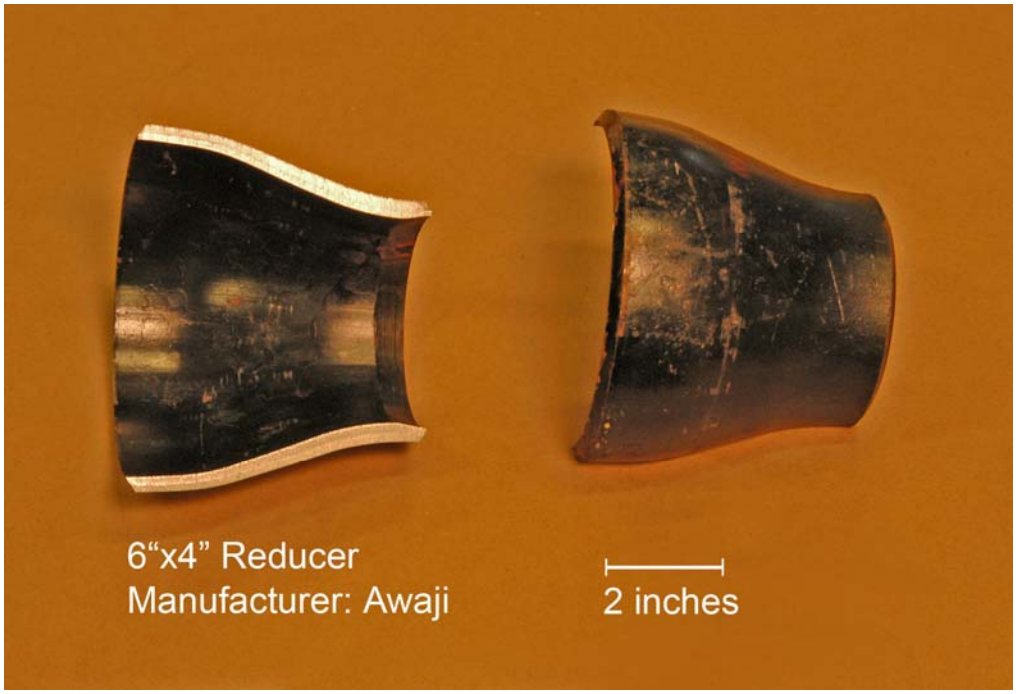

Figure D.2 Scaled photo of 6x4-inch concentric reducer manufactured by Awaji.

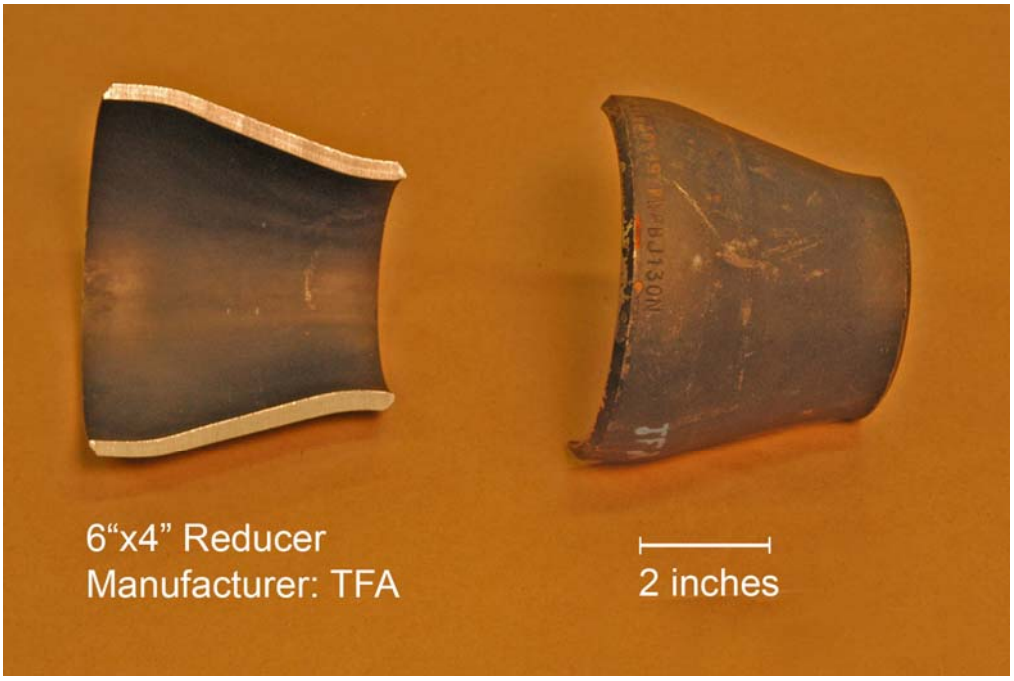

Figure D.3. Scaled photo of 6x4-inch concentric reducer manufactured by TFA.

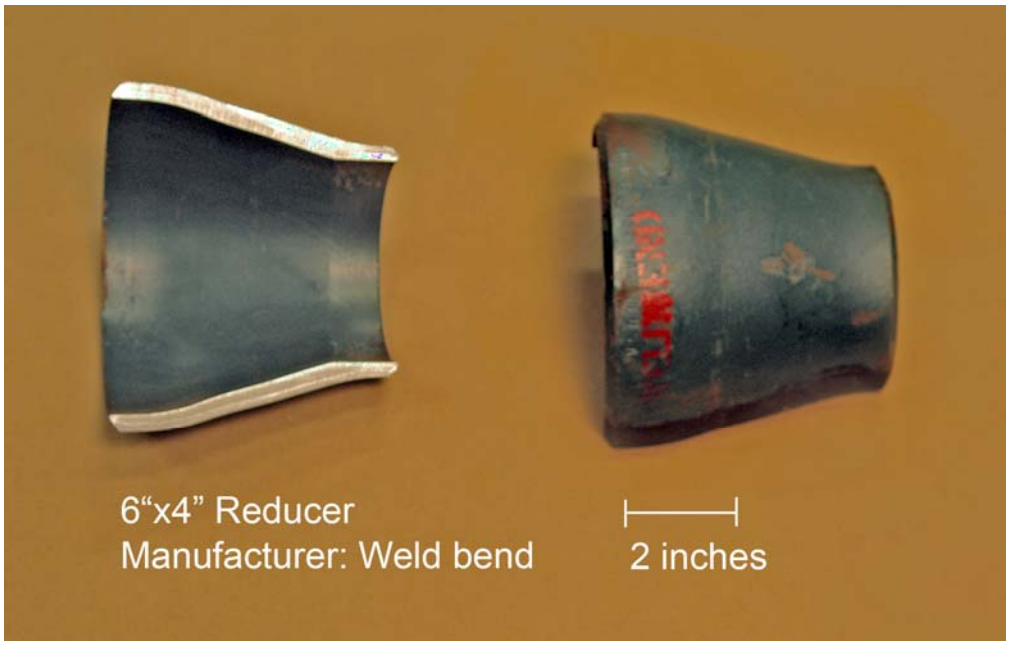

Figure D.4 Scaled photo of 6x4-inch concentric reducer manufactured by Weldbend.

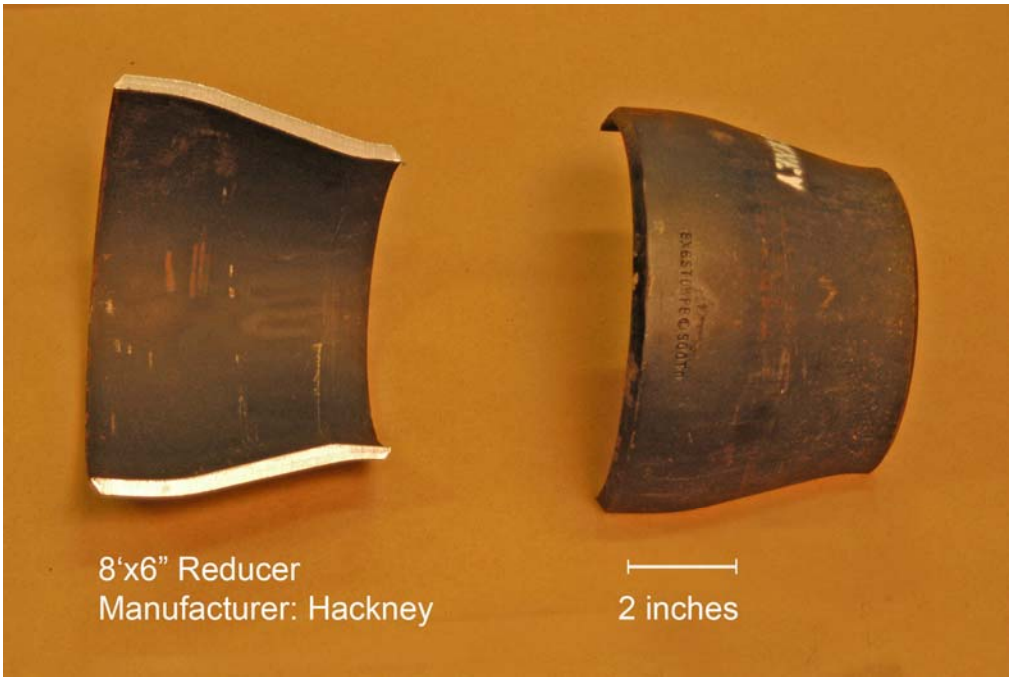

Figure D.5 Scaled photo of 8x6-inch concentric reducer manufactured by Hackney.

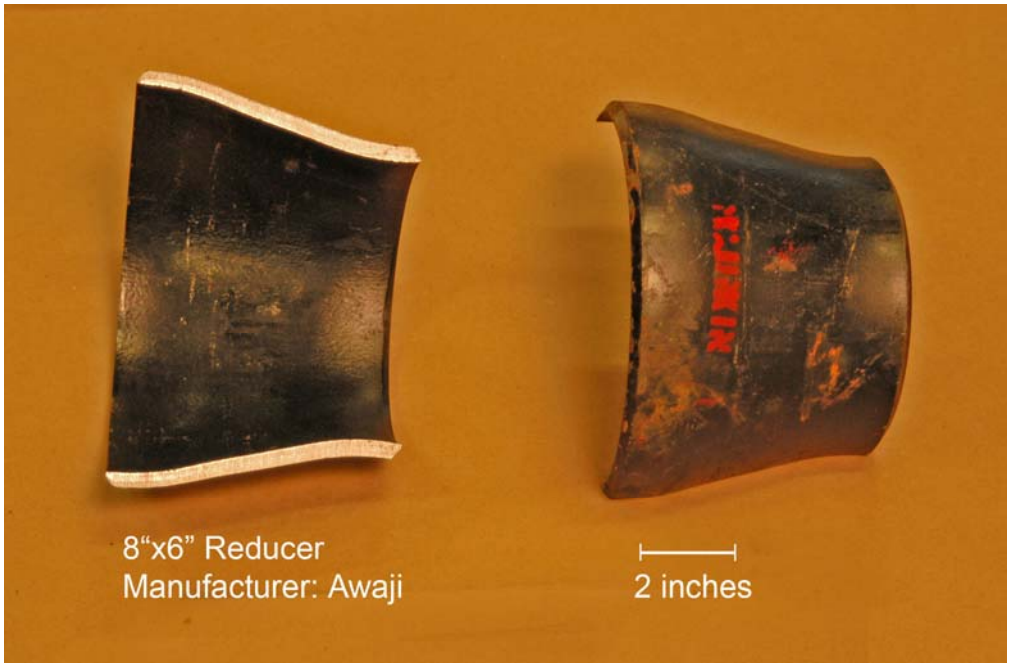

Figure D.6 Scaled photo of 8x6-inch concentric reducer manufactured by Awaji.

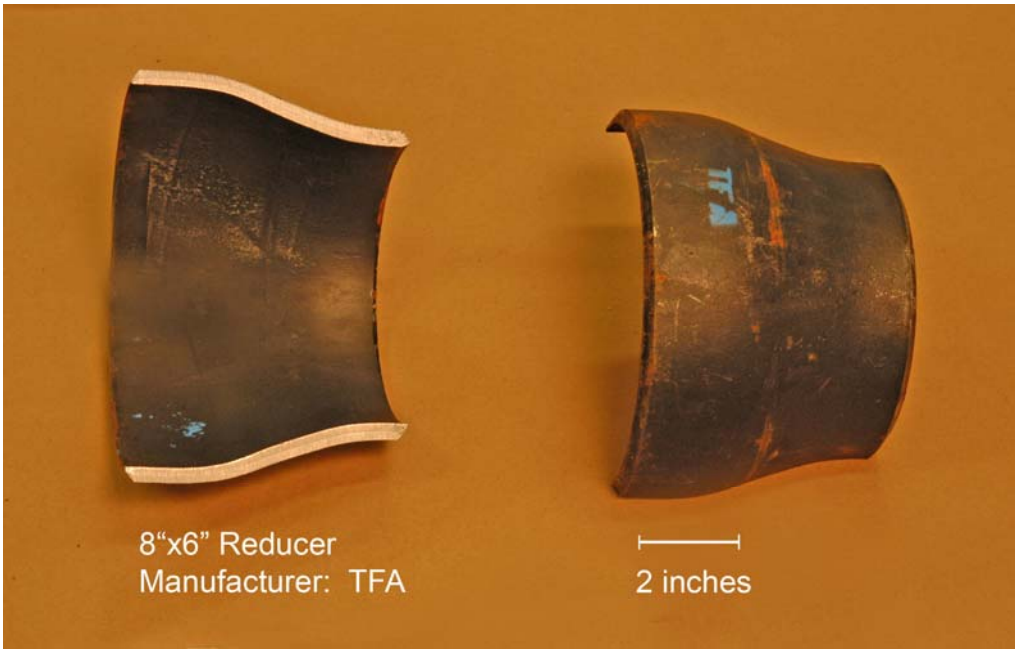

Figure D.7 Scaled photo of 8x6-inch concentric reducer manufactured by TFA.

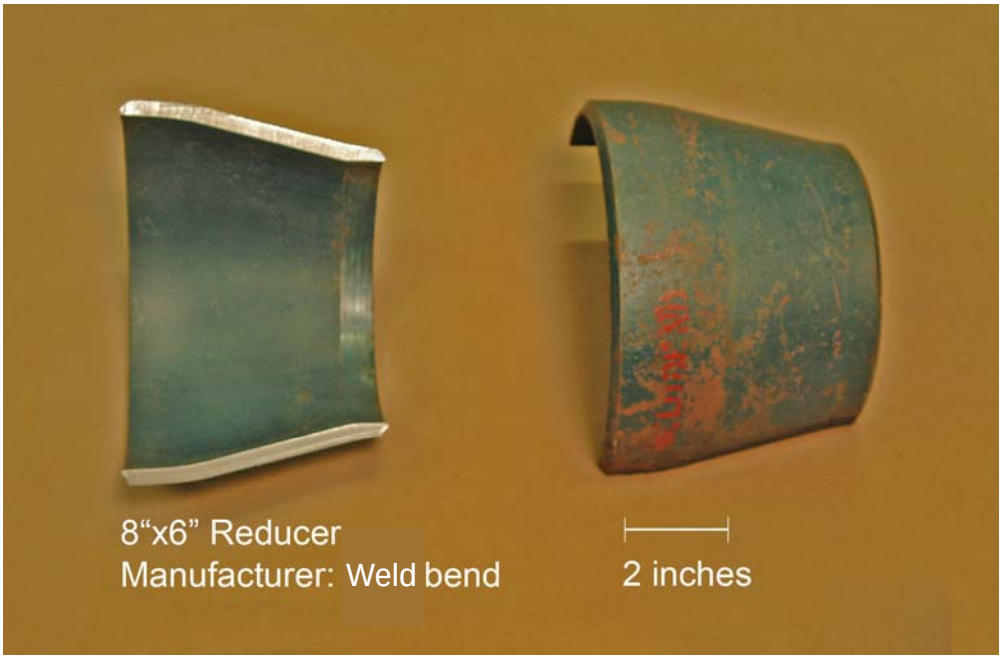

Figure D.8 Scaled photo of 8x6-inch concentric reducer manufactured by Weldbend.

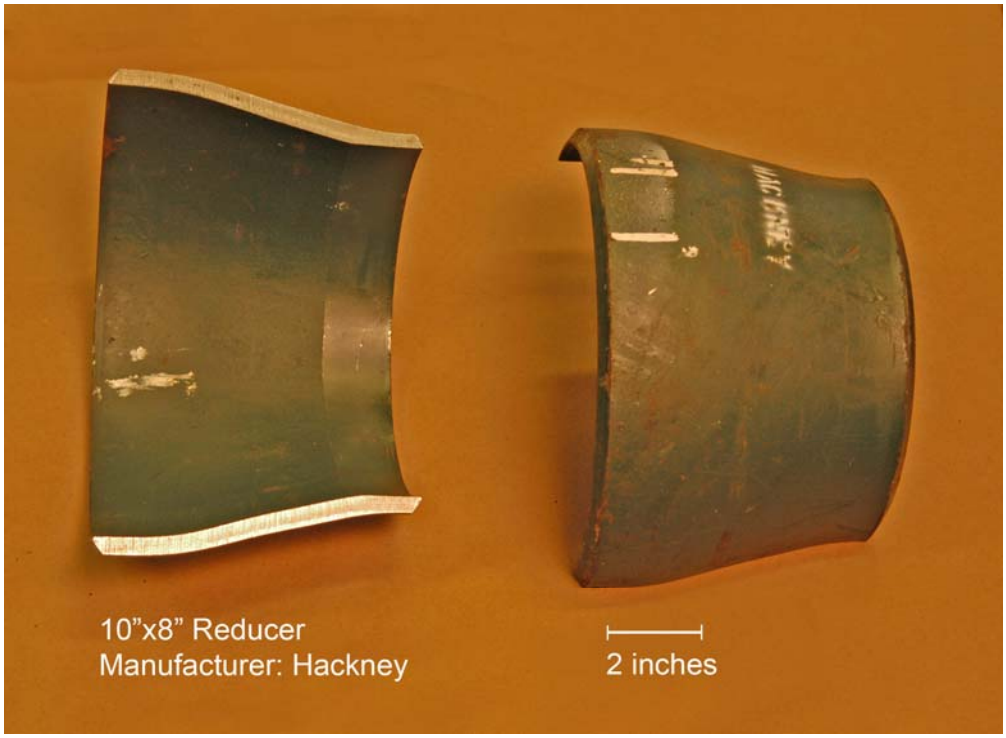

Figure D.9 Scaled photo of 10x8-inch concentric reducer manufactured by Hackney.

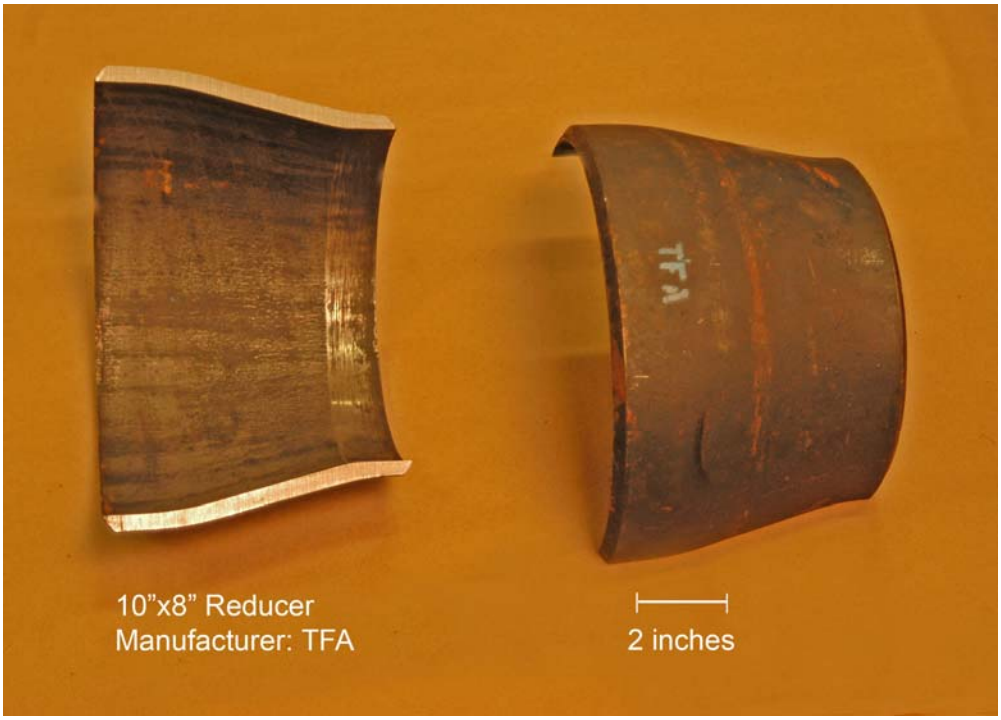

Figure D.10 Scaled photo of 10x8-inch concentric reducer manufactured by TFA.

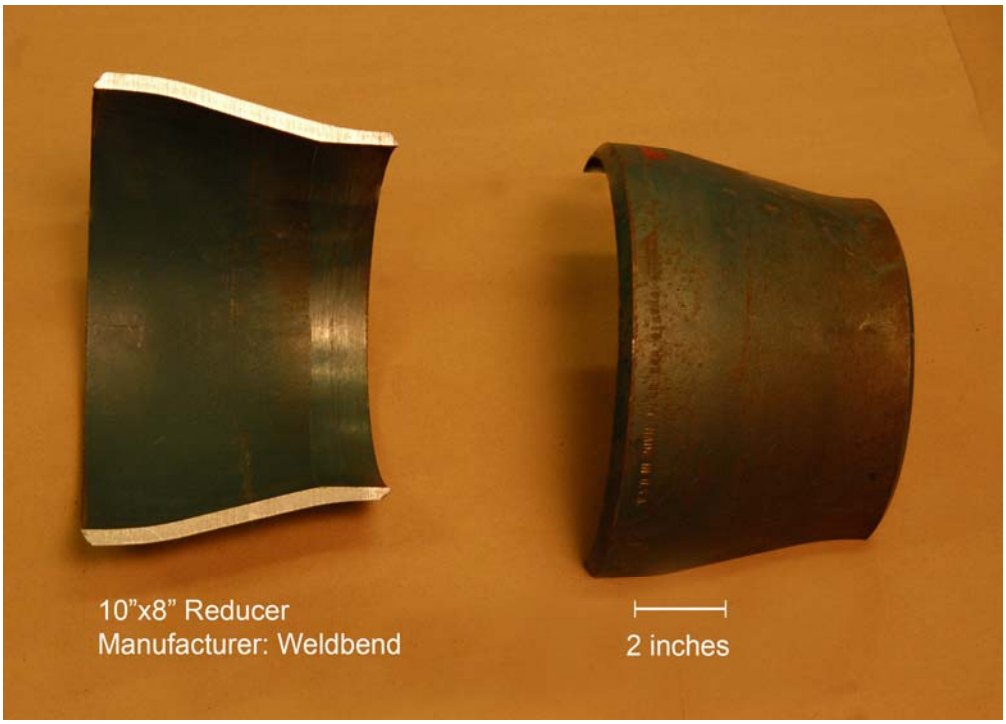

Figure D.11 Scaled photo of 10x8-inch concentric reducer manufactured by Weldbend.